EUR 4486 e

INVESTIGATION ON
REACTIVITY VALUES OF Pu-U ROD CLUSTERS
BY AN OSCILLATION METHOD

by

A. BOEUF, E. MACKE and S. TASSAN

1970

This report is on sale at the addresses listed on cover page 4

at the price of FF 25.—   FB 225.—   DM 16.50   Lit. 2,800   Fl. 16.—

When ordering, please quote the EUR number and the title, which are indicated on the cover of each report.

This document was reproduced on the basis of the best available copy.

EUR 4486 e

INVESTIGATION ON REACTIVITY VALUES OF Pu-U ROD CLUSTERS
BY AN OSCILLATION METHOD by A. BOEUF, E. MACKE and S. TASSAN

The reactivity worths of synthetic Pu-U clustered fuel elements, in a D_2O moderated assembly, have been experimentally determined using the reactor oscillation method.

Five different test-fuel compositions have been investigated, representing varying degrees of fuel burn-up and burn-up distributions; two uranium samples with different U^{235} enrichment have been used as standard.

The technique selected was aimed to establish "clean" experimental conditions, so as to effectively simplify the analysis of the results. Basically, it consisted in oscillating, according to a square-wave pattern, a 6 m long fuel element containing a 50 cm high test section with the investigated fuel composi-

tion : the corresponding neutron density modulation was interpreted in terms of a Fourier analysis.

The results of the experiment form a consistent set of data, which can be used as test values for refined reactor burn-up calculation codes. The overall experimental error, typically $\pm$ 0.015 pcm, is considered remarkably low, in view of the massive and complex experimental set-up used.

The report contains a detailed description of the experimental work; particular evidence is given to the peculiar aspect of the measurement, i.e., : oscillation of heavy load, complex geometry fuel elements in a D_2O moderated reactor, for high precision reactivity determinations.

A chapter devoted to the error analysis, which is based on the results of an extensive series of tests, puts in evidence the flexibility of the experimental technique, in view of its use under more severe conditions for the determination of minor differential reactivity effects (as temperature coefficient of Pu vs. U fuel, etc.).

EUR 4486 e

INVESTIGATION ON REACTIVITY VALUES OF Pu-U ROD CLUSTERS BY AN OSCILLATION METHOD

by

A. BOEUF, E. MACKE and S. TASSAN

1970

ABSTRACT

The reactivity worths of synthetic Pu-U clustered fuel elements, in a D_2O moderated assembly, have been experimentally determined using the reactor oscillation method.

Five different test-fuel compositions have been investigated, representing varying degrees of fuel burn-up and burn-up distributions; two uranium samples with different U^{235} enrichment have been used as standard.

The technique selected was aimed to establish "clean" experimental conditions, so as to effectively simplify the analysis of the results. Basically, it consisted in oscillating, according to a square-wave pattern, a 6 m long fuel element containing a 50 cm high test section with the investigated fuel composition : the corresponding neutron density modulation was interpreted in terms of a Fourier analysis.

The results of the experiment form a consistent set of data, which can be used as test values for refined reactor burn-up calculation codes. The overall experimental error, typically $\pm$ 0.015 pcm, is considered remarkably low, in view of the massive and complex experimental set-up used.

The report contains a detailed description of the experimental work; particular evidence is given to the peculiar aspect of the measurement, i.e., : oscillation of heavy load, complex geometry fuel elements in a D_2O moderated reactor, for high precision reactivity determinations.

A chapter devoted to the error analysis, which is based on the results of an extensive series of tests, puts in evidence the flexibility of the experimental technique, in view of its use under more severe conditions for the determination of minor differential reactivity effects (as temperature coefficient of Pu vs. U fuel, etc.).

CONTENTS
_____

GENERAL CONSIDERATIONS *)

0. INTRODUCTION

0.1. The evolution of the fuel composition during operation
conditions the core life of nuclear power reactors.
Fissile isotopes are progressively consumed, forming
fission products which cause parasitic neutron capture,
while fertile isotopes (U^{238}, Th^{232}) generate additional
fissile isotopes (Pu^{239}, U^{233}). The knowledge of the
corresponding variation in the multiplication factor is
of fundamental importance for the life prediction of
power reactor cores. Due to the complexity of the problem
the theoretical work must be supported by extensive
experimental effort.

It is generally preferable to simplify the investigation,
by separating the effects of fission products accumulation
from those of fissile isotopes build-up by a two step
procedure. The first phase involves consideration of
fictitious fuel consisting of a known mixture of fissile
and fertile isotopes (e.g. : U^{235}, Pu^{239}, U^{238}) with a
range of compositions extending over the fuel evolution
of interest. Having determined the reactivity of this
"simplified" fuel, consideration of the real fuel with
different degrees of burn-up (second phase), allows to
appreciate the reactivity effects of the fission products
content. In consideration of the very high cost (base
material and fabrication) of such fuel elements, it is
imperative to use experimental techniques which require
the lowest amount of fuel.

---

*) Manuscript received on 31 March 1970

0.2. The report describes an extensive series of measurements of the reactivity values (also referred to as : reactivity worths, reactivities, etc.) of synthetic Pu-U fuel elements of known composition, performed in the D_2O moderated critical facility ECO by the reactor oscillation method.

The fuel element geometry considered was that of the fuel forming the basic lattice of ECO, i.e. : a cluster of 19 natural U metal rods, each 12-mm-dia, clad by 1-mm-thick aluminum and cooled by organic liquid ("diphyl" : 26.5%, $C_{12}H_{10}$, 73.5% $C_{12}H_{10}O$) (1).

The nominal compositions of the four Pu-U test-elements (also referred to as : test-samples, test-sections, test-fuels, etc.) investigated are listed in the Table below.

| | | weight % ratios | |
identification	Pu/U	Pu^{240}/Pu^{239}	U^{235}/U
Pu I	0.05	8	0.714
Pu II	0.30	8	0.20
Pu III	0.05	25	0.714
Pu IV	0.30	25	0.20

The reactivity values of the Pu-U fuels were determined relative to the reactivity of the natural U fuel element of the ECO basic lattice. The reactor oscillation method was selected because of its high intrinsec accuracy, in view of the small relative reactivity values of the test-elements.

The overall experimental error obtained, typically ±0.015 pcm, is considered remarkably low, in view of the massive and complex experimental set-up, and is in fact close to the lowest limit of error reported for reactor oscillation type experiments.

The results of the measurements form a consistent set of data, which can be used as test values for refined reactor burn-up calculation codes.

0.3. The report contains a detailed description of the experimental work, but no reference is made to the results of theoretical calculations which will be presented in a later report. Particular evidence is given to the peculiar aspect of the experiment, i.e.: oscillation of heavy-load, complex-geometry, fuel elements in a D_2O moderated critical assembly, for high precision reactivity determinations.

1. MAIN FEATURES OF THE EXPERIMENT

1.1. Schematically, the experiment consisted in oscillating with constant period a 50-cm-long section of the fuel investigated, inserted inside an extended-length natural U fuel element of the basic lattice of ECO, in-out the core of ECO along the reactor axis. The oscillation pattern approximated a square-wave function.

The corresponding modulation of the neutron density population, detected by an ionization chamber placed inside the reflector and recorded in digital form on magnetic tape, was analysed to obtain the amplitude of the first harmonic of its Fourier series expansion divided by the mean value (= $\Delta n/n$).

Provided that the requirements for the validity of
the linear reactor kinetics equations were met, $\Delta n / n$
was proportional to the reactivity value of the test
fuel section in the selected reactor position. The
normalization factor was obtained by measuring "reference"
test-sections of U enriched and, respectively, depleted
in U^{235}, whose reactivity values could be calculated with
adequate precision from basic nuclear data. The composi-
tion of the reference fuels was chosen so as to cover the
range of reactivities under study.

1.2.   The main features of the experimental method are briefly
        outlined in the following paragraphs; more detailed
        information is presented in the appropriate sections of
        the report.

1.2.1. The quasi-square oscillation was performed between the
        extreme positions : "test-section midplane at the maximum
        of the thermal flux axial distribution in the core"
        (position in); and "test-section completely above the
        D_2O free level" (position out). As a consequence reacti-
        vity effects from neutron scattering by the test section
        were negligible.

        The experiment was essentially a substitution measurement,
        using the reactor oscillation method to increase the
        accuracy of the results (in fact in a D_2O moderated
        assembly substitution measurements carried out by static
        methods on test-sections having reactivity worths of few
        tens pcm, as those considered, would not yield precise
        results, mainly due to the presence of delayed photoneutrons:
        see chapters 3 and 12).

1.2.2. The square-wave function was closely approximated by the
actual oscillation function (typically 2 sec transit
time vs 28 sec rest time). This feature reduced the
importance of the reactivity signal originating during
the transfer of the test-section (e.g. the spurious
signal generated by the joints of the test-sections),
contributing to "clean" the data of the measurement (see
chapter 11). It also avoided systematic errors arising
from the neutron spectrum variations close to the
boundaries of the core (see 2.4).

1.2.3. The insertion of the 50-cm-long test-section in a
geometrically identical fuel element of the lattice
minimized the "end-effects" to be considered in the
analysis of the data (conversely, the interpretation
of measurements made with the same test-section in the
empty oscillation channel would have required the
evaluation of important end-effects in order to infer
the test-section reactivity from the experimental result).

1.2.4. The oscillation of an extended-length (6 meters) fuel
element, allowed that the reactor core and bottom
reflector were completed (i.e. : filled) by the element
at all times during the oscillation.

Thus the reactivity signal generated by the oscillation
closely approached that caused by an ideal migration of
the 50-cm-long test fuel composition along a stationary
natural U fuel element.

This feature made the neutron modulation signal substan-
tially "clean" and considerably simplified the analysis
of the data (see chapters 6 and 11).

1.3. The characteristics of the experimental method outlined
in 1.2.1. to 1.2.4. were selected with the aim to
improve the analysis of the experimental data, as well
as to reduce the importance of the sources of systematic
errors.

Some of the above features, namely those indicated in
1.2.2. and 1.2.4., implying the oscillation of a heavy
load, extended length fuel element according to a
square-wave function, were very demanding from the
point of view of the design and performance of the expe-
rimental equipment, particularly the oscillator and
the oscillating fuel element.

For this reason the report contains the detailed descrip-
tion of the relevant characteristics of the equipment
and of the whole series of off-pile and in-pile tests,
carried out to optimize the parameters of the experiment
as well as to define the limits of the experimental
errors, also in view of further applications of the
method.

2. PRINCIPLE OF THE REACTOR OSCILLATION METHOD

2.1. Basing on some simplifying assumptions one can establish,
for a nuclear reactor, the relation between a small
sinusoidal oscillation of the reactivity (e.g. generated
by the oscillation of a little absorbing sample in-out
the critical reactor) and the corresponding oscillation
of the neutron population. Such assumptions and the
derivation of the "transfer function", relating neutron
population and reactivity oscillations, are recalled in
the Appendix.

The two basic differential equations involved are linear so that the neutron population oscillates also in a sinusoidal way. Between the complex magnitudes of those two signals one obtains the relationship :

$$\frac{\Delta \bar{n}}{n} = \frac{\Delta \bar{k}}{A(T) + j B(T)}$$ (2.1.)

between the amplitudes :

$$\Delta k = \frac{\Delta n}{n} (A^2 + B^2)^{\frac{1}{2}}$$ (2.2.)

and between the phases :

$$t_g(\Delta \bar{k}, \Delta n) = \frac{B}{A}$$ (2.3.)

The quantities A and B are independent of the perturbation function and of the power level n, as long as the assumptions presented in the Appendix hold. They depend only on the type of reactor concerned (e.g. : due to differences in the parameters for the delayed neutron groups) and on the period T.

2.2. For experimental applications one can immediately verify that :

A. In the case that the reactor transfer function is accurately known and that, by some mean, a sinusoidal oscillation of the neutron population of relative amplitude $\Delta n / n$ is generated, the corresponding amplitude of the reactivity signal can be deduced.

B. If the transfer function is not known with sufficient precision, relative measurements can be performed, yielding the ratio between the magnitudes of two reactivities (provided the parameters of the oscillation, as the oscillation period, are kept constant).

Normally, case A does not occur, i.e. the transfer function of the reactor is known with accuracies about a factor of ten worse than the measured $\Delta n/n$ values, and measurements are performed relative to a reactivity standard (or reference reactivity).

2.3. In the general case, the knowledge of the absolute reactivity value of a sample at a given point of a critical reactor is required. This can be obtained as the difference in the reactor reactivity between the two configurations "sample out of the reactor" and "sample in the reactor" at the selected position.

Thus, ideally, the experiment consists in oscillating the sample in-out the critical reactor with constant frequency, and in recording the corresponding modulation of the neutron density in the reactor. The ratio of the amplitude of the first harmonic of the Fourier series expansion of the recorded signal to its mean value is proportional to the reactivity worth of the sample, through the appropriate transfer function.

2.4. In the case of relative measurements, it is not necessary to know the shape of the periodic reactivity signal. It suffices that the reactivity signals of the "test" sample and of the "reference" sample be proportional at any moment during the oscillation cycle. Provided the variation of the neutron spectrum along the oscillation path in the reactor has a negligible influence, this condition is met if the oscillation pattern (i.e. sample position versus time) is identical for the test and the reference sample.

In fact the influence of neutron spectrum variations
(mainly close to the reactor core boundaries) is difficult
to appreciate a priori, specially if the sample absorption
cross section has an important resonance structure.

This source of error is minimized by reducing the sample
transfer-time relative to the rest-time at the "in reactor"
and "out of reactor" positions, i.e. by generating a
"sample position vs time" function which approaches the
square-wave function.

3. COMPARISON BETWEEN STATIC AND DYNAMIC METHODS FOR REACTIVITY
   DETERMINATIONS

3.1. The general features of static and dynamic techniques for
   reactivity measurements have been discussed in detail by
   several authors (2,3).

   In the following section some considerations are made specific
   to heavy water moderated assemblies, where the delayed photo-
   neutrons produced by the 1.6 MeV threshold (γ ,n) reaction
   in D_2O considerably affect the reactivity worth of heavy-
   weight fuel test-sections, and to the operational characteri-
   stics of the ECO reactor.

3.2. Static method

   The following procedure is used for routine determinations
   of small reactivities in the ECO reactor.

   The critical states corresponding to the conditions "test-
   section at core center" and test-section out of core"
   are obtained by adjustement of the D_2O level in the reactor
   vessel.

The reactivity worth of the test-section is inferred from the measured difference in the D_2O critical levels, on the basis of a previously established relation between reactivity and D_2O level variation (pcm/mm D_2O) in the neighbourhood of the experimental critical levels.

Such relation is derived from measurements of the stable reactor periods corresponding to varving D_2O level steps, starting from the critical state, through the standard in-hour equation. The parameters of the equation are adjusted to account for the effect of delayed photoneutrons, including corrections for self-absorption of the gamma radiation in the fuel elements, etc.

3.3.   Factors affecting the precision of the static method

3.3.1. Measurement of reactor periods

Due to the presence of long living delayed photoneutrons, in D_2O moderated assemblies the asymptotic period corresponding to small reactivity additions establishes too slowly to be accurately measurable (delayed neutrons half-lifes range : 0.18 to 54.5 sec for U^{235} fission neutrons, 2.5 to 1.1×10^6 sec for photoneutrons from (γ,n) reaction in D_2O). A long period reactor power rise may be overridden by minor power drifts meanwhile occurred due to variations in atmospheric pressure, D_2O moderator local temperatures, etc.

Thus in the ECO reactor the maximum measurable period is around 200 sec corresponding to a reactivity addition of the order of 55 pcm. As a consequence, the reactivity worths of most of the considered test-sections, being of the order of 10-40 pcm, cannot be directly measured following the reactor divergence from the critical state.

The reactivity value of the D_2O mm height is determined
by the measurement of a series of periods, corresponding
to reactivity additions from about 150 pcm (about 35 mm D_2O)
upward, i.e. through an important downward extrapolation
of the experimental data implying a reduction of accuracy.

3.3.2. Measurement of D_2O levels

The reactivity worth of the D_2O moderator level being of
the order of 2.5 to 4 pcm/mm D_2O, an error of +0.1 mm
in the measured level corresponds to a +0.25 to 0.4 pcm
error in the reactivity.

The measurement of D_2O levels with errors around +0.1 mm
over the entire range of possible critical levels in a
flexible critical facility, which might well be of the
order of 100 cm, is an upper limit in accuracy very difficult
to achieve.

3.3.3. Delayed photoneutron parameters

The available data (yield, energy, decay period, etc.)
regarding delayed photoneutron emission in D_2O-moderated
critical assemblies are less accurate than the corresponding
data relative to delayed U^{235} fission neutrons, at least
by an order of magnitude. The self-absorption and energy
degradation of the emitted fission gamma radiation by the
fuel elements is difficult to evaluate for complex-geometry
D_2O power reactor elements.

While some of the above sources of uncertainty (3.3.1., 3.3.2)
can be appreciably reduced in importance by a very careful
selection of the experimental conditions, it is evident
that the presence of delayed photoneutrons limits the
validity of static methods for small reactivity measurements
in D_2O moderated reactors.

3.4. Dynamic method

The periodic oscillation of the test section "in-out" the reactor core is started, reactor at preselected power, D_2O level set to the average value between the critical levels corresponding to the conditions "test-section at core center" and "test-section out of core". The D_2O level is finely adjusted untill the residual reactor power drift is not significant:

The measurement is performed, recording the signal of a compensated ionization chamber which is proportional to the global reactor neutron density modulation. The first harmonic in the Fourier series expansion of the periodic signal, easily calculated by numerical methods, divided by the average value of the signal, is proportional to the reactivity worth of the test section, i.e.

$$\Delta k = \frac{\Delta n}{n} \cdot F(\tau)$$

F(T) being the reactor transfer function inferred from elementary linear reactor kinetics.

3.5. Factors affecting the precision of the dynamic method

3.5.1. Oscillator assembly

In the present case the oscillator assembly is an elaborate mechanical device operating on a massive load (250-kg fuel element suspended to a 350-kg rack) with strict specifications to follow a precise oscillation pattern, limiting at the same time the stresses in the materials to acceptable values.

The design and construction of the oscillator assembly (including the oscillating fuel element) presents considerable difficulties.

3.5.2. <u>Adjustement of experimental parameters</u>

The greater instrumental complexity of the dynamic method
may be the source of important experimental errors, e.g.
those arising from poor reproducibility of : test-sample
"in-pile" position, oscillation period, "in-out" sample
transit and rest time, as well as from a faulty design or
operation of the electronic equipment for the signal
detection and recording.

3.5.3. <u>Reactor and electronic instrumentation noise</u>

The ultimate accuracy of measurements implying reactor
power modulation is set by the random fluctuations of reactor
power known as reactor noise, which arise from statistical
variations occurring at various stages of the neutron chain
reaction.

An estimate of this limiting accuracy which is adequate
for the present considerations is obtained from the simplified
expression (4)

$$\frac{S}{N} = \frac{\Delta \rho}{\pi} (2 \, N_F T)^{1/2}$$

Where : $\frac{S}{N}$ = signal to noise ratio (i.e. ratio of fractional
modulation of flux produced by reactivity modu-
lation to the statistical variation in the flux)

N_F = mean fission rate in the reactor

T = total time of measurement.

The value of $\Delta \rho$ which makes the signal to noise ratio unity
gives the error to be expected from reactor noise.

For a typical oscillator measurement in ECO :

$N_F \sim 1.15 \times 10^{12}$ (power level 50 W)

T = 15 min.

Hence = $7 \times 10^{-8} \sim 0.01$ pcm.

3.5.4. <u>Reactor power drift</u>

The reactor power drift during one oscillation period, ranging from 10 to 120 sec, is normally insianificant. At most the minor drift occurring can be approximated to a linear power variation and easily corrected for in the analysis of the experimental data. (Ref.Appendix).

3.5.5. <u>Reactor transfer function value</u>

The reactor transfer function, relating the neutron density modulation to the reactivity oscillation (F(T) in Eq.2.1), is generally known with an accuracy lower by a least one order of magnitude than that attained in the measurement of the fractional neutron density modulation $(\Delta n/n)$.

As a consequence, Eq.2.1 is normally not used for the interpretation of oscillation measurements, which are rather performed relative to the reactor response to the oscillation of a standard (or : reference) sample, whose reactivity value can be calculated with high precision from primary nuclear data. In the actual case two test-sections of U with 0.80% and respectively 0.64% U^{235} content, geometrically identical to the investigated test-sections, have been used as standard samples.

3.5.6. <u>Validity of the transfer function approximation</u>

The derivation of Eq.2.1, expressing the proportionality between reactivity oscillation and neutron density fractional modulation, is based on a linearization of the reactor kinetic equations involving several approximations in the theoretical treatment.

The validity of the simplified theory is restricted
to small reactivity perturbations. The limits of the
linear approximation extend to around 200 pcm reactivity
input (3), and can be tested experimentally by the
oscillation of proper samples with increasing absorption
cross section. In practice these limits are not
approached, since for test samples with reactivity
values above some 50 pcm the static method is preferred
due to its greater instrumental simplicity (except
for D_2O moderated reactors : ref.3.3.1).

3.6. Conclusion

In conclusion the dynamic method, which is in general
required for high accuracy determinations of small
reactivities (less than 5 pcm), extends its field of
application to samples worth some tens pcm in D_2O
moderated reactors, where the presence of delayed
photoneutrons negatively affects the application of
static methods. However, special attention must be
devoted to the design and performance of the experimental
equipment.

E X P E R I M E N T A L   E Q U I P M E N T

4. THE ECO REACTOR

4.1. General

The critical facility ECO (1) is a low-power assembly,
intended for the experimental determination of the
lattice parameters of heavy-water-moderated reactors
(in particular : organic-cooled ORGEL-type reactors).

The size of the reactor core, as well as other technolo-
gical features, were determined with particular reference
to the requirements of the programmed buckling measu-
rements by the "progressive substitution" method, which
implied the progressive replacement of the lattice fuel
elements (reference elements) located in the central
zone of the reactor with the fuel elements to be tested.
The buckling of the reference lattice is measured by
flux mapping, the difference ΔB^2 between the bucklings
of the two lattices is determined by measuring the
variation of the D_2O critical level corresponding to each
substitution.

4.2. Fuel element of the reference lattice

The fuel element of the reference lattice, which was
selected so as to satisfy the experimental requirements
(essentially neutron spectrum matching) for a large range
of lattices to be examined, is a 2.9-m-long cluster of
nineteen 12-mm-dia natural U rods, canned by 1-mm-thick
aluminum, contained in a 76.8-mm-dia, 1.5-mm-thick
aluminum pressure tube filled with liquid "diphyl"
($C_{10}H_{12}$ 26.5%, $C_{10}H_{12}$ O 73.5%), in turn contained in a
81.8-mm-dia, 1.5-mm-thick aluminum calandria tube.
Other details of the fuel element geometry are shown in
Fig.1.

4.3. Core, reflector, shielding

The core of ECO is contained in a 3-m-dia, 4.2-m-high cylindrical aluminum tank. The wall of the tank is 10-mm-thick, the base is 15-mm-thick. The tank is surrounded laterally and underneath by a thermal insulating layer and by a 90-cm-thick graphite reflector (Fig.2).

A 6.0 x 6.0 x 1.3 m parallelepiped-shaped aluminum caisson is connected through a neoprene joint to the top of the tank. It contains the fuel element suspension mechanism, formed by 17 lower rails bearing small carriages under which the fuel elements hang, guided by 17 upper rails placed at right angles with the others.

The rails move parallel and symmetrically with respect to the fixed central one by the means of an array of articulated lozenges. In this way, it is possible to continuously vary the lattice pitch, from 180 to 300 mm, using only two remotely driven devices.

In the caisson top there is a circular hole having a diameter greater than that of the tank, closed by a rotating cover either 10-cm-thick (used at zero reactor power) or 110-cm-thick (used when operating around 1 kW, i.e. at maximum reactor power). The cover has a radial slot which allows access to every point of the reactor core. The reactor vessel and caisson are under a slight nitrogen overpressure to prevent entry of atmosphere moisture which would degrade the D_2O moderator. Gas tightness is ensured by means of an inflatable rubber seal adherent to the rotating cover.

The lateral shielding is a 1.70-m-thick ordinary concrete wall. A passage between the reflector and the shield leads to flux detectors and control servomechanisms. The caisson is provided with a barite concrete shield, forming with the cover the upper protection. This is completed by two 60-cm-thick concrete plates sliding on rails. Shielding allows work around and over the reactor at 1 KW power.

4.4. Control and safety

Reactor criticality is usually achieved and maintained by adjustement of the D_2O level in the core vessel. A boral sheath, sliding between the tank and the reflector, follows the heavy water level with its lower edge, thus preventing neutron reflection beyond the free water level.

Fast and slow filling pumps are provided for the water level variation. The accurate determination of the D_2O level is carried out by a temperature-compensated meter, which consists of a pneumatic probe suspended on an invar perforated tape, wound on a take-up reel via a sprocket wheel; the take-up reel is connected to a digital recorder with visual display. The probe senses a floating reference head with a ± 0.1 mm overall accuracy, over the whole 1.5 m D_2O level range.

Four absorbing plates (two vertical and two horizontal), sliding into holes in the reflector, allow automatic control of the reactor power.

Two stainless steel sheathed, boron carbide safety
rods, may fall by gravity into the center of the core.
In addition a remotely controlled valve opens when
either the power is too high or the period too short,
permitting rapid (10 m^3/min) damping of the water
contained in the tank. A device for measuring and
continuously recording the heavy water isotopic
concentration is also provided.

4.5. Experimental facility for the oscillation of a fuel
element

The experimental facility for the oscillation of the
fuel element at the lattice center is a 110-mm-dia,
6-mm-thick, 11-m-long aluminum tube, which can be
inserted in the reactor assembly on the core axis.
The tube passes through : rotating cover, variable pitch
mechanism, D_2O moderator, graphite bottom reflector
and concrete bottom shield via a removable graphite
plug. It is rigidly fixed to three points : the rotating
cover (with a gas tight seal), the variable pitch
mechanism and the bottom plug. Vertical allignment is
achieved by means of an automatic sensing device.

The lower end of the tube, closed by a thin membrane,
is fitted to a containment block for the recovery
of the oscillating load and leaking-out D_2O moderator,
in case of a major accidental break-down of the
equipment during operation, resulting in the fall of
the load accompanied by the laceration of the oscillation
tube wall. The block includes a ".bee-have" type shock
absorber, to limit the damage to the fuel element at the
inpact, and an enclosure to collect the heavy water
escaping from the core vessel before intervention of the
fast dump valve. A general view of the facility is shown
in Fig.2.

5.   MECHANICAL OSCILLATOR

5.1.   General considerations

5.1.1. The mechanical oscillator was designed for oscillating
        a fuel element on the axis of the core of the ECO reactor,
        following a trapezoidal wave function.

        The oscillation function is shown in Fig.3.   The denomina-
        tions adopted for the different parts of the function
        are clearly indicated in the figure, as : transit time,
        rest time, translation (or run); etc.. The actual
        oscillation pattern differred to some extent from the
        basic function, due to the presence of damped oscillations
        at the points of discontinuity : these are often referred
        to as "transients".

        Characteristic design parameters for the oscillator were :
        oscillating fuel element length and weight : about 6 m
        and 250 kg, respectively; amplitude of oscillation :
        about 250 cm, oscillation period : 60 sec, fuel element
        transit time : 3 sec.

5.1.2. The experimental requirement was the precise performance
        of the oscillation pattern of Fig.3; in particular :
        equal and constant upward and downward rack translation
        speed, accurate and reproducible rack rest position and
        rest time, absence of important and persistent rack
        vibrations during transients, accurate and reproducible
        oscillation period.

        The limitation of the stresses in the structural materials
        (in particular the oscillating fuel element), to avoid
        deformations and breakdown of the equipment, set the
        requirement of low accelerations during the oscillation
        transients.

Obviouslv the experimental and mechanical requirements were conflicting, to the extent that the compromise solutions selected often were at the borderline of the correspondina acceptance limits. As a consequence, an extensive series of preliminary tests of the whole assemblv and of its components was carried out, to verifv that the design specifications were met, that the material stresses in the most severe foreseen operatinq conditions were below the fatique breakdown as well as deformation limits, that operation of the oscillator accordina to the desian specifications aenerated the proper experimental conditions.

5.1.3. The main specifications set for the oscillator performance were :

oscillation amplitude : max 400 cm

oscillation period   : continuously variable from 0 to 200 sec

rack rest time   : continuously variable from 0 to 100 sec

rack transit speed   : continuously variable from 0.1 to 1 m/sec

motor speed   : continuously variable from 300 to 3000 rpm

reproducibility of
rack rest position   : $\pm$ 3 mm

transient duration   : 0.2 sec

reproducibility of
oscillation period   : $\pm$ 0.2 sec

5.2. Description of the assembly

A complete description of the oscillator assembly is given in Ref.5. Its main components, as schematically shown in Fig.4, are :

- a 6.5-m-long vertical rack (weight about 350 kg) crossing a 2-m-high framework and a coupling block fixed on the reactor top platform. Its upper part is guided by two rails, its lower part is rigidly connected to the oscillating fuel element.

- a massive framework holding : the main pinion driving the rack, two pinions driven by the rack and connected to two independent hydraulic circuits used to control the rack transit speed, the rack guiding rollers, and the electromagnetic safety brake of the rack.

- a coupling block, which is also the base plate for the whole oscillator. This block holds the mechanism necessary to couple the lower end of the rack to the oscillating fuel element.

- a gear box with four electromagnetic clutches and a differential coupling, commanding the movement (rise, descent, rest) of the rack. Two nitrogen oil type shock absorbers limiting the oscillations of the gear box about its horizontal axis during transients.

- a 25 kW d.c. motor, whose speed can be varied from 300 to 3000 rpm.

The general view of the mechanical oscillator is presented in Fig.5.

3.   Principle of operation

3.1.   A block diagram illustrating the principle of operation
        of the oscillator is presented in Fig.6.   The oscillation
        function is defined by presetting :

        - rack rest time

        - motor speed

        - oscillation amplitude ,resulting from the addition
          of upward a downward run, independently selected, with
          respect to an adjustable reference level)

        - characteristics of electromagnetic clutches and shock
          absorbers of main gear box.

        Thus neither the rack transit time nor the oscillation
        period are directly selected.   The oscillation period is
        the combination of two rest times (preset) and two
        transit times : the required period is obtained by the
        fine adjustement of the oscillator motor speed.

3.2.   The oscillation pattern (rise, stop, descent, stop) is
        generated in the gear box, through the action of clutches
        and differential couplings, following the principle of
        operation outlined in Fig.7.   The main operation features
        are summarized in the following paragraphs.

3.2.1. Driving motor speed
        The speed is continuously adjustable, by controlled
        diodes, in the range from 300 to 3000 rpm (corresponding
        transit speed of the rack : 0.1 to 1 m/sec).

5.3.2.2. **Electromagnetic clutches**

During each operation mode (rest, rise, descent) two
of the four diode controlled electromagnetic clutches
are actuated by independent power supply circuits.
The circuits contain an adjustable dissipative resi-
stance which permits to modify the time constant of
the clutch.

5.3.2.3. **Shock absorbers**

The rotational oscillation of the gear box during
transients is limited and damped by two air/oil type
shock absorbers. The static pressure of nitrogen
and the loss of head of the secondary oil circuit
are adjustable.

5.3.2.4. **Rack reference position**

It is selected by adjusting the position of a photo-
electric cell, fixed on a sliding rule (range   1 m,
reproducibility of position : $\pm$ 0.5 mm), which gives
an electrical impulse at each upward passage of the
leading edge of the rack head.

5.3.2.5. **Rack rest position**

The rack low and high rest positions are independently
selected by prefixing the upward and downward run
relative to the reference position. The position of the
rack relative to the reference position is measured by
a bidirectional digital encoder (sensitivity 2,5 pulses
per mm translation), and visually displayed in terms
of equivalent pulses of the digital encoder. A reset
of the system is made at each passage through the
reference position.

The actual rest position differs by few mm from the
preselected value, due to the time lag for the clutches
intervention (120 μsec) and the high moment of inertia
of the moving masses (rack and oscillating fuel element
weight : 600 kg).

.3.2.6. Rack rest time

It is independently selected for the high and low rest
position of the rack in the range from 0 to 99.9 sec,
with a 0.1 sec precision.

.3.3. Additional instrumentation provides information on the
following parameters (some for safety reasons).

.3.3.1. Oscillation period

A 2000 cycles/sec diapason generator, coupled to a
counting circuit and a digital indicator, measures the
actual oscillation period with a 0.01 sec precision.

The counting time is determined by the electric signal
generated by the rack when passing the reference position
during the upward run. The measured oscillation period
is maintained on display for 10 sec.

.3.3.2. Instantaneous rack position

Is measured by a rotating potentiometer coupled to the rack,
whose signal is displayed on a fast paper recorder. With
proper signal amplification and bias, the transients
(e.g. the oscillations around the rack rest position) are
recorded with adequate precision.

5.3.3.3. <u>Instantaneous accelerations of the rack</u>

Are measured by a strain gauge accelerometer (range ± 2.5 g) mounted on the rack top whose signal, after proper impedance adjustement, is displayed on a fast paper recorder.

5.3.3.4. <u>Fluctuations of the driving motor speed</u>

Are detected by a dynamo mounted on the motor shaft. The signal from the dynamo, after subtraction of the average value, is displayed on a fast recorder.

5.4. <u>Main safety devices</u>

5.4.1. The maximum admissible rack translation is limited by two switches, respectively for the low and for the high position. These switches command the safety brakes which act by loss of current.

5.4.2. The hydraulic circuits are adjusted for each operating condition so that, during the downward translation, the load (rack plus fuel element) falls freely at the selected speed without charging the motor.

5.4.3. At the end of the maximum admissible downward run the rack acts on a cam, which causes a drastic increase in the head loss of the hydraulic circuit. This produces a reduction of the rack speed from 1 m/sec to 40 cm/sec within 15 cm, in the worst case of not intervention of the safety brake. Two rubber shock absorbers are then adequate to stop the movement of the rack without damage to the assembly.

5.5.   Results of preliminary off-pile tests of the oscillator
        performance

5.5.1. Only the results of the tests performed for the most
        severe operating conditions are presented in condensed form.

        The operating conditions were : 3000 rpm driving motor
        speed (i.e. 1 m/sec rack translation speed), 80 cm run,
        2 sec rest time, oscillation of full-size mock-up of
        load, reproducing overall dimensions, weight and mecha-
        nical properties of actual fuel element.

        The results are classified according to the performance
        parameters individually considered.

        The oscillator assembly for off-pile testing is shown
        in Fig.8.

5.5.2. Driving motor speed
        It was constant to within 0.5% during the complete
        oscillation cycle, except at the start of the upward
        rack translation where a minor (less than 5%) decreases
        in the motor speed was observed, damping out in about
        3 sec.

5.5.3. Rack accelerations
        During the 0.2 sec long transient (start and stop of rack
        translation) maximum peak accelerations of 1.5 g were
        observed. The duration of the peaks was less than 0.03 sec.
        Once constant rack speed was attained, the acceleration
        values oscillated around zero with 0.4 g peak-to-peak
        amplitude. A typical record of the observed accelerations
        is shown in Fig.9.

5.5.4. Rack transit time

The upward and downward average rack speeds were constant over extended series of oscillations and basically equal, e.g. : the observed differences in the corresponding transit times were lower than 0.1 sec for 80-cm-long rack runs over the whole range of driving motor speeds.

5.5.5. Rack rest position

Repeated observations of series of 20 consecutive oscillations showed dispersions in the values of the actual rest position for the rack with average absolute deviations around 0.5 pulses, or 0.6 mm.

High-amplification recording of the instantaneous rack position during transients showed no significant fluctuation about the rest position.

5.5.6. Oscillation period

It showed an average absolute deviation of about 0.01 sec over a series of 20 consecutive oscillations.

5.5.7. Clutches condition

The dispersion in the values of rack rest position and oscillation period was affected by the thermal conditions of the electromagnetic clutches. Preheating of the clutche by 10 oscillation cycles was verified to yield the asymptot values of dispersion indicated above.

5.5.8. Transversal vibrations of the oscillation tube

The transversal vibrations of the oscillation tube generate by the oscillating fuel element (mainly during the transients)were investigated on an off-pile assembly reproducing the constraints on the tube (see 4.5 and Fig.8)

The characteristic values of the observed vibrations
were : maximum amplitude : 13 μ, frequency : about 25 Hz.

It was concluded that the induced oscillations of the
D_2O free level would have had negligible effect on the
reactivity of ECO, as confirmed by the results of
preliminary in-pile measurements (Ref.Chapter 11).

5.5.9. The results of the off-pile tests reported above showed
that the oscillator performance met the design specifi-
cations (see 5.1), and in some respect was better then
required (e.g. : with respect to the reproducibility
of the rack rest position).

The verification that the operation of the oscillator
according to the design values generated the proper
experimental conditions was carried out through an
extensive series of in-pile preliminary measurements
described in detail in Chapter11.

6.   OSCILLATING FUEL ELEMENT

6.1.   In principle, the oscillating fuel element was a 19-rod
natural U element of the ECO reference lattice, contai-
ning a 50-cm-long test section which, during the square
wave oscillation of the element through the reactor
core, was periodically moved between the two rest positions
"core-mid-plane" ("in" position) and "above the D_2O
critical level" ("out" position).

6.2.   In fact, the actual oscillating fuel element differred
to some extent from the fuel element of the basic lattice
of ECO (Fig.1) in order to meet a number of requirements
of varying nature. These requirements were set by :

a) stresses in the structural materials due to the
   accelerations originating during the transients
   following the "start" and "stop" signals for the
   oscillations, which might have led to deformation
   and/or collapse of the structure or part of it ;

b) connection between test-section and rest of fuel
   element, requiring the use of joints not present
   in the basic fuel element ;

c) experimental requirement that during the oscillation
   cycle the oscillation tube were filled by the fuel
   element over the whole "active" zone of the reactor
   (i.e. : the zone where a material perturbation
   affected the reactor criticality) ;

d) experimental requirement that at the two rest positions,
   "test-section in" and "test-section out", the oscilla-
   ting fuel element configurations relative to the
   reactor were identical over the active zone, except
   for the fuel composition in the 50-cm-long test-section
   (i.e. : the only perturbation to the reactor criticality
   were due to the substitution Pu-U vs. natural U over
   a 50-cm-long section of the fuel, about the core center)

6.3. Condition a) led to a compact mechanical design of the
     fuel element, implying the following modification with
     respect to the ECO basic fuel element (see 4.2.) :
     a.1. Replacement of the liquid organic coolant (diphyl)
          filling the fuel pressure tube with a solid organic
          compound matrix, reproducing the liquid coolant
          volume (i.e. : a cylindrical matrix pierced with
          circular holes closely fitting the fuel rods outer
          diameter).

a.2. Replacement of the 1.5-mm-thick aluminum pressure
tube with a 3-mm-thick zircalloy tube. The super-
imposed segments composing the oscillating fuel
element were maintained alligned in the tube under
an axial compression generated by a threaded plug
from the upper end of the tube.

Thus the tensile stresses, produced by the accelera-
tions originating during the oscillation of the fuel
element, acted only on the high resistance zircalloy
tube, while the compression loads acted on a compact
fuel rods assembly without producing deformation or
collapse of the structure (1).

Condition c) set the overall length of the oscillating
fuel element, so as to fill the oscillation tube over
the whole "active" zone of the reactor during the oscilla-
tion cycle.

The active zone of ECO may be assumed to extend axially
from the critical D_2O free level to the lower end of
the 90-cm-thick graphite bottom reflector, in the sense
that minor material perturbations occurring in such zone
affect the reactor criticality. The D_2O critical height
obviously depends on the lattice pitch and fuel loading
pattern : for the situations investigated its maximum
value was evaluated as 240 cm (corresponding maximum in
the flux axial distribution 130 cm below the D_2O free
level). The maximum height of the active zone considered
was then 350 cm.

---

(1) The fuel rods could not stand important tensile stresses
since they consisted of trains of adjacent U pellets,
maintained together by the 1-mm-thick Al cladding.

The upward translation to transfer the 50-cm-long test
section from the "maximum flux" position to above the
D_2O free level (joints included) was then 232 cm,
resulting in an overall active length of the oscillating
fuel element of 610 cm. The situation is clarified in
Fig.10.

6.5. Condition d) required that, when the 50-cm-long test-
section was in the "out" position, an identical section
containing natural U were in the "in" position.

This led to a design of the fuel element in five segments :
the two identical 50-cm-long segments were separated
by a central segment of proper length, to meet the
above requirement for the maximum value of the fuel
translation, the two outer segments had lengths adequate
to satisfy condition c). The actual fuel segments
had the following U lengths from top to bottom :
145, 50, 175, 50, 173.5 cm (see Fig.10).

Each segment consisted of 19 rods fixed to two end-plates
with the prescribed geometry. The 12-mm-dia fuel rods
were clad by 1-mm-thick Al tubes, with welded-in 10 mm-
thick Al caps provided with a threaded hole for fixation
to the end-plates.

The connection among the five fuel segments was through
their end-plates, which acted also as centering discs
in the fuel containment tube. In order to reduce the
flux perturbation, the plates were made with zircalloy
and their size was the minimum compatible with the mechanic
resistance of the assembly. The thickness of the joint
(two Zr end-plates plus two Al caps of the fuel rods)
was 32 mm.

The two end plugs of the 6-m-long fuel element containement tube were provided with rollers, for centering and guiding the oscillating fuel element in the oscillation tube. The rollers were kept against the tube wall by a double-action spring system.

As assembly view of the oscillating fuel element is presented in Fig.11. Some details of the fuel segments are shown in Fig.12.

6.5. From the point of view of the theoretical analysis of the experimental results, the most important modifications with respect to the ECO reference fuel element were the replacement of :
the liquid organic coolant (diphyl) by a solid organic compound (plexiglass, polystirol);
segments of fuel by Al-Zr joints;
the 1.5-mm-thick Al pressure tube by a 3-mm-thick Zr tube;
the 81.8 mm dia, 1.5-mm-thick Al calandria tube by the 110 mm dia, 6-mm-thick Al oscillation tube.

The substitution "diphyl-plexiglass , polystirol" resulted in a variation in the density and composition of the coolant as indicated in Table 6.1. The correction to the measured reactivity worths to obtain the values for diphyl coolant could be easily carried out by calculation.

The 32-mm-thick Al-Zr joints introduced an appreciable perturbation in the reactor neutron balance, and local flux distribution, but meeting condition d) (i.e. identical lattice configuration with test-section in positions "in" and "out") allowed to eliminate the effect of such perturbation on the experimental results.

The substitution Al-Zr in the fuel element containement tube did not significantly affect the neutron balance, and could be easily accounted for by calculation.

The replacement of the original calandria tube by the larger diameter oscillation tube produced an appreciable modification in the configuration of the lattice central fuel cell (essentially the quantity of D_2O moderator associated with the central cell was less than in the standard lattice cell). Clearly, the modification was more important at small lattice pitches. The calculation developed for the analysis of the experiment included consideration of such lattice anomaly.

7. FUEL TEST SECTIONS

7.1. The fuel under study was assembled in 50-cm-long test-sections, to be inserted in the oscillating fuel element. The test-sections were identical, except for the fuel isotopic composition, to the equal-length natural U segment of the oscillating fuel element (Ref.6.5).

As assembly drawing of the test-section is shown in Fig.13. The 50-cm-long fuel rods were clad by 1-mm-thick pure Al tubes with welded-in Al threaded plugs. The canned rods were fixed to zircalloy end-plates by zircalloy screws. The solid organic matrix, reproducing the liquid coolant volume, was provided with cylindrical holes into which the fuel rods were inserted (0.1 mm clearance), and consisted of a train of 5-cm-long sections snuggly fitted between the end-plates.

7.2. The isotopic compositions of the fuels investiqated
are shown in Table 7.1. The compositions were selected
on the basis of the following requirements

- limit the macroscopic absorption cross section
  variations relative to the natural U fuel cross
  section to few percent, in order to maintain the
  local flux perturbations within the limits of
  validity of perturbation theory (1) ;

- obtain experimental information relative to fuel
  compositions corresponding to a range of burn-up of
  interest for the ORGEL reactor design, i.e. :
  3.000 - 10.000 MWD/T (Pu I and Pu IV) ;

- put in evidence the effect of the Pu^{240} resonance
  capture (Pu I vs Pu II and Pu III vs Pu IV) ;

- provide a set of "reference" fuel samples, whose
  reactivity worths could be accurately calculated from
  primary data, covering the range of reactivities (≥ 0)
  of the fuels under study (UD and UE).

The non-uniform Pu distribution across the actual power
reactor fuel elements, due to the thermal flux depression
in the fuel resulting in higher burn-up at the fuel
periphery (outer ring rods of cluster), was simulated
by mixed test-sections, with the outer-ring fuel rods
having higher Pu content than the inner-ring and central
rods (Pu V and Pu VI).

---

(1) More specifically, at the selected compositions, the
    flux perturbations due to the test-samples were shown
    to be significantly only in their immediate vicinity (6),
    so that the calculation for the interpretation of the
    experimental results could be limited to a macrocell
    surrounding the central fuel element.

7.3. In order to provide test values for the theoretical models used in the treatment of the hydrogeneous coolant, two different solid organic compounds were used to mock-up the fuel element coolant : plexiglass ($C_5H_8O_2$) and polystirol (C_nH_n). The chemical and physical properties of the plexiglass and polystirol used are shown in Table 6.1. The main variation resulting from the substitution plexiglass-polystirol was a 10% change in the hydrogen content of the coolant (atoms/cm^3).

7.4. The extreme case of air coolant was also investigated, at the limits of validity of both perturbation theory and linear reactor kinetics. In order to maintain the overall compactness of the oscillating fuel element, such configuration was obtained by removing the solid organic matrix from the test-section only.

Due also to the resulting mismatch between the composition of the test section and the adjacent natural uranium segments of the oscillating fuel element, this voided-channel experiment was intended only to provide rough data for the prediction of the consequence of accidental voiding of the fuel channel, as well as to test the limits of the experimental technique in view of its future uses.

7.5. Detailed information on the specifications for the fuel rods of the test-sections, as well as on the quality control tests performed, is presented in the Appendix.

8. NEUTRON DETECTION AND SIGNAL RECORDING INSTRUMENTATION

8.1. The primary experimental data were electrical signals proportional to the reactor neutron density level as a function of time, during a cycle of oscillations of the fuel test-section in-out the critical reactor core.

The analyzed data were the ratios of the "amplitude of the first harmonic of the Fourier series expansion" to the "average value" of the primary data. The analysis was performed on a digital computer, by a mathematical code operating on the primary data recorded in digital form on magnetic tape.

In parallel to the digital recording, the primary data were continuously displayed on a multitrack recorder, to visualize the progress of the measurement to the operator's convenience, as well as to provide auxiliary information. Additional data displayed on the recorder were the instantaneous positions of the oscillating fuel element.

The main features of the instrumentation used are summarized below. A block diagram is presented in Fig.14.

8.2. Neutron detection instrumentation

8.2.1. Gamma compensated ionization chamber with following characteristics : size 100-mm-dia, 203-mm-length; coating B^{10} 88% enriched boron; sensitivity 2.10^{-14} A/ $\underline{/}$n/sec.cm^2 $\underline{/}$; range from 10 to 10^9 n/cm^2 s.

The chamber was placed inside a 11-cm-dia radial channel in the 90-cm-thick lateral graphite reflector of the reactor, in the place around the maximum in the axial distribution of the neutron density in the core. Graphite inserts of varying length allowed to modify the distance of the chamber from the reactor axis over a 40 cm range (i.e. from 175 to 215 cm). Reproducibility of chamber radial position : $\pm$ 0.1 mm.

8.2.2. Preamplifier, with impedance adjustement for low noise pick-up to the 15-m-long cable connecting the chamber to the amplifier unit of the general control panel, located inside the reactor control room. A 100 Hz cut-off filter, incorporated in the preamplifier, eliminated the high frequency noise without affecting the 0.017 Hz main signal.

8.2.3. High-speed picoammeter with the following performance : range : 10^{-13} to 10^{-5} A full scale; zero drift : less than 1% of full scale per 8 hours; accuracy : 2% to 3% of full scale; calibrated current suppression : up to 1000 full scales, max. suppression : 10^{-4} A; visual display.

8.3. Digital recording instrumentation

High-accuracy digital measurements of the continuous dc output of the ionization chamber were performed by a DYMEC 2010H data acquisition system, consisting of scanner programmer, integrating digital voltmeter, magnetic tape coupler and incremental magnetic tape recorder, set to the following operation mode : single-channel automatic scanning of dc signal, sampling rate of 5 readings/sec, 0.10 sec reading time, 5 effective digits per reading, data recorded in standard IBM 7-channel 200 bits/inch format.

An exceptionally high degree of noise rejection was
provided through two special design features of
the system. Firstly the voltmeter was average-reading,
thereby greatly reducing the effects of noise super-
imposed on the signal to be measured : at the usual hum
frequencies cancellation of the superimposed noise was
virtually infinite. Secondly errors due to common
mode pickup from "ground" loop currents were reduced
to negligible proportions by guarding. Averaging and
guarding together provided an effective common mode
rejection of 105 db minimum for any noise frequency.

This feature permitted to operate without applying a
backing-off voltage to cancel the constant component
of the signal (average value), thus avoiding the source
of error arising from the instability of the compen-
sating unit.

8.4. Continuous display

8.4.1. The picoammeter output signal was continuously displayed
on a multitrack, self developing, photographic fast
recorder, with the following characteristics : paper
speed : 6 steps from 0.5 to 2000 cm/sec; paper recording
width : 15 cm; max. channels number : 14; galvanometers
natural frequency : 160 cps; frequency range for flat
response : 0-80 cps; electromagnetic damping; continuous
sensitivity adjustement; time marker. The constant
component of the picoammeter signal was suppressed
before display on the recorder.

8.4.2. Also displayed on the paper recorder were :

a) The dc output of the turning potentiometer mounted on the oscillator rack, giving the instantaneous position of the oscillating fuel element (Ref.5.3.3.2). The track reading error was 0.5 mm, corresponding to 7 mm uncertainty in fuel element position for a 2 meter run displayed on the paper.

b) A signal picked-up from the driving unit of the incremental magnetic recorder, which allowed to check the paper recorder speed.

c) The zero line.

A typical four-track record is shown in Fig.15.

9.   FUEL ELEMENT ASSEMBLY CELL AND ANNEX

9.1.   The assembly of the 6-m-long oscillating fuel element was carried out inside a cell, protecting the personnel against the radiation emitted by the element as well as the contamination released in case of accidental breakage of the fuel cladding.

The cell, containing a mechanical system to perform the operations for the assembly/disassembly of the fuel element components, was located in the hall housing the ECO reactor. The fuel element was transferred from the reactor to the cell by remote crane operation.

The cell was a normal-concrete construction (10 m height, 1 x 1 m^2 cross section, 50 cm wall thickness) provided with several protected inlets, and kept under a 8-mm-H_2O depression by a filtered air ventilation system.

The assembly drawing in Fig.16 shows the operation place
(operator protected by a 5-cm-thick lead wall, interior
of the cell viewed through two 20 x 20 cm lead-glass
windows, fuel handling made using heavy rubber gloves),
the vertical tube for the fuel element insertion, the
350-kg crane, the equipment for the assembly/disassembly
of the fuel element components.

9.2. Schematically, the fuel assembly system consisted of
a wheel rotating about a vertical axis and provided with
a crown of circular cavities, inside which the segments
of the oscillating fuel element were separately hung.
This operation was carried out by crane, rotating the
wheel so as to present a free cavity on the crane axis.
The assembling was performed inserting in the zircalloy
pressure tube, also hanging through a cavity of the
wheel, the fuel segments, which were connected at the
end-plates by screwed-in joints. Finally the zircalloy
pressure tube was closed with a threaded plug, keeping
the train of fuel segments under axial compression.

9.3. The assembly of the 50-cm-long, Al-clad, Pu-U rods
into sections was carried out inside a hood, housed
in a sealed plexiglass-aluminum room (4-m-high x 2.5-m-
large x 4.5-m-long) connected to the assembly cell
through a protected passage. The room and the hood
were kept under depression of 6 mm H_2O and 15 mm H_2O,
respectively, by a filtered air ventilation system.

The sealed room also housed a glove box (15 mm H_2O
depression), to be used for handling the Pu-U test
sections contaminated following an accidental rupture
of the fuel cladding. A top view of the assembly cell
and related facilities is shown in Fig.17.

D E S C R I P T I O N   OF   E X P E R I M E N T   AND   R E S U L T S

10.   EXPERIMENTAL PROCEDURE

10.1. The following is a description of the experimental
      procedure. For completeness it contains also some
      information presented in the previous chapters.

      The experimental cases are listed in Table 10.1.
      They included six different test-samples (Pu I to Pu VI),
      two "reference" samples (UE and UD), two organic
      coolants with different hydrogen density, as well as
      air coolant, three (ECO) lattice pitches (18.8, 23.5
      and 28.05 cm).

      The compositions of the test-samples were selected
      so as to : provide reactivity values over a range of
      fuel burn-up of interest for ORGEL type reactors
      (i.e. : 3.000 - 10.000 MWD/t; samples I and IV),
      put in evidence the effect of the Pu^{240} resonance
      capture (samples I vs. III and II vs. IV); study more
      realistic situations characterized by a nonuniform
      distribution of the Pu content in the cluster (samples V
      and VI), provide a set of reactivity standards (or
      reference values) for the interpretation of the reactor
      oscillation experiments (samples UE and UD).
      The compositions of the test-samples are listed in
      Table 7.1.

The variation of the hydrogen content in the solid
mock-up of the organic coolant (plexiglass, $C_5H_8O_2$,
and polystirol, C_nH_n, with H_2 densities 5.37 and
$4.86.10^{22}$ atoms/cm^3, respectively) was intended
mainly to provide data for a test of the theoretical
model used in the treatment of neutron scattering by
the coolant.

10.2. During the experiment, the lattice of the ECO reactor
consisted of a fixed number of fuel elements, namely
88 19-rod natural U metal clusters. Thus only at the
lattice pitch 28.05 cm the fuel elements arrangement
completely filled the core vessel cross section, while
at pitches 23.5 and 18.8 cm a D_2O moderator layer of
increasing thickness existed between the lattice boundary
and the core vessel wall (Fig.18). This situation was
easily accounted for in the theoretical calculation.
Incidentally, the number of fuel elements was kept
constant due to the considerable difficulties which
would have arisen in the fuel loading operation, once
the oscillator assembly was installed on the reactor
top plates.

The average temperature of the D_2O moderator was recorded
before and after each measurement. The observed variation
was in general less than .1°C. Both this variation and
the spread in the D_2O temperatures over the complete series
of measurements (±1.5°C) did not affect in an appreciable
way the experimental results (from the consideration of
the typical features of the reactor oscillation method,
see Chapter 3).

The axial distribution of the thermal neutron density
along the oscillation tube, at the three selected lattice
pitches, was determined by activation of bare and cadmium
covered Mn detectors. The measured distributions, shown
in Fig.19 (typical experimental error $\pm 1\%$), allowed to
localize the maximum in the flux and to evaluate the
order of magnitude of the experimental error following
an incorrect positioning of the test section in the
reactor core. In fact the distribution was rather flat,
with a $\pm 5\%$ variation over the range ± 25 cm around the
flux maximum.

10.3. The oscillating fuel element contained the test-section
and an identical natural U section, respectively in the
upper and in the lower position (see 6.5). The element,
coupled to the oscillator rack, was introduced in the
oscillation tube (reactor shut-down, no D_2O in), untill
the test-section mid-plane coincided with the flux
maximum in the axial distributions of Fig.19. The D_2O
critical level was determined through a standard approach
to criticality.

Prior to each oscillation experiment the curve "reactivity
value of the oscillating fuel element versus axial position
of the element in the oscillating tube" was experimentally
determined for a range extending over the foreseen oscilla-
tion amplitude (or : run). A typical reactivity curve
of this kind is shown in Fig.20.

These curves were used to : define the correct value
of the test-section "in core" position (the position
corresponding to the maximum or the minimum in the curve),
to establish in the first approximation the reactivity
value of the test-section relative to natural U fuel
(the difference between maximum and minimum in the curve)
as a check on the reactivity value measured with the
reactor oscillation method, to verify the general
features of the reactivity signal during the oscillation.

The reactivity value of the oscillating fuel element at
varying position in the core was inferred from the
corresponding variation in the D_2O critical levels, on
the basis of a previously established relation between
reactivity and D_2O level variation (pcm/mm D_2O). Such
relation had been derived from measurements of the
stable reactor periods corresponding to varying D_2O
level steps, starting from the critical state, through
the standard "in-hour" equation with adjusted parameters
(see 3.2).

Mainly due to the special features of D_2O moderated
systems (photoneutron production, etc.), the accuracy
of the above measurement was lower, by a factor estimated
around 20, than that of the corresponding reactor
oscillation measurement (see 3.2 and 3.3).

At the lattice pitches 18.8, 23.5 and 28.05 cm the measured
reactivity values of the mm D_2O were 2.3+.5, 4.9∓.5 and
3.9∓.5 pcm/mm respectively. The typical overall error
in the data points of Fig.20 was estimated as ±0.4 pcm
(the typical overall experimental error in the reactor
oscillation measurement was ±0.02 pcm).

10.4. The values for the parameters characterizing the periodic
oscillation of the test fuel element were chosen on the
basis of the results of the preliminary off-pile and in-pile
tests, described in some detail in chapters 5 and 11,
respectivelv. Two sets of parameters were used for the
complete series of measurements, as shown in the table
below :

	set 1	set 2
period of the oscillation	60 sec	60 sec
run	2320 mm	2320 mm
transit speed	1 m/sec	0.50 m/sec
transit time	2.2 sec	4.4 sec
reactor power	50W	50W

Both sets represented a satisfactory compromise among the
opposing requirements of the experiment. The second set,
characterized by a lower transit speed, was used for the
last series of measurements in order to reduce the stresses
in the oscillating fuel element.

10.5. The reactor was stabilized critical at about 50 W power,
the oscillating fuel element being in the oscillation tube,
with the test-section at the correct "in-core" position.

After starting the oscillation of the fuel element in the
mode defined by the selected set of parameters, the D_2O
moderator level was brought to the value midway between
the critical levels corresponding to the positions test-secti
"in core" and "out core", and subsequently adjusted untill
the average reactor power was stabilized at 50 W.

Meanwhile the amplitude of the fuel element oscillation
and the effective oscillation period were set to the
correct value, by the fine adjustement of the preset
"upward" and "downward" run relative to the reference
position and of the preset "rest time", respectively
(see 5.3.2.).

It is reminded (see 6.5.) that the oscillation amplitude
was so selected that, when the test-section was in the
"in-core" and "outside the reactor" (above the D_2O level)
position, the identical natural U section was outside
(below) the reactor and in the "in-core" position,
respectively (Fig.10). Neglecting the transit times,
the reactor core configuration (and thus the reactivity)
was equal for the states test-section "in" and "out",
except for the replacement of a 50-cm-long section of
the central fuel element by an identical test-section with
different fuel composition. The analysis of the reactor
oscillation experiment yielded directly the reactivity
effect of such replacement, referred to as "reactivity
value" or, alternatively "reactivity worth" of the test-
section.

Second order reactivity effects, due to non uniformity
of the oscillating fuel element (e.g. in axial distribution
of effective fuel density, fuel rod diameter, rod-to-rod
spacing, Zr joints mass, etc.), were cancelled out by
subtracting from the measured "reactivity value" of the
considered test-section the "reactivity value" determined
for a natural U test-section placed at the same position
in the oscillating fuel element. Since the reactivity
worth of natural U was null by definition, the measured
value was in fact the reactivity difference between the
two rest positions of the oscillating fuel element, due
to the above mentioned non uniformity. Such reactivity
effect was typically 1 pcm at pitch 23.5 cm.

10.6. Having achieved the correct experimental conditions, the actual measurement was carried out by collecting the following data :

1. "Upper" and "lower rest positions of the oscillating fuel element, in terms of the readings of the digital encoder, at each cycle. Accuracy of reading : 1 digit, corresponding to ± 0.393 mm displacement.

2. Effective value of the oscillation period, at each cycle, Accuracy of reading : 0.01 sec.

3. Instantaneous position of the fuel element during the oscillation, continuously displayed on a fast paper recorder. Accuracy of fuel position reading : 10 mm.

4. Modulation of the neutron density in the reactor, as detected by the compensated ionization chamber placed in the reflector, continuously displayed on a fast paper recorder after substraction of the constant component of the signal.

5. Modulation of the neutron density in the reactor as detected by the ionization chamber, converted to digital form and recorded on magnetic tape. The DYMEC-2010 H Data Acquisition System used was set to the following operation mode : automatic single-channel scanning of the d.c. output of the ionization chamber, sampling rate of 5 readings per sec, 0.10 sec reading time, 5 effective digits per reading, data recorded in standard IBM, 7-channel, 200 bits per inch format, record length 500 words.

6. Pulses corresponding to single readings (see above) and to "end-of-record" signals, displayed on fast paper recorder.

More details about the features of the equipment used
are presented in chapter 8. Prior to use the components
of the equipment were tested to be in proper operating
conditions by standard routine checks. A typical record
of signals 3, 4 and 6 its shown in Fig.15 (sample Pu II).

The data were collected over a series of (usually) 24 test-
section oscillations, lasting 24 minutes (= one measurement).
The primary data, i.e. the modulation of the neutron density,
were grouped on the magnetic tape in (usually) 15 "records",
each containing the information relative to 1.5 test-section
oscillations.

10.7. The records were analysed by a mathematical code, based on
numerical integration methods, following the scheme reported
in the Appendix. The calculation, carried out record by
record, yielded the value of the amplitude of the first
harmonic (fundamental) in the Fourier series expansion of
the periodic neutron density signal generated by the
oscillatioh of the fuel test section in-out the critical
reactor core ($=\Delta n$), as well as the mean value of the same
signal during each analyzed oscillation period ($= n$).

The experimental result was thus the ratio $\frac{\Delta n}{n}$, proportional
(see chapter 2) to the reactivity introduced in the ECO
reactor by the replacement of a 50-cm-long section of the
natural U fuel element at the core center with an identical
test section with different fuel composition.

The treatment of the data included : correction for linear
drift in the reactor neutron density, evaluation of the
linear drift coefficient, evaluation of the mean value and
of the standard deviation of the 15 results ($= \frac{\Delta n}{n}$) of
the measurement.

10.8. The other data recorded (data type 1,2,3,4,6) allowed to have a continuous display of the characteristic parameters of the experiment, in order to verify the correct operation of the equipment, as well as to derive auxiliary information, as phase angle between test-section oscillation and neutron density modulation.

11. PRELIMINARY MEASUREMENTS AND ERROR ANALYSIS

11.1. An extensive series of preliminary measurements was carried out in ECO, in order to :

1. verify that the off-pile tested oscillator performance (see 5.5) met the experimental requirements ;

2. investigate the sources of experimental error (both random and systematic) and estimate the overall experimental uncertainty ;

3. optimize the free parameters of the experiment, so as to establish the most suitable experimental routine (see 10.4) ;

4. investigate the general features of the experimental technique, in view of further applications.

11.2. The different sources of error considered were :

Reactor   Noise; reactivity drifts (due to imperfect initial reactor balance or to varying external causes, as temperature and pressure); uncertainty in lattice geometrical configuration (e.g. : lattice pitch).

<u>Oscillator</u>	Uncertainty in the preset values, as well as fluctuations during operation, of : position of test-section in reactor core, oscillation-period, test-section transit time.
<u>Oscillating fuel element</u>	Reproducibility of geometric arrangement of the test-fuel rods in the cluster assembly; mass differencies in structural materials of test-sections (Zr end-plates, solid organic matrix, Al cladding); uncertainty in the position of the test section in the oscillating fuel element assembly; end-of-run damped oscillations.
<u>Oscillation tube</u>	Transversal vibrations, generated by the oscillating fuel element and transmitted to the D_2O moderator.
<u>Neutron detection and signal recording equipment</u>	Radial position of ionization chamber; drifts in components of neutron density measuring channel (e.g. in the "zero" of the d.c. amplifier unit); integration time of single reading for digital conversion; fluctuations in frequency.
<u>Oscillator control instrumentation</u>	Inaccuracy in the determination of oscillation period, test-section transit time, test-section position in core, oscillator motor speed.
<u>Data analysis</u>	Discontinuous record of the neutron modulation signal; correction for linear drift of reactor power.

11.3. Of paramount importance were the tests aimed to verify
that the selected experimental arrangement was not affected
by appreciable systematic errors. For instance, there was
some concern about the correct positioning of the ionization
chamber detecting the neutron density modulation;
Such a position, by the definition of the experimental metho
must be where the local perturbation of the neutron density
distribution in space and energy caused by the test-sample
had reduced to a negligible value (see chapter 2).

The test-sections investigated were varying mixtures of
fissile and absorbing materials. Since fissile and absorbin
samples cause local perturbations which propagate in the
reactor core in a different way, the corresponding residual
perturbations at the ionization chamber location might
appreciably differ in magnitude for the different samples.
As there was some evidence that this could be the case,
a test was carried out by measuring different fissile and
absorbing test-samples with the ionization chamber placed
at varying distance from the core axis.

11.4. The fourth type of tests (see 11.1) was intended to
explore the flexibility of the technique, in view of its
use under more severe conditions. The main concern was
for the problems associated with the oscillation of fuel
elements of lower mechanical resistance, as fuel in the
oxide state, with liquid coolant, or maintained at rela-
tively high temperature (for the determination of the
temperature coefficient of reactivity). In this respect
it was of interest to investigate the possibility of
reducing the stress on the oscillating fuel element by
decreasing the transit speed and thus the end-of-run
accelerations, keeping the oscillation period constant.

It was evident that the resulting reduction of the "rest time/transit time" value of the oscillation would (in principle) negatively affect the experimental accuracy, due to the increase of the relative importance of that part of the signal generated during the transient which was not proportional to the reactivity worth of the test section (i.e. : signal due to the translation of the zirconium joints). This effect would set a limit to the decrease in the transit speed of the oscillating fuel element.

On the other side, maintaining constant the "rest time/transit time" value by a proper increase of the oscillation period, would have augmented the relative importance of the correction to the data for possible reactor power drifts, eventually reaching the situation where the drift could be no longer approximated by a linear function. It is reminded that the model used for the interpretation of the experimental data completely eliminated the effect of the power drift, provided it was linear.

Although being extensive, the series of tests performed was not exhaustive, mainly due to the lack of reactor time. The performed tests are described below, classified according to the oscillation parameter considered. The results are generally presented in detail in tables and figures. The overall conclusion drawn from the tests is stated at the end of the chapter.

11.5. In-core rest position of the test-section

The estimated uncertainty in the selected value of the rest position was +2 mm; the observed spread of values during one series of oscillations (see 5.5.5.) was +0.6 mm.

The tests consisted in oscillating several fuel samples with "in-core" positions in the range ± 10 cm around the correct value. The oscillation of natural U test-sections with low reactivity values, put in evidence the importance of a correct position with respect to the reactivity worth of the Zr joints of the oscillating fuel element.

The results of a part of these tests are presented in Tables 11.1 and 11.2. The error caused by a ± 1 cm variation from the correct in-core rest positions was slightly above the combined experimental uncertainty of the measurements at the two positions (typically : 4×10^{-5} vs $3 \times 10^{-5} \frac{\Delta n}{n}$). A ± 5 cm variation introduced an error of the order of 1% of the correct reactivity worth of a typical test-sample.

It was concluded that the effect of operational fluctuations in the value of the test-sample in core rest position during one experiment, as well as of "probable" errors in the selection of the correct position, was definitively negligibl Only gross errors (e.g. ± 5 cm) could appreciably affect the experimental results.

11.6. <u>Oscillation period</u>

The estimated uncertainty in the selected value of the oscillation period was ± 0.02 sec (the period was not selected directly, but resulted from the preset parameters : rack rest time, amplitude of rack translation, driving motor speed : see 5.3.1.). The observed fluctuations during extended series of oscillations were contained to within ± 0.01 sec (5.5.6.).

Two series of tests were performed : the first, to verify
the effect of the above "instrumental" uncertainties,
consisted in varying the oscillation period ± 0.6 sec around
the correct value; the second test, to obtain indications
on the influence of the choice of the period on the experi-
mental accuracy, consisted in changing the rack rest time
(at constant rack speed and translation amplitude of
1 m/sec and 204 cm, respectively) so as to vary the oscilla-
tion period from 40 to 80 sec.

The results of the first test, presented in Table 11.3 showed
the negligible contribution of the sources of error linked
to the instrumentation (often referred to as operational
errors). In fact the mean relative variation of $\Delta n/n$
observed for a 0.4 sec change in the oscillation period being
0.3%, the error in $\Delta n/n$ corresponding to the instrumental
uncertainty in the period of ± 0.02 sec was of the order of
$\pm 0.015\%$.

The results of the second test (Table 11.4) indicated that
the oscillation period could be increased to the maximum
preset value of 80 sec, without incurring in non linear
reactor power drift phaenomena (i.e. : since the linear
drift correction included into the data analysis code was
adequate to equalize the results of measurements at varying
oscillation period to within the standard experimental
uncertainty of $2 \times 10^{-5} \Delta n/n$).

11.7. Test section transit time

The transit time of the test-section resulted from the
selection of the proper driving motor speed for the given
translation amplitude : the corresponding estimated uncertainty
was $\pm 2\%$ of the nominal value, i.e. ± 0.04 sec in the transit
time for a 100-cm-long translation with transit speed
1 m/sec.

Actually the value of the transit time could be approached
to the correct value to within 0.01 sec, by adjusting the
motor speed so as to obtain the required oscillation period
with fixed rest time.

Two series of tests were performed : the first, to verify
the effect of the above uncertainties, consisted in varying
the transit time $\pm$0.1 sec around the correct value;
the second test, to investigate the influence of important
variations of the "rest time/transit time" value in view
of reducing the transit speed and thus the accelerations
of the oscillating fuel element, consisted in varying the
transit speed from 1 to 0.2 m/sec, with constant oscillation
period and translation amplitude (60 sec and 204 cm,
respectively).

The results of the first test (not reported) showed the
negligible effect of the sources of error relative to the
instrumentation.

The results of the second test are presented in Table 11.5.
Over the range of transit times from 2.2 to 6.5 sec,
corresponding to "rest time/transit time" values from 12.6
to 3.6, the reactivity worths of the fuel samples considered
were essentially constant within the typical experimental
error. At transit speeds lower than 0.25 m/sec the d.c.
motor became unstable.

It was concluded that satisfactory experimental conditions
were obtained at the lowest tested (stable) transit speed
of 0.33 m/s, and could probably be achieved even at lower
speeds (once the oscillator motor were properly modified.
for stabilization at these speeds), provided the oscillation
period were increased to the higher tested values (see 11.6).

11.8. Ionization chamber position

Since fissile and absorbing samples cause local neutron
flux perturbations which propagate differently through
the reactor core and reflector, residual flux perturbations
at the ionization chamber location can introduce a systematic
error in the experimental data (see 10.3). The magnitude
of the error is clearly position dependant, and can be put
into evidence by measuring fissile and absorbing samples
with the ionization chamber placed at different radial
positions.

To verify that no significant flux perturbation caused by
the test section still existed at the ionization chamber
location, the distance from the core axis of the chamber
placed in the lateral graphite reflector, was varied in the
range from 175 to 215 cm. For this test the oscillation
period was 60 sec, the transit speed 0.5 m/sec, the lattice
pitches 23.5 and 28.05 cm, the fuel samples considered were :
Pu III (positive reactivity signal, fission prevailing),
Pu IV (negative reactivity signal, capture prevailing), UN.

The results of the test, are presented in Table 11.6.
Since the experimental data $(\Delta n/n)$ are independent of the
chamber location (typically within 0.15% and with no
preferential trend in the variation), there is strong
evidence that the systematic error due to flux perturbations
about the ionization chamber is indeed negligible. In fact
an appreciable error caused by perturbation phoenomena
of this kind would produce a space-dependant experimental
result when comparing fissile and absorbing samples.

11.9. Test-section assembly

Since the test-sections were segments of the oscillating
fuel element including Al canning, solid organic matrix
and Zr end-plates, systematic errors could be introduced
in the experimental results due to differences in the masses
and/or geometries of such structural materials.

In order to limit the magnitude of this error to negligible
values, great care was taken to equalize the structural
materials in the various test-sections by proper design
specifications and quality control tests (see Chapter 6 and
the Appendix).

In fact all the test-sections oscillated were assembled
using only two sets of Zr end-plates and solid organic
matrices. The relative masses differred by 0.1 gr (Zr)
and 2.3 g (plexiglass). The effect of such mass difference
was experimentally determined measuring the same fuel sample
in the two assemblies. The sample selected for the test
was UN for which the absorption in the structural materials
is relatively more important. The oscillation parameters
were : period 60 sec, transit speed 1 m/sec.

The results of the test, shown in Table 11.7, indicated a
$20.10^{-5} \, \Delta \eta / \eta$ effect due to the structural material
replacement, corresponding to about $1\%_0$ of the signal for
a typical Pu-U test-section. Consequently all the experiment
data relative to fuel samples with plexiglass mocking-up the
coolant were normalized to the same Zr-plexiglass structure
using the data of Table 11-7. A similar normalization was
made for the data relative to the fuel samples with the
polystirol matrix.

The weights of the Al canning of the rods of the test-sections were inferred from accurate measurements of the weights of the bare and canned fuel rods. The average canning weight of each set of test-fuel rods, with the standard deviation relative to the weight distribution of the canning of the set, is given in Table 11.8. It was concluded that the minor weight difference observed could not have any appreciable effect on the experimental results.

Another source of systematic error in the experimental data could have conceivably been the uncertainty in the test-section geometry following the mechanical tolerances of the structure. In order to investigate this situation some test-sections were measured twice (at several lattice pitches) having completely disassembled the cluster segments between the two experiments.

The results of the test are reported in Table 11.9. The reproducibility of the results was between 0.06 and 0.6%, except for the Pu III sample. The 1% to 3% discrepancy observed for the results relative to the test-section Pu III was about òne order of magnitude larger than any experimental error observed in all the tests. It was therefore ascribed to some gross error (not detected) in the performance of the test. Due to lack of reactor time this test could not be repeated.

11.10. Lattice pitch

The pitch of the fuel elements lattice in ECO could be continuously varied by a remotely controlled mechanism. The reproducibility attainable, relative to the selected pitch value, was nominally around ± 0.1 mm, averaged on the whole lattice.

The importance of the correct assessment of the lattice pitch appeared from the observed dependence of the experimental results $(\Delta n/n)$ on the value of the pitch, as reproduced for a typical sample (Pu II) in Fig.21.

At the three selected pitches of 18.8, 23.5 and 28.05 cm the measured $\Delta n/n$ values were $2.83.10^{-2}$, $4.94.10^{-2}$ and $5.41.10^{-2}$, respectively. The slope of the typical curve " $\Delta n/n$ vs. pitch" was steeper at low lattice pitches : thus at pitch 18.8 cm to a ± 0.1 mm error in the lattice-averaged pitch corresponded a $\pm 0.4\%$ error in the measured $\Delta n/n$ value of the test-section.

The effect on the experiment of the reproducibility of the lattice pitch was verified by repeating several times the same experiment, having modified and then fixed again to the correct value (18.8 cm) the lattice pitch in-between successive measurements.

The results of the test, presented in Table 11.10, showed that the error due to the uncertainty in the lattice pitch value did not increase the margin of error relative to a single measurement at fixed pitch, even in the most sensitive situation, i.e. : lattice pitch 18.8 cm.

11.11. Reactor noise

The reactor power fluctuations (reactor noise), following the statistical nature of the neutron reactions, introduce an error in the experimental data obtained from reactor oscillation experiments, which becomes more important at low reactor power, i.e. when the rate of neutron events is lower (3,4).

In order to appreciate the magnitude of the error due to
the reactor noise as well as to the noise of the neutron
detection instrumentation a test was performed, consisting
of recording the neutron density vs. time at constant
reactor power, and subsequently analyzing the data by
the code used for the interpretation of the reactor
oscillation experiments.

The mean square deviation of the average $\Delta n/n$ value from
10 records, each extending over a hypothetic 60 sec.
period oscillation, was taken as an index of the overall
error introduced in the (reactor oscillation) experimental
data by the reactor and instrumentation noise. The
results of the test, carried out at reactor powers from
10 W to 60 watts, are presented in Table 11.11.

The error due to noise decreased asymptotically over the
considered power range. The 50 W power level was selected
for all the oscillation experiments, in consideration of
the fuel activation problems which could have arisen
operating the reactor at appreciably higher power levels.

11.12. Oscillations cycle

A standard reactor oscillation measurement consisted of a
series of 15 records. Each record, containing the data
relative to one oscillation period, was separately
analyzed for the determination of the value $\Delta n/n$; the result
of the measurement was the average of the $\Delta n/n$ values
inferred from the 15 records, with associated the standard
deviation corresponding to the distribution of the single
$\Delta n/n$ value about the mean.

In order to verify whether an extension of the number
of records per measurement would result into an appreciable
reduction in the dispersion of the results, a test was
performed collecting 45 records per measurement. The
results of the test, presented in Table 11.12, showed
no significant decrease in the value of the standard
deviation of the mean with respect to the measurement
collecting 15 records only.

11.13. Discontinuous record of the neutron density modulation

The continuous output of the ionization chamber measuring
the neutron density modulation in the reactor was
converted to digital form, with a sampling rate of 5
readings/sec, and reading (integrating) time of 0.1 sec.
Thus the data analysis code operated on a discrete (i.e.:
discontinuous) set of values, averaged over 0.1 sec
and spaced at 0.2 sec intervals, rather than on the
original continuous signal.

By calculation (presented in the Appendix) it was proved
that, for the selected experimental conditions (300
averaged data over the 60 sec oscillation period), the
value of the amplitude of the first harmonic in the
Fourier expansion of the neutron density modulation
was not (appreciably) affected by the above approximation.

11.14. The above described series of tests is considered to
represent an extensive investigation of the sources of
error, both systematic and random, relative to the experimen

Other sources of error than these individually studied,
were estimated by calculation to negligibly affect the margi
of uncertainty of the experimental data.

In fact, the error contributions from some of these sources (as D_2O moderator temperature variations during the oscillation experiments, transversal vibrations of oscillation tube transmitted to the D_2O moderator, etc.) were included in the overall uncertainty of the results of the tests, and thus could be globally evaluated.

For the purpose of the error analysis the experiments were divided into two classes : "single-experiment", consisting in a series of oscillations of one assembled test-section and yielding a standard set of 15 analyzed oscillation periods, i.e. 15 values of $\Delta n/n$ (Δn = amplitude of the first harmonic in the Fourier expansion of the recorded neutron density modulation signal; n = mean value of the neutron density signal during one oscillation period); "repeated experiments", consisting of the repetition of "single experiments" spaced in time and with test-sections completely reassembled for each test.

11.15. The dispersion of the 15 (=N) data of a "single experiment" was analyzed in terms of a normal distribution, yielding the mean square deviation of the mean,

$$\sigma = \left\{ \frac{\sum[(\overline{\Delta n/n}) - (\Delta n/n)]^2}{N(N-1)} \right\}^{1/2}$$

This error index included the full contribution of such error sources as : fluctuations and/or drifts during the experiment of reactor power, neutron detection instrumentation, data recording frequency, oscillation period, test-section transit time and rest position; reactor noise; transversal vibrations of oscillation tube, etc.

By artificially varying some oscillation parameters over
proper intervals, it was possible to evaluate the experi-
mental uncertainty following "probable" errors in the
selection of : oscillation period, oscillator motor speed,
test-section rest position and rest time, etc.. It was
verified that "operational" errors of this kind (i.e.
likely to occur during the performance of the experiment)
did not appreciably increase the margin of error typical
of the "single experiment" and that gross errors in the
assessment of a main oscillation parameter were needed
to affect the experimental results. For example :
a ± 5 cm error in the in-core rest position of the test-
section resulted in $\pm 0.5\%$ error in the measured reactivity
worth of a typical sample; however the upper limit of the
corresponding "operational" error was ± 0.25 cm and did not
modify the uncertainty of the result of the "single
experiment" (see Tables 11.1 and 11.2).

When expressed in terms of the mean square deviation of
the mean of a standard set of 15 experimental data, the
error of the "single experiment" was typically $2.10^{-5} \frac{\Delta n}{n}$.
The magnitude of the error was independent of the amplitude
of the recorded reactor neutron density modulation.
The corresponding reactivity uncertainty was, for the three
lattice pitches considered (18.8, 23.5, and 28.05 cm),
around 0.01 pcm. Relative to the reactivity worths of
the bulk of the test-sections investigated (10 to 40 pcm)
the experimental error was thus in the range from 0.1 to
0.025%.

11.16. The "repeated experiment" permitted to appreciate the
error contributions from the test-section "assembly",
such as : uncertainty in test-section geometry due to
mechanical tolerances, variations in the mass of
structural components and in the position of the test-
section in the oscillating element, as well as the error
contributions from the installations of the oscillator
on the reactor.

It was verified that the repetition of the experiment
increased the uncertainty of the result of the "single
experiment" by about a factor of 3 (see Table 11.9).
The corresponding relative error was however still below
$\pm$0.15% for the typical fuel test-section (the error due
to the mechanical tolerances in the test-section design
is roughly proportional to the reactivity worth of the
test section).

Since the error following the uncertainty in the Pu-U alloy
composition of the samples used was appreciably higher
than the above experimental error, there was no immediate
interest for attempting to reduce the error of the
"repeated experiment" [1]. However, taking into account
the complexity of oscillating fuel assembly, mechanical
oscillator and associated equipment, the "overall"
experimental uncertainty attained (typically $\pm$0.15% of
the measured value) was considered remarkably small.

11.17. The investigation of the sources of systematic error led
to the conclusion that neither the experimental method
nor the equipment entrained appreciable systematic errors.

---

(1) Actually the error could have been substantially
diminuished (probably by a factor of about 2) simply
by "repeating" many times the same experiment. This
lengthy test was not carried out due to lack of reactor
time.

The "repeated experiment" error which is associated to
the mechanical tolerance in the fuel element design,
is specific to the particular fuel element investigated
(essentially is an increasing function of the complexity
in the geometry of the fuel element) and cannot be
considered typical of the oscillation experiment.

Thus the error analvsis for the reactor oscillation
experiment described in this report led to the estimate
of an error for the "single experiment", which was
representative of the uncertainty inherent to the expe-
rimental equipment and method (including the data analvsis
procedure) but neglected the source of error represented
bv the fuel element assembly, and of an error for the
"repeated experiment", which was specific to the fuel
element assembly actually studied.

The two errors were estimated to be, respectively,
$2.10^{-5} \Delta n/n$ (or 0.01 pcm) and $3.10^{-5} \Delta n/n$ (or 0.015 pcm)
(see foot note before). In consideration of the massive
and complex experimental equipment used, these errors
are considered remarkably little, being in fact close
to the lowest limit of error observed in reactor oscilla-
tion experiments with small samples (i.e. little weight,
no geometrical complexity, small and simplified sample
oscillator, etc.).

11.18. The high accuracy of the results, maintained even for
small reactor modulation signals, makes the experimental
technique particularly suited to the investigation of
differential reactivity effects, such as those from
variations in density or composition (basically hydrogen
content) of the coolant, temperature of fuel element
or fuel channel, etc.

The test performed to investigate the flexibility of the experimental technique, in view of this new application, indicated that the test-section transit speed could be significantly reduced, eventually increasing the oscillation period to about 120 sec, without affecting the precision of the experimental results (see 11.6, 11.7).

Operating at transit speeds around 0.2 m/sec and with an improved shock-absorbing device, the stresses in the oscillating fuel element would be greatly reduced, and a less compact design of the element should be possible, abbandoning the "solid coolant" concept.

This observation opens the way to "liquid coolant" solutions of different type, permitting to measure the reactivity effects of varying temperature and hydrogen density of the coolant. An extensive series of tests on mock-ups would however be required, to verify the validity of the solution proposed, which depends to a large extent on the features of the particular fuel element considered.

12. EXPERIMENTAL RESULTS

12.1. The experimental results are presented in Fig.22 to 26 and Tables 12.1 to 12.6.

The Figures 22 to 26 are smooth curves through the measured reactivity worths (relative to UN fuel) of the fuel test-sections Pu I to Pu VI, UD and UE, plotted versus the ECO lattice pitch.

Specifically the results are : test-sections in plexiglass
relative to UN in plexiglass (Fig.22), test-sections in
polystirol relative to UN in polystirol (Fig.23), test-
sections in polystirol relative to UN in plexiglass
(Fig.24), test-sections in air relative to UN in air
(Fig.25), test-sections in air relative to UN in plexiglass
(Fig.26).

The same data are listed in Tables 12.1 to 12.5, with the
corresponding overall experimental error. The error was
evaluated by adding to the error of the "single experiment"
an average value for the "repeated experiment" error
contribution, as inferred from the results of the test
presented in Table 11.9. It is reminded that the "repeated
experiment" error contribution results mainly from the
mechanical tolerances in the design of the fuel test-section
(Ref.11.16).

This error was typically $3.10^{-5} \frac{\Delta n}{n}$ or 0.015 pcm. The
corresponding relative error was from 0.1% to 0.025%,
for the measured reactivity worths in the range from 10
to 40 pcm.

The anomalous uncertainty quoted for the test-section Pu III
is explained in 11.9. In fact the quoted total error could
have easily been reduced by a factor of at least two,
simply by carrying out a series of "repeated experiments"
(Ref.11.9). This was not done, due to lack of time, in
view of the fact that the error associated with the uncer-
tainty in the Pu-U fuel composition was substantially higher
than the experimental error.

12.2. A comparison between the results of the reactor oscillation experiments and of the reactivity measurements by the static method outlined in 3.2 and 10.3 is presented in Fig.27 to 29, for the ECO lattice pitches 18.8, 23.5 and 28.05 cm, respectively.

The co-ordinates of the diagrams are the values obtained by the oscillation measurements (ordinates), expressed as $\Delta n/n$ x 10^2, and the corresponding values measured by the static procedure (abscissas), expressed in pcm i.e. Δk x 10^{-5}. To each test fuel measured corresponds a point in the diagram. Provided that the assumption of linearity of the reactor response to small perturbations is valid for the fuel test-sections investigated (see 7.2), the points should be aligned within the combined experimental errors, and the straight line fitted to them should pass through the zero of the co-ordinates system.

It is reminded that the typical error of the static measurement is about one order of magnitude larger than the error of the oscillation experiment (see chapter 3). Thus the alignement of the data points would represent only in the first approximation a test for the consistency of the experimental results. Evidently, the test would put into evidence gross errors in the performance of the oscillation experiments.

Straight lines ($y = a\,x + b$) have been fitted through the experimental points by the least square method. In general the spread of the single data points from the line is within the limits of the experimental error, and the lines are through the origin of the co-ordinates system.

In fact the alignment of the points is better than what
expected from the estimated error of the static measurements
It is of interest to note that the linearity is conserved
even for the highest reactivity worths measured (140 pcm).

On the basis of the satisfactory result of the test, the
curves of Fig.27 to 29 were used to infer the absolute
values for the reactivity worths of the test fuels. With
as entry the measured $\Delta n/n$ value of the test-section
(zero error assumed), the corresponding reactivity worth
in pcm was read as the abscissa of the intersection with
the straight line fitted through the data points.

The uncertainty of the absolute reactivity worth thus
obtained was estimated by elementary considerations, using
the basic data for the error of the single static measu-
rement given in 3.3 and 10.3, as ± 0.4 pcm. The corresponding
relative error was 4% to 1%, over the range of the measured
reactivity worths (from 10 to 40 pcm). The error in the
absolute reactivity values is thus over a factor of twenty
higher than the error in the corresponding relative value,
$\Delta n/n$ (see 11.17).

The information provided by the absolute reactivity values
is considered nevertheless useful, and is presented in
Table 12.6.

12.3. The experimental results seem to form a consistent set,
in the sense that they conform to the theoretical predictions
that smooth lines connect the discrete measured values
(e.g. the $\Delta n/n$ values for one test fuel versus the ECO
lattice pitch) showing the correct trend, that the correspon-
dance between the results of the measurements with the test-
sections in plexiglass and in polystirol is correctly
observed, etc.

The only apparent exception is the set of data for the
Pu I fuel which, still being internally consistent, lies
below the corresponding set for the Pu III fuel, while
elementary considerations based on the isotopic composition
of the two fuels indicate that the Pu I data should
actually be somewhat higher than the corresponding Pu III
data (see Table 12.1.).

In fact the various tests on the composition of the rods
of the Pu I fuel (described in the Appendix) showed some
important discrepancies, not yet clarified. Thus, at
present, the above mentioned inconsistency between the
experimental results for Pu I and Pu III is ascribed
to an important error in the measured composition of
the Pu I fuel. The same hypothesis was made basing
on preliminary results of theoretical calculations of
the relative worths of the test samples. An effort is
being made to obtain a satisfactory definition of the
composition of the Pu I test-section.

A P P E N D I X

A.1. RESPONSE OF A THERMAL REACTOR TO A SMALL PERIODIC
PERTURBATION FUNCTION

For completeness, the derivation of the reactor transfer function is briefly recalled, with emphasis on the limits of validity of the approximations involved in the theory.

The effective multiplication factor k_{eff} can be defined as

$$k_{eff} = \underbrace{\begin{array}{l} \text{average pro-} \\ \text{bability that} \\ \text{the life of a} \\ \text{thermal neutron} \\ \text{in the reactor} \\ \text{ends by giving} \\ \text{a fission} \end{array}}_{P_f} \times \underbrace{\begin{array}{l} \text{average} \\ \text{number of} \\ \text{neutrons} \\ \text{issuing} \\ \text{from one} \\ \text{fission} \end{array}}_{\nu} \times \underbrace{\begin{array}{l} \text{average pro-} \\ \text{bability that} \\ \text{one fast} \\ \text{neutron issuing} \\ \text{from a fission} \\ \text{be the source} \\ \text{of one thermal} \\ \text{neutron} \end{array}}_{P_t} \quad (1$$

The following two assumptions are valid for small perturbations in thermal systems.

1. The overall perturbation of the energy spectrum and spatial distribution of the neutrons is negligible : thus the reactor averaged probabilities for the events encountered by a neutron can be considered as time-independent.

2. The thermalization time is negligible compared to the average life time of the neutron.

The neutrons and precursors balances relative to an elementar time interval dt around t can be written ;

for the neutron population :

variation of thermal neutron population during dt	=	thermal neutron population at time t	×	average probability for one thermal neutron to disappear during dt	×
dn		n		dt/τ	

×	average probability that the life of a thermal neutron in the reactor end by giving a fission	×	average number of fast neutrons immediately released from fission	×	average probability that a neutron issued from a fission be the source of one thermal neutron	+
	P_f		$(1-\beta)\,\nu$		P_t	(2)

+	summation over all precursors		number of neutrons emitted by precursors i during dt	×	average probability that a neutron emitted by precursors i be the source of one thermal neutron
	$\sum_i$		$\lambda_i\,C_i\,dt$		P_{t_i}

for the precursors of type i :

variation of the total number of precursors of the type i during dt	=	thermal neutron population at time t	×	average pro- bability for one thermal neutron to disappear during dt	×
$d\,C_i$		n		dt/τ	

×	average probability that the life of a thermal neutron in the reactor ends by giving a fission	×	average number of precursors of type i created by one fission	−
	P_f		$\beta_i \nu$	(3)

−	loss of precursors of type i during dt
	$\lambda_i\, C_i\, dt$

From eq(2) and (3) using (1)

$$\frac{dn}{dt} = \frac{n}{\tau}\left\{ k\,(1-\beta) - 1 \right\} + \sum_i \lambda_i C_i\, P_{t_i} \tag{4a}$$

$$\frac{dC_i}{dt} = \frac{n}{\tau} \cdot \frac{k\beta_i}{P_t} - \lambda_i C_i \tag{4b}$$

The solution of the system of equations (4a) and (4b) in the case of a small sinusoidal oscillation of the multiplication factor k around unity, $\bar{k} = 1 + \bar{\delta k}\, e^{j\omega t}$,

may be written in the form

$$\bar{n} = n_o + \delta\bar{n}\, e^{j\omega t}$$
$$\bar{C}_i = C_{i_o} + \delta\bar{C}_i\, e^{j\omega t}$$

Neglecting second order terms, assuming $P_{t_i} = P_t$ and with

$$\frac{n_o}{\tau} \cdot \frac{\beta_i}{P_t} = \lambda_i C_{i_o}$$

(4b) yields

$$j\omega\, \delta\bar{C}_i = \frac{\beta_i}{\tau P_t}\left\{ n_o\, \delta\bar{k} + \delta\bar{n} \right\} - \lambda_i\, \delta\bar{C}_i$$

being $\delta n \gg \delta k\, n_o$

$$\delta\bar{C}_i = \frac{\beta_i}{\tau P_t} \cdot \frac{\delta\bar{n}}{\lambda_i + j\omega}$$

From (4a) and (4b)

$$\frac{d\bar{n}}{dt} + P_t \sum_i \frac{d\bar{C}_i}{dt} = \frac{n}{\tau}\,(\bar{k}-1)$$

$$j\omega\, \delta\bar{n} + j\omega\, \frac{\delta\bar{n}}{\tau} \sum_i \left(\frac{\beta_i}{\lambda_i + j\omega} \right) = \frac{n_o\, \delta\bar{k}}{\tau}$$

and finally

$$\delta \bar{k} \quad = \quad (A + jB) \, \frac{\delta \bar{n}}{n_o}$$

with

$$A \; = \; \omega^2 \; \sum_{\text{all precursors}} \left(\beta_i / \lambda_i^2 - \omega^2 \right) \; , \; B \; = \; \omega \tau + \omega \sum_{\text{all precursors}} \left(\lambda_i \beta_i / \lambda_i^2 + \omega \right)$$

Within the limits of validity of the simplified theory outlined above, the transfer function $\bar{F} = A + jB$ relates sinusoidal oscillations of reactivity and neutron density in the critical reactor.

In case of a non-sinusoidal oscillation of the multiplication factor the same relation applies between the various harmonics in the Fourier expansion of the reactivity and neutron density functions.

In heavy water moderated reactors an appreciable fraction of delayed neutrons originates from the 1.6 MeV threshold (γ ,n) reaction in D_2O. These delayed photoneutrons have lower energy and longer mean lifes than delayed fission neutrons; their yield depends on the self-absorption of the gamma radiation in the fuel elements. The relatively poor knowledge of the delayed photoneutrons parameters, as well as the difficulty of the gamma self-absorption calculation in the complex-geometry fuel element of D_2O moderated reactors, considerably complicates the theoretical treatment in the case of D_2O moderated assemblies.

In fact, even in the absence of photoneutrons, difficulties of various nature limit the usefulness of the transfer function for the direct interpretation of reactor oscillation experiments in absolute terms (e.g. : pcm). Rather, the

experiments are generally performed relative to a standard element, geometrically identical to the investigated elements, whose reactivity worth can be calculated with adequate precision from primary data.

In this sense in D_2O moderated reactors the presence of delayed photoneutrons does not introduce additional experimental or theoretical problems, the only condition to be met being the equality of the oscillation function for the investigated elements and the standard element.

A.2.   DESIGN SPECIFICATIONS AND QUALITY CONTROL OF THE
          TEST-SECTIONS

A.2.1.   Design specifications

          The following paragraphs are excerpts from the original
          design specifications.

A.2.1.1. Alloy chemical composition

          1. The nominal composition of the fuel test-sections
             shall be that listed in Table A.2.1.

          2. The actual composition shall not differ more than 10%
             from the nominal value.

          3. The actual composition shall be uniform radially and
             axially throughout each rod to within 3%.

          4. The dispersion in the average compositions of the rods
             of one set, expressed by the mean square deviation (1σ),
             shall not exceed one percent.

          5. The overall impurities content of the alloy shall not
             exceed 2 ppm boron equivalent.

A.2.1.2. Physical properties of the fuel rods

          1. The average alloy density of each rod shall not be
             lower than 18.7 gr/cm^3, or 99% of the theoretical U
             density.

          2. The fuel rods shall have the following dimensions :
             diameter 12 $\pm$ 0.02 mm, length 250 $\pm$ 0.1 mm (note that
             the 50-cm-long rods of the test-sections were obtained
             by cladding together two 25-cm-long rod segments).

          3. The rods surface shall be free from evident defects,
             as tool marks, open cavities, etc.; the rods ends will
             have sharp edges.

A.2.2.   Quality control tests

A.2.2.1. Alloy chemical composition

1. The Pu-U content ratio was measured for each cast by
    chemical analysis of samples taken at both ends of one
    ingot of the cast, with a $\pm 2\%$ accuracy. This measu-
    rement served as production control test (i.e. to
    reject ingots before proceeding further in the
    fabrication) as well as a check of the uniformity
    in the axial distribution of the composition of the
    alloy. The results are reported in Table A.2.2.
    The measured uniformity generally met the design
    specifications.

2. The normalized distribution curve for the Pu-U average
    ratios in the rods of each set was experimentally
    determined, by a technique based on the detection of
    the spontaneous fissions of Pu^{240} ($T_{\frac{1}{2}} = 1.2.10^{11}$ y,
    $\nu = 2.2$) and U^{238} ($T_{\frac{1}{2}} = 6.10^{15}$ y, $\nu = 2.2$).
    The Pu^{240} fission rate in the Pu-U rod was isolated
    by substracting from the rod overall fission rate that
    measured for a geometrically identical U rod.

    The experimental equipment consisted in a set of 20 BF3
    counters arranged in concentric crowns in a paraffine
    matrix. The rod to be measured was placed inside a
    cylindrical hole on the axis of the assembly. The
    fast neutrons emitted by spontaneous fission in the rod
    were thermalized by collisions with the paraffine
    atoms and detected with high efficiency by the counters.

The normalized Pu content of the rod of the set (R_i) was obtained, with a $\pm$ 1% accuracy, from the expression :

$$R_i = \left\{ \frac{C_i}{W_i} - \frac{C_u}{W_u} \right\} \Big/ \left\{ \frac{C_N}{W_N} - \frac{C_u}{W_u} \right\}$$

where C is the measured count rate, W is the rod weight and the subscripts U and N refer, respectively, to the natural U rod and normalizing Pu-U rod of the set.

Due to proper geometrical arrangement, the axial efficiency of the BF3 counters set was flat over the 25-cm-length of the Pu-U rods. Thus the detected count rate was an accurate measure of the average Pu content of the rod, regardless of possible small variations in its axial distribution. More details on this experimental technique are presented in Ref.7.

The measured normalized distributions of the Pu/U average values in the rods of each set are shown in Fig.30 to 32. The satisfactory uniformity of the Pu content is expressed in terms of the number of rods (per cent) whose Pu content differred from the set average content less than 1% (see A.2.1.1.4).

Taking advantage from the radial symmetry of the 19-rod fuel element, the rods used for the assembly of the test-sections were properly selected from the above distribution curves, so as to further homogeneize the Pu content in the two rings of rods of the clusters. The average Pu/U values thus obtained for the rings of rods of the test-sections are shown in Table A.2.3.

3. The determination of the absolute Pu/U value of the rods used for the normalization of the relative Pu/U distribution curve was performed by a technique consisting of a double isotopic dilution followed by a mass spectrographic analysis (8).

By analyzing a sample taken from the acid solution
of the complete rod, the average Pu/U value of the rod
was measured with a $\pm 1\%$ accuracy over the entire
range of Pu contents. The results of the analysis
are listed in Table A.2.4.

4. The above samples were also analysed by mass spectrography
   techniques for the determination of the isotopic compo-
   sition of Pu and U. The following experimental accuracies
   were obtained over the whole range of isotopic compositions
   considered :

   Pu^{239}/Pu 1%, Pu^{240}/Pu 5%, Pu^{241}/Pu 5%, U^{235}/U 0.3%.
   The results are listed in Table A.2.4.

5. The average compositions of the fuel test-sections, as
   obtained combining the results of tests 2,3 and 4 above
   to the measured fuel rods weight, are listed in Table A.2.3.

A.2.2.2. Physical properties of the fuel rods
   The measured weights, densities and dimensions of the rods
   of each set (Tables A.2.5,6,7,8) were within the design
   specifications, except for the density of the set Pu-III
   which was about 0.5% below the required value. Since the
   overall weights of the test sections were all equal to
   within 300 g (or 1.5%), the effect of the reduced density
   of the Pu-III could be easily accounted for by calculation.

A.3. SCHEME OF CALCULATION OF THE AMPLITUDE OF THE FIRST
HARMONIC IN THE FOURIER EXPANSION OF THE RECORDED SIGNAL

1. The data registered in digital form on the magnetic
tape are subdivided in records, i.e. sets of data
used for a single determination of the first harmonic
amplitude and average value of the signal, and files,
i.e. the records concerning a single oscillation
experiment.

The calculation yields the value of the amplitude of
the first harmonic in the Fourier expansion of the
periodic neutron density signal generated by the
oscillation of the fuel test section in-out the critical
reactor core, as well as the mean value of the same
signal during each analysed oscillation period.

The treatment of the data includes : correction for
linear drift in the reactor neutron density, evaluation
of the linear drift coefficient, evaluation of the mean
and standard deviation of the results relative to one
file.

2. On the assumption that the recorded global signal F is
formed by the combination of a periodic signal FP, due
to the periodic sample oscillation, and of a linear
drift kt in the reactor neutron density (first order
approximation to the effect of slowly varying conditions
on reactor criticality, as D_2O temperature, air
pressure, imperfect initial balancing, etc.), and that
time integration is started at random with respect to
the periodic signal, the cosine and sine components and
the amplitude of the first harmonic in the Fourier
expansion of F are

$$A \;=\; 2/_T \int_0^T F(t) \cos \Omega t \; dt \;=\; 2/_T \int_0^T F_P(t) \cos \Omega t \; dt$$

$$=\; A_P$$

$$B \;=\; 2/_T \int_0^T F(t) \sin \Omega t \; dt \;=\; 2/_T \int_0^T F_P(t) \sin \Omega t \; dt \;-\; \frac{kT}{\pi}$$

$$=\; B_P \;-\; k\frac{T}{\pi}$$

$$\left(A^2 + B^2\right)^{\frac{1}{2}} \;=\; \left(A_P^2 + B_P^2 + \frac{k^2 T^2}{\pi^2} - 2 B_P \frac{kT}{\pi} \right)^{\frac{1}{2}}$$

being normally k≪1

$$\left(A^2 + B^2\right)^{\frac{1}{2}} \;=\; \left(A_P^2 + B_P^2\right)^{\frac{1}{2}} \left\{ 1 + BkT/\pi (A^2 + B^2) \right\}$$

Thus the amplitude of the measured signal F differs from the amplitude of the periodic function FP by the factor

$$BkT/\pi (A^2 + B^2)$$

3. A record covers over 1.5 oscillation period. A first integration started at the beginning of the record yields the first harmonic components A_1 and B_1, a second integration from T/2 to 3 T/2 yields A_2 and B_2. The linear drift coefficient is calculated from

$$A_1 \;=\; A_{P_1} \qquad\qquad A_2 \;=\; A_{P_2}$$

$$B_1 \;=\; B_{P_1} - kT/\pi \qquad B_2 \;=\; B_{P_2} - kT/\pi$$

assuming FP to be a pure periodic function

$$\left(A_{P_1}^2 + B_{P_1}^2\right) = \left(A_{P_2}^2 + B_{P_2}^2\right)$$

one obtains

$$k = \frac{\pi}{2T} \cdot \frac{A_1^2 + B_1^2 - \left(A_2^2 - B_2^2\right)}{B_2 - B_1}$$

4. Using this value for k one calculates the periodic function FP = F - kt, as well as the phase of its first harmonic maximum (or minimum) relative to the beginning of the record

$$tg\left(\Omega t_o\right) = \frac{\int_0^T F_P(t) \sin \Omega t \, dt}{\int_0^T F_P(t) \cos \Omega t \, dt}$$

(the above expression is obtained writing

$$B_{P_o} = 2/T \int_0^T F_P(t + t_o) \sin \Omega t \, dt = 0 \Big)$$

5. Integration of the global signal F is performed over the time interval $(t_o, t_o + T)$ yielding A_o, B_o (nominally $B_o = 0$) and $(A_o^2 + B_o^2)^{\frac{1}{2}}$.

6. Following the choice of the integration origin about the maximum (or minimum) of the first harmonic of the periodic signal FP (i.e. at t_o), $B_o/A_o \ll 1$ and

$$\left(A_o^2 + B_o^2\right)^{\frac{1}{2}} \sim \left(A_P^2 + B_P^2\right)^{\frac{1}{2}} \left\{ 1 + B_o kT/\pi \left(A_o^2 + B_o^2\right) \right\}$$

$$\sim \left(A_P^2 + B_P^2\right)^{\frac{1}{2}}$$

7. In the normal case

$$B_o/A_o \sim 0.01$$

$$k \sim 2 \cdot 10^{-5}$$

$$\left(A_o^2 + B_o^2\right)^{\frac{1}{2}} / \left(A_P^2 + B_P^2\right)^{\frac{1}{2}} \sim 1.00002$$

8. <u>Data input</u>
   - digitalized relative neutron density signal, subdivided in records (covering over 1.5 oscillation period) and files (15 records relative to a single oscillation experiment) ;
   - file identification number ;
   - number of signal readings per unit time (normally 5 readings/sec) ;
   - oscillation period (normally 60 sec).

9. Data output

For each record :

$H_1 = (A_1^2 + B_1^2)^{\frac{1}{2}}$ amplitude of first harmonic of recorded (global) signal F when origin of integration set at beginning of record ;

$H_2 = (A_2^2 + B_2^2)^{\frac{1}{2}}$ amplitude of first harmonic of recorded (global) signal F when origin of integration set T/2 after beginning of record ;

B_o sine component of first harmonic of F when origin of integration set to t_o, i.e. at the maximum of the pure periodic signal FP ;

k linear drift coefficient;

PH   phase of first harmonic maximum of the pure periodic signal FP relative to the beginning of the record ;

$H = (A_o^2 + B_o^2)^{\frac{1}{2}}$ amplitude of the first harmonic of F when integration started at t_o. Practical equal to amplitude of the first harmonic of the pure periodic signal FP ;

$FM = \frac{1}{t} \int_o^t F(t)dt$ average value of the recorded signal F, over a period of oscillation, equal to the average value of the pure periodic signal on the assumption of linear neutron density drift.

H/FM

For each file :

      AVE   mean of the H/FM values obtained for each of the N records of the file ;

      SIGMA   standard deviation of the mean

$$\left(= \left[\frac{\sum \left(AVE - \frac{H}{FM} \right)^2}{N(N-1)} \right]^{\frac{1}{2}} \right)$$

10. A typical set of output data, allowing to appreciate the dispersion of the results, is shown in Table A.3.1.

A.4. EVALUATION OF THE ERROR INTRODUCED IN THE DATA ANALYSIS BY THE DISCONTINUOUS RECORD OF THE SIGNAL

The signal is recorded at discrete time intervals in digital form, the data analysis calculates the amplitude of the first harmonic in the Fourier expansion of the recorded signal by numerical integration through the Simpson rule. The following is an evaluation of the error in the analysed data stemming from the discontinuous record of the signal.

The data recording system registers the average value of the signal over the time ε at time intervals $\delta t > \varepsilon$.

In the case of a sinusoidal signal $g \cos(\omega t - \varphi)$, the average value registered in the incremental recorder at time $t = k \, \delta t$ is

$$\frac{1}{\varepsilon} \int_{t-\varepsilon/2}^{t+\varepsilon/2} g \cos(\omega t - \varphi) \, dt = \frac{2g}{\omega \varepsilon} \sin \omega \varepsilon/2 \, \cos(\omega t - \varphi)$$

The sine component of the first harmonic in the Fourier expansion of the signal in the time interval $(0,T)$ is theoretically given by

$$a(\Omega, \omega) = \frac{2}{T} \int_0^T \frac{2g}{\omega \varepsilon} \sin \omega \varepsilon/2 \, \cos(\omega t - \varphi) \, \sin \Omega t \, dt$$

where ω is not necessarily a multiple of $\Omega = \frac{2\pi}{T}$.

Actually the computer carries out the time integration using the Simpson rule over $2m$ intervals δt and calculates

$$a^*(\Omega, \omega) = \left\{ \frac{2}{T} \cdot \frac{2g}{\omega \varepsilon} \cdot \frac{\delta t}{3} \cdot \sin \omega \varepsilon/2 \right\} \cdot \tag{1}$$

$$\cdot \left\{ y_0 + y_{2m} + 4 \sum_{n=0}^{n=m-1} y_{2n+1} + 2 \sum_{n=0}^{n=m-2} y_{2n+2} \right\}$$

with

$$\gamma_k = \cos(k\omega\,\delta t - \varphi)\,\sin(k\omega\,\delta t)$$

$$2m\,\delta t = T = 2\pi/\Omega$$

Similarly for the second component of the first harmonic

$$b^*(\Omega,\omega) = \frac{2}{T}\cdot\frac{2g}{\omega\varepsilon}\cdot\sin\frac{\omega\varepsilon}{2}\cdot\frac{\delta t}{3}\cdot$$

$$\cdot\left\{\gamma_0 + \gamma_{2m} + 4\sum_{n=0}^{n=m-1}\gamma_{2n+1} + 2\sum_{n=0}^{n=m-2}\gamma_{2n+2}\right\}$$

After tedious calculation one obtains, for $m > 1$:

$$a^*(\Omega,\omega) = \frac{8}{3}\cdot\frac{g\sin\omega\varepsilon/2}{\omega\varepsilon}\cdot\frac{1}{m}\cdot\frac{\sin\frac{\pi}{m}\left(2\cos\frac{\pi\omega}{m\Omega}+\cos\frac{\pi}{m}\right)}{\cos\frac{2\pi}{m}-\cos\frac{2\pi\omega}{m\Omega}}$$

$$\cdot\sin\frac{\pi\omega}{\Omega}\cdot\sin\left(\varphi-\frac{\pi\omega}{\Omega}\right) \qquad (2)$$

$$b^*(\Omega,\omega) = \frac{8}{3}\cdot\frac{g\sin\omega\varepsilon/2}{\omega\varepsilon}\cdot\frac{1}{m}\cdot\frac{\sin\frac{\pi\omega}{m\Omega}\left(2\cos\frac{\pi}{m}+\cos\frac{\pi\omega}{m\Omega}\right)}{\cos\frac{2\pi}{m}-\cos\frac{2\pi\omega}{m\Omega}}\cdot$$

$$\cdot\sin\frac{\pi\omega}{\Omega}\cos\left(\varphi-\frac{\pi\omega}{\Omega}\right)$$

If $\omega \to \Omega$, for $\Omega\varepsilon = \dfrac{\pi\varepsilon}{m\,\delta t}$ sufficiently small

and $m > 2$:

$$a^* = g\sin\varphi = a$$

$$b^* = g\cos\varphi = b$$

The only condition to be met being that the signal be recorded for 2m time intervals δt ranging from 0 to $2\ m\ \delta t = T = \frac{2\pi}{\Omega}$ and that $m > 2$.

Analyzing under the same conditions a complex periodic signal

$$G \;=\; g_0 + g_1 \cos(\Omega t - \varphi_1) + g_2 \cos(2\Omega t - \varphi_2) + \cdots$$
$$\cdots + g_s \cos(s\Omega t - \varphi_s) + \cdots$$

due to the presence of the $\sin \pi\omega/\Omega$ term, the contribution of higher harmonics vanishes except for the $(1 + km)^{th}$ harmonic. Thus

$$\lim_{\omega \to \Omega(1+km)} \left\{ \frac{\sin \pi\omega/\Omega}{\cos 2\pi/\Omega - \cos 2\pi\omega/m\Omega} \right\} =$$

$$= \frac{(-1)^{km+1}\ m}{2\ \sin 2\pi/m}$$

and

$$A_1^* = \sum_{s=0}^{s=\infty} \tfrac{1}{3}\, q_{sm+1} \frac{\sin \frac{(sm+1)\,\Omega\varepsilon}{2}}{\frac{(sm+1)\,\Omega\varepsilon}{2}} \left[2\,(-1)^s + 1\right] \sin \varphi_{sm+1}$$

$$(3)$$

$$B_1^* = \sum_{s=0}^{s=\infty} \tfrac{1}{3}\, q_{sm+1} \frac{\sin \frac{(sm+1)\,\Omega\varepsilon}{2}}{\frac{(sm+1)\,\Omega\varepsilon}{2}} \left[2\,(-1)^s + 1\right] \cos \varphi_{sm+1}$$

instead of the exact result

$$A_1 = q_1 \sin \varphi_1$$

$$B_1 = q_1 \cos \varphi_1$$

The advantage of taking a high number of signal
measurements during one oscillation period stems from
the large frequency gap (1 + km) existing between
the fundamental and the perturbing harmonics. For
the selected experimental conditions (2 m = 300 and
T = 60 sec) the first perturbing harmonic has a 2.5 cps
frequency, which can be considered as low level noise
and be easily filtered out without affecting the
first harmonic amplitude.

A.5. SOME REMARKS ON THE SHAPE OF THE NEUTRON DENSITY
MODULATION SIGNAL

Some typical records of the main primary data, i.e.
the neutron density modulation and the test-section
position versus time (ref.8.4), are shown in Fig.33 to 36.
They refer to the samples UN (Fig.33), Pu I (for two
translation speeds, 1 m/sec and 0.5 m/sec; Fig.34 and 35),
Pu II (Fig.36).

Samples Pu I and Pu II are representative of the samples
with positive and negative reactivity worths, respecti-
vely; the record of the data for the sample UN puts in
evidence the reactivity effect of the translation of
the Zr-Al joints of the segments forming the oscillating
fuel element.

The translation of the joints in either direction gave
rise to a significant peak in the neutron density, extending
over a fraction of the translation time.

The peak was the result of the composite reactivity effects
of the replacement of absorber (Zr-Al joint) with fissile
material (fuel element) in regions of varying neutron
importance, with the positive effect (exit of the test-
section from the core center) prevailing first and the
negative effect (approach of the reference section to the
core center) following.

Such a component of the global modulation of the neutron
density was clearly unrelated to the reactivity worth
of the test-sample and had to be cancelled out in the
data analysis.

Specifically, the Fourier analysis of the density
modulation greatly reduced the importance of the joints
transit effect. The residual effect was totally eliminated
in the subtraction of the UN sample signal amplitude from
the test-section signal amplitudes (see 10.5).

The direct subtraction of signal amplitudes was a valid
procedure, provided the two signals had the same phase
angle with respect to the sample oscillation function.
The latter hypothesis was verified for some typical cases,
as shown in Table A.5.1 (phase expressed in terms of period
subintervals).

The oscillation of the extended length fuel element
resulted in the extraction of delayed neutron precursors
from the reactor core. In fact, in the translation between
the two rest positions for the test-section, a portion of
the oscillating fuel element previously exposed to the
neutron flux was extracted from the reactor lattice (above
or below it). Since the transit times were from 2 to 4 sec,
as compared to rest times of 28 to 26 sec, a large
fraction of the delayed neutrons were emitted outside
the reactor core.

This continuous loss of neutrons from the core had a
negative reactivity worth, which was evident in the
oscillation of the UN sample. Thus it was not possible
to maintain the reactor stable critical during the oscilla-
tion of this sample, as shown in Fig.33 (in this measurement
the reactor was initially set slightly supercritical to
compensate for the effect of the delayed neutrons loss).
Evidently also this spurious reactivity effect was completely
cancelled out when subtracting the UN sample signal from
the test samples signals (10.5).

———

REFERENCES

1. G.BLAESSER, P.BONNAURE, G.CASINI, R.CENERINI,
   V.RAIEVSKI, F.TOSELLI

   Report EUR-130f (1962)

2. O.R.FRISCH, D.J.LITTLER

   Phil.Mag. 45, 126 (1954)

3. R.B.TATTERSALL, V.G.SMALL, I.J.MACBEAN, W.H.DOWE
   Report AEEW-376 (1964)

4. C.E.COHN
   Nucl.Sci.Eng. 7, 472 (1960)

5. R.ARHAN, J.ELBAZ, E.MACKE, C.PAGNY, P.VAREKAMP
   Communication EUR-1935 (1968)

6. E.DIANA
   Personal communication (1964)

7. D.BRUNET, L.DE LAPPARENT, P.LOURME
   Report CEA R-2-613 (1964)

8. Standard UKAEA analytical isotope dilution procedure
   (PGR 340-W)

compound	chemical formula	density g/cm^3	atoms/cm^3		
			C	H	O
diphyl	26.5% $C_{12}H_{10}$ 73.5% $C_{12}H_{10}O$	1.062	$4.64 \cdot 10^{22}$	$3.86 \cdot 10^{22}$	$2.76 \cdot 10^{2}$
plexiglass	$C_5H_8O_2$	1.189	$3.58 \cdot 10^{22}$	$5.73 \cdot 10^{22}$	$1.43 \cdot 10^{2}$
polystirol	$(CH)_n$	1.057	$4.89 \cdot 10^{22}$	$4.89 \cdot 10^{22}$	-

Table 6.1. : Compositions of organic compounds used to simulate the fuel channel coolant.

sample identification	Pu/U %	Pu^{240}/Pu^{239} %	Pu^{241}/Pu^{239} %	U^{235}/U %
Pu I	0.057	6.20	0.57	0.714 (nat)
Pu II	0.299	8.45	0.69	0.208
Pu III	0.046	25.52	4.22	0.714 (nat)
Pu IV	0.256	27.80	4.79	0.227
Pu V	12 outer rods of cluster : Pu II rods 7 inner rods of cluster : Pu I rods			
Pu VI	12 outer rods of cluster : Pu IV rods 7 inner rods of cluster : Pu I rods			
UE				0.804
UD				0.643

Table 7.1. : Isotopic compositions of fuels investigated

Sample	plexiglas coolant	polystirol coolant	void
UE	X		
UD	X		
Pu I	X	X	X
Pu II	X	X	X
Pu III	X	X	X
Pu IV	X	X	
Pu V	X		
Pu VI	X		

Table 10.1. : Synopsis of experimental configurations; measurements carried out at lattice pitches 18.8, 23.5 and 28.05 cm.

test fuel	correct position	correct position + 5 cm	correct position + 10 cm
UN/ plexiglass	$0.4169.10^{-2}$ $\mp1.2.10^{-5}$	$0.3926.10^{-2}$ $\mp1.2.10^{-5}$	$0.3514.10^{-2}$ $\mp1.3.10^{-5}$
Pu IV/ plexiglass	$-18.417.10^{-2}$ $\mp2.5.10^{-5}$	$-18.402.10^{-2}$ $\mp4.3.10^{-5}$	$-18.186.10^{-2}$ $\mp7.6.10^{-5}$
Pu III/ plexiglass	$5.6707.10^{-2}$ $\mp1.6.10^{-5}$	$5.6052.10^{-2}$ $\mp1.7.10^{-5}$	$5.5044.10^{-2}$ $\pm1.2.10^{-5}$

Table 11.1. : Effect of important variations of the "in-core" position of the test-section on the experimental results ($\Delta n/n$).

Oscillation data : period = 60 sec
transit speed = 0.5 m/sec
lattice pitch = 23.5 cm

test fuel	correct position	correct position + 1 cm	$\Delta(0,+1)$	correct position - 1 cm	$\Delta(0,-1)$
UN/ plexiglass	0.4643 ±0.0015	0.4607 ±0.0021	-0.0036	0.4684 ±0.0019	+0.0041
Pu I/ plexiglass	5.1132 ±0.0019	5.1093 ±0.0015	-0.0039	5.1152 ±0.0017	+0.0020
Pu II/ plexiglass	-5.4144 ±0.0058	-5.4082 ±0.0120	-0.0062	-5.4079 ±0.0013	-0.0065
Pu III/ plexiglass	6.0581 ±0.003	6.0462 ±0.0020	-0.0120	6.0549 ±0.0018	-0.0032
UD/ plexiglass	-7.4490 ±0.0021	-7.4512 ±0.0010	+0.0022	7.4423 ±0.0013	-0.0067

<u>Table 11.2</u> : Effect of small variations in the "in core" position of the test-section on the experimental results ($\Delta n/n$ x 10^2)

Oscillation data : period   = 60 sec
                          transit speed = 0.5 m/sec
                          lattice pitch = 28.05 cm

lattice pitch cm	oscillation period sec	rest time sec	$\Delta n/n$ x 10^{-2}	
18.8	59.67	27.6	7.8809	$\pm$ 0 005
	60.05	27.8	7.9263	$\pm$ 0.008
	60.47	28.0	7.9360	$\pm$ 0.017
23.5	59.65	27.6	16.490	$\pm$ 0.002
	60.05	27.8	16.541	$\pm$ 0.007
	60.47	28.0	16.583	$\pm$ 0.007
	60.86	28.2	16.627	$\pm$ 0.004
28.05	59.70	27.6	20.019	$\pm$ 0.009
	60.10	27.8	20.063	$\pm$ 0.006
	60.49	28.0	20.146	$\pm$ 0.005

Table 11.3 : Dependence of the experimental results ($\Delta n/n$) on small variations of the oscillation period

Oscillation data : test fuel   = UN/void
                  transit speed = 1 m/sec

period sec	sample 1 (UN + 120 gr Cu)	sample 2 (UN + 200 gr Cu)	$\frac{\text{sample 2}}{\text{sample 1}}$
40	-3.9590 ± .0017	-6.2139 ± .0015	1.5695
60	-4.7407 ± .002	-7.4192 ± .0015	1.5650
80	-5.3747	-8.4318 ± .0027	1.5688

Table 11.4 : Dependence of the experimental results
($\Delta n/n$ x 10^2) on the choice of the oscillation
period.

Oscillation data : transit speed 1 m/sec
lattice pitch 23.5 cm

transit speed m/sec	transit time sec	rest time sec	rest time/ transit time	PuI	UA	UA/PuI
1.000	2.2	27.8	12.6	3.4655	6.2882	1.8145
0.833	2.6	27.3	10.5	3.4679	6.2795	1.8107
0.666	3.3	26.7	7.9	3.4643	6.2863	1.8145
0.500	4.3	25.7	6.0	3.4580	6.2691	1.8129
0.333	6.5	23.5	3.6	3.4278	6.2198	1.8145
0.266	8.25	21.7	2.6	3.3959	6.1770	1.8189

Table 11.5 : Dependence of the experimental results ($\Delta n/n \times 10^2$) on the "rest time/transit time" value of the oscillation

Oscillation data : period   : 60 sec
                   lattice pitch: 18.8 cm
                   test fuel   : PuI/plexiglass, UA/plexiglass

fuel sample	lattice pitch cm	chamber in normal position (175 cm from core axis)	chamber outward (215 cm from core axis)	relative variation in results
Pu III/ polystyrol	23.5	5.6707 $\mp$0.0016	5.6685 $\mp$0.0021	- 0.4 °/$_{oo}$
	28.05	5.8448 $\mp$0.0030	5.8548 $\mp$0.0012	+ 1.7 °/$_{oo}$
Pu IV/ polystyrol	23.5	16.992 $\mp$0.0025	17.018 $\mp$0.008	+ 1.5 °/$_{oo}$
	28.05	17.122 $\mp$0.003	17.131 $\mp$0.013	+ 0.6 °/$_{oo}$
UN/ plexiglass	23.5	0.4169 $\mp$0.0012	0.4139 $\mp$0.0015	- 7 °/$_{oo}$
Pu IV/ plexiglass	23.5	18.414 $\mp$0.003	18.435 $\mp$0.003	+ 1.1 °/$_{oo}$
Pu IV/ polystyrol	23.5	3.155	3.159	+ 1.3 °/$_{oo}$
Pu III polystyrol	28.05	3.0776	3.0724	- 1.7 °/$_{oo}$

Table 11.6 : Dependence of the experimental results
($\Delta n/n \times 10^2$) on the radial position of
the ionization chamber

Oscillation data : period   : 60 sec
                  transit speed : 0.5 m/sec

lattice pitch cm	matrix 1	matrix 2	1-2
18.8	0.3508 ±0.001	0.3332 ±0.002	-0.018
23.5	0.4434 ±0.0013	0.4221 ±0.002	-0.021
28.05	0.4938 ±0.0012	0.4719 ±0.002	-0.022

Table 11.7 : Dependence of the experimental results
($\Delta n/n.10^2$) for the UN test fuel on the
mass differences in the structural
materials (plexiglass and Zr)

Oscillation data : period : 60 sec
transit speed : 1 m/sec

	plexiglass gr	Zr gr
matrix 1	929.58	586.28
matrix 2	927.25	586.20

	Pu I	Pu II	Pu III	Pu IV
Al canning (gr)	55.6$\overline{+}$1	55.4$\overline{+}$1	56.6$\overline{+}$1	62.5$\overline{+}$1

Table 11.8 : MEAN VALUE OF THE AL CANNING WEIGHT FOR EACH SET OF TEST FUEL RODS, WITH STANDARD DEVIATION FROM THE MEAN.

lattice pitch cm	test fuel	measu-rement 1	measu-rement 2	(1-2)	(1-2) $^o/_{oo}$
18.8	UD/plexiglass	5.294	5.297	0.003	0.6
	UE/plexiglass	6.318	6.297	0.021	3.3
	PuI/plexiglass	3.480	3.460	0.020	6
	PuIII/plexiglass	3.589	3.549	0.040	10.1
23.5	PuI/plexiglass	4.823	4.835	0.012	2.5
	PuIII/plexiglass	5.334	5.270	0.064	12.1
28.05	UD/plexiglass	7.934	7.943	0.009	1.1
	PuIII/plexiglass	5.564	5.416	0.148	27.1

Table 11.9 : Dependence of the experimental results ($\Delta n/n \times 10^2$) on the mechanical tolerances of the fuel test-sections

Oscillation data :   period   : 60 sec
                       transit speed : 1 m/sec

lattice pitch cm			mean square deviation of single measurement $^o/_{oo}$	deviation from the mean value $^o/_{oo}$
18.8	1.0845	$\mp$ 0.0015	1.3	0.9
	1.0876	$\mp$ 0.0014	1.2	1.9
	1.0859	$\mp$ 0.0017	1.3	0.4
	1.0840	$\mp$ 0.0014	1.3	1.4
	mean	: 1.0855		
23.5	2.2934	$\mp$ 0.0017	0.7	1.1
	2.2883	$\mp$ 0.0024	1.0	1.1
	mean	: 2.2909		
28.05	2.7582	$\mp$ 0.0014	0.5	0.4
	2.7566	$\mp$ 0.0020	0.7	0.2
	2.7569	$\mp$ 0.0015	0.6	0.1
	mean	: 2.7572		

Table 11.10 : Dependence of experimental results
($\Delta n/n$ x 10^2) on the reproducibility
of the lattice pitch values

oscillation data : period   : 60.05 sec
                    transit time : 1 m/sec
                    test fuel   : Pu V/plexiglass

reactor power (watts)	error in measured $\Delta n/n$
10	$8.8 \cdot 10^{-5}$
20	$3.4 \cdot 10^{-5}$
30	$5.4 \cdot 10^{-5}$
40	$2.3 \cdot 10^{-5}$
50	$2.0 \cdot 10^{-5}$
60	$1.8 \cdot 10^{-5}$

Table 11.11 : Error due to reactor and instrumentation noise

oscillation data :   test fuel : UN/plexiglass (fixed position)
lattice pitch : 23.5 cm
oscillation period : 60 sec
(fictitious)

lattice pitch cm	number of oscillations		mean square deviation $(\times 10^{-3})$
18.8	15	0.3325 ∓ 0.0010	3.0
	15	0.3339 ∓ 0.0012	3.6
	15	0.3337 ∓ 0.0012	3.5
	45	0.3328 ∓ 0.0009	2.7
23.5	15	0.4232 ∓ 0.0019	4.5
	15	0.4204 ∓ 0.0024	5.7
	15	0.4227 ∓ 0.0015	3.5
	45	0.4224 ∓ 0.0014	3.3
28.05	15	0.4719 ∓ 0.0017	3.6
	15	0.4728 ∓ 0.0014	3.0
	15	0.4702 ∓ 0.0018	3.8
	45	0.4718 ∓ 0.0012	2.5

Table 11.12 : Dependence of the dispersion in the experimental results ($\Delta n/n \times 10^2$) on the number of analysed oscillations

oscillation data : period : 60.05 sec
transit speed : 1 m/sec
test fuel : UN/plexiglass

$$\Delta n/n \times 10^2$$

pitch (cm)	UD	UE	Pu I	Pu II	Pu III	Pu IV	Pu V	Pu VI
18.8	−5.296	+6.308	+3.470	−3.178	+3.569	−13.244	−1.436	−8.745
23.5	−7.694	+9.219	+4.829	−5.264	+5.302	−18.915	−2.734	−12.747
28.05	−7.939	+9.538	+4.804	−5.882	+5.490	−19.311	−3.251	−13.167

Table 12.1. : Experimental results. Reactivity worths of test-fuels in plexiglass matrix relative to UN in plexiglass matrix. Typical experimental error : $\pm 0.003 \times 10^{-2}$.

pitch (cm)	$\Delta n/n \times 10^2$			
	Pu I	Pu II	Pu III	Pu IV
18.8	+3.444	-3.052	+3.541	-13.168
23.5	+4.837	-5.129	+5.331	-18.997
28.05	+4.801	-5.719	+5.521	-19.594

Table 12.2. : Experimental results.
Reactivity worth of test-fuels in
polystirol matrix relative to UN in
polystirol matrix. Typical experimental
error : $\pm 0.003 \times 10^{-2}$.

pitch (cm)	$\Delta n/n \times 10^2$				
	UN	Pu I	Pu II	Pu III	Pu IV
18.8	+0.648	+4.091	-2.405	+4.194	-12.519
23.5	+1.628	+6.475	-3.491	+6.968	-17.361
28.05	+2.032	+6.845	-3.674	+7.566	-17.550

Table 12.3. : Experimental results.
Reactivity worths of test-fuels in
polystirol matrix relative to UN in
plexiglass matrix. Typical experimental
error : $\pm 0.003 \times 10^{-2}$.

Pitch (cm)	$\Delta n/n \times 10^2$		
	Pu I	Pu II	Pu III
18.8	+3.755	−3.872	+4.003
23.5	+5.591	−6.571	+6.310
28.05	+5.722	−7.523	+6.662

Table 12.4. : Experimental results.
Reactivity worths of test-fuels in
air relative to UN in air. Typical
experimental error : $\pm$ 0.003 $\times$ 10^{-2}.

pitch (cm)	$\Delta n/n \times 10^2$			
	UN	Pu I	Pu II	Pu III
18.8	+7.578	+11.333	+4.402	11.581
23.5	+16.108	+21.699	+10.403	22.418
28.05	+19.582	+25.304	+13.021	26.244

Table 12.5. : Experimental results.
Reactivity worths of test-fuels in
air relative to UN in plexiglass
matrix. Typical experimental error :
$\pm$ 0.003 $\times$ 10^{-2}.

test fuel	organic coolant mock-up	lattice pitch (cm)		
UD	plexiglass	-25.5	-39.5	-40.5
UE	"	34.0	53.2	54.0
Pu I	"	18.7	27.5	27.5
Pu II	"	-10.2	-26.2	-29.2
Pu III	"	20	31.2	32.2
Pu IV	"	-66.2	-102.5	-101.5
Pu V	"	-5.2	-11.7	-15.2
Pu VI	"	-43.0	-67.7	-68.0
UN	polystirol	5.7	12.2	14.7
Pu I	"	25.2	41.0	43.2
Pu II	"	-11.7	-18.5	-18.7
Pu III	"	25.2	43.7	43.2
Pu IV	"	-69.7	-101.5	-101.5
UN	air	40.5	91.5	108.0
Pu I	"	60.2	123.0	139.7
Pu II	"	20.2	55.0	67.0
Pu III	"	61.2	127.0	145.0

Table 12.6 : Reactivity worths of the test fuels relative to UN in plexiglass as inferred from the diagrams of Fig.27 to 29. Values given in pcm,typical experimental error : +0.4 pcm.

Identification	weight % ratios		
	Pu/U	Pu^{240}/Pu^{239}	U^{235}/U
Pu I	0.05	8	0.714
Pu II	0.30	8	0.20
Pu III	0.05	25	0.714
Pu IV	0.30	25	0.20
UE	−	−	0.80
UD	−	−	0.60

Table A.2.1. : Nominal compositions of test fuels.

test fuel	cast identifi- cation	Pu/U Wt% ratios top	bottom
Pu I	1	0.059	0.059
	2	0.059	0.059
	3	0.043	0.043
	4	0.047	0.045
	5	0.044	0.045
	6	0.045	0.044
	7	0.044	0.045
	8	0.047	0.046
	9	0.047	0.044
	10	0.047	0.044
	11	0.049	0.045
	12	0.047	0.050
	13	0.046	0.045
Pu II	1	0.283	0.245
	2	0.288	0.293
	3	0.294	0.298
	4	0.299	0.298
	5	0.294	0.296
	6	0.304	0.299
	7	0.292	0.300
Pu III	1	0.047	0.046
	2	0.046	0.047
	3	0.046	0.046
	4	0.047	0.045
	5	0.046	0.045
	6	0.048	0.048
	7	0.047	0.046
	8	0.048	0.048
	9	0.039	0.057
	10	0.049	0.049
	11	0.049	0.049
	12	0.048	0.048
Pu IV	1	0.258	0.278
	2	0.274	0.271
	3	0.279	0.252

Table A.2.2. : Weight percent Pu/U ratios for samples taken at top and bottom of one ingot for each cast; results of chemical analysis (typical accuracy : +2%).

sample identi-fication	Pu/U (%) central rod	inner ring	outer ring
Pu I	0.0567	0.0569	0.0568
Pu II	0.300	0.299	0.299
Pu III	0.0454	0.0458	0.0458
Pu IV	0.259	0.255	0.257
Pu V	0.0567	0.0569	0.299
Pu VI	0.0567	0.0569	0.257

<u>A.2.3.:</u> Average values of weight percent Pu/U ratios for central rod, inner ring rod (6 **rods**) and outer ring rod (12 **rods**).

sample identi-fication	Pu/U(%) $\overline{+}1\%$	Pu^{240}/Pu^{239} (%) $\overline{+}1\%$	Pu^{241}/Pu^{239} (%) $\overline{+}5\%$	Pu^{242}/Pu^{239}	U^{235}/U tot (%) $\overline{+}$ 0.3%
Pu I	0.0573	6.22	0.57	–	natural
Pu II	0.301	8.48	0.69	0.03	0.208
PuIII	0.0457	25.52	4.22	1.1	natural
PuIV	0.269	27.80	4.79	1.0	0.227

Table A.2.4. :   Isotopic compositions of test fuels

position of the rod in the cluster	rod number	weight kg	density gr/cm^3	average diameter mm	length mm
center	111	1.0638	18.785	12.01	499.85
inner ring	107	1.0586	18.696	12.00	499.80
	112	1.0593	18.697	12.01	499.75
	114	1.0556	18.726	11.98	499.80
	117	1.0632	18.791	12.00	499.85
	119	1.0609	18.775	12.00	499.90
	106	1.0608	18.723	12.01	499.85
outer ring	101	1.0625	18.846	12.00	499.80
	102	1.0675	18.796	12.03	499.80
	103	1.0660	18.775	12.01	499.85
	105	1.0625	18.757	12.01	499.90
	108	1.0594	18.725	12.01	499.85
	109	1.0598	18.737	12.00	499.85
	110	1.0592	18.728	12.00	499.90
	113	1.0594	18.733	12.00	499.90
	116	1.0613	18.734	12.01	499.80
	118	1.0655	18.794	12.02	499.90
	123	1.0637	18.793	12.01	499.90
	115	1.0586	18.760	11.99	499.85

Table A.2.5. : Measured weights, densities and dimensions of test fuel rods : Pu I

position of the rod in the cluster	rod number	weight kg	density gr/cm^3	average diameter mm	length mm
center	206	1.0572	18.718	12.00	499.95
inner ring	205	1.0621	18.695	12.03	499.95
	207	1.0651	18.757	12.01	500.00
	208	1.0630	18.757	12.01	500.00
	209	1.0605	18.720	12.01	499.95
	212	1.0636	18.759	12.01	499.90
	213	1.0667	18.800	12.02	499.90
outer ring	201	1.0549	18.635	12.01	500.05
	202	1.0638	18.839	11.99	500.00
	203	1.0610	18.700	12.03	500.00
	204	1.0604	18.695	12.03	499.90
	210	1.0660	18.775	12.03	499.95
	211	1.0641	18.757	12.02	499.95
	214	1.0674	18.805	12.03	449.95
	215	1.0572	18.680	12.00	500.00
	216	1.0616	18.687	12.03	499.95
	217	1.0647	18.736	12.03	499.95
	218	1.0644	18.741	12.01	500.00
	219	1.0606	18.727	12.02	499.95

Table A.2.6. : Measured weights, densities and dimensions of test fuel rods : Pu II

position of the rod in the cluster	rod number	weight kg	density gr/cm^3	average diameter mm	length mm
center	313	1.0558	18.642	12.01	499.95
inner ring	301	1.0557	18.673	12.00	500.00
	303	1.0443	18.562	11.99	500.00
	305	1.0486	18.570	12.00	500.00
	307	1.0473	18.541	12.00	500.00
	312	1.0611	18.720	11.99	499.95
	306	1.0466	18.553	12.00	499.95
outer ring	302	1.0545	18.679	11.99	500.00
	304	1.0453	18.578	11.99	500.00
	308	1.0480	18.559	12.02	500.00
	309	1.0434	18.504	12.01	500.00
	310	1.0520	18.675	11.98	500.05
	311	1.0610	18.735	12.01	500.05
	314	1.0581	18.670	12.01	500.00
	315	1.0552	18.631	12.00	499.95
	316	1.0530	18.660	12.00	499.85
	317	1.0566	18.635	12.02	499.90
	318	1.0438	18.568	11.98	500.05
	319	1.0576	18.685	12.02	499.90

Table A.2.7. : Measured weights, densities and dimensions of test fuel rods : Pu III

position of the rod in the cluster	rod number	weight kg	density gr/cm^3	average diameter mm	length mm
center	408	1.0712	18.973	12.01	499.98
inner ring	402	1.0666	18.973	11.99	499.98
	403	1.0727	18.973	12.01	499.98
	409	1.0671	18.947	12.01	500.00
	410	1.0709	18.947	12.00	499.98
	416	1.0601	18.798	12.00	500.00
	417	1.0618	18.798	12.02	500.00
outer ring	404	1.0647	18.973	11.99	499.00
	405	1.0721	18.973	11.99	499.98
	406	1.0715	18.973	12.00	499.98
	407	1.0689	18.973	12.01	499.98
	411	1.0697	18.947	12.01	499.98
	412	1.0714	18.947	12.01	499.98
	413	1.0708	18.947	12.00	499.98
	414	1.0706	18.947	11.99	499.98
	418	1.0614	18.798	12.00	499.98
	419	1.0605	18.798	12.01	499.98
	420	1.0602	18.798	12.02	499.98
	421	1.0618	18.798	12.01	499.98

Table A.2.8. : Measured weights, densities and dimensions
of test fuel rods : Pu IV

record number	$\left(\dfrac{\Delta n}{n}\right).10^2$
1	2.8400
2	2.8400
3	2.8285
4	2.8298
5	2.8304
6	2.8329
7	2.8290
8	2.8383
9	2.8352
10	2.8274
11	2.8369
12	2.8294
13	2.8383
14	2.8264
15	2.8345
16	2.8236
average	2.8325
	∓ 0.0013

Table A.3.1. :   Typical set of experimental data :
$\Delta n/n$ values for 16 analysed records
relative to sample PuII/plexiglass
at pitch 18.8 cm.

Test sample	Pu III plexiglas	Pu II plexiglas	Pu II plexiglas	Pu II plexiglas	Pu IV polystirol	Pu IV polystirol	Pu IV polystirol
Lattice pitch (cm)	28.05	18.8	23.5	28.05	18.8	23.5	28.05
Phase angle between the beginning of record and the middle of of sample "in" position	133.5	17.2	155.5	197	316	132	298
Phase angle between the beginning of record and the maximum of first harmonic of signal	166.6	50.6	189.1	231.9	347.4	165.3	331
	33.0	33.4	33.6	34.9	31.4	33.3	33.0

Table A.5.1. : Phase angle of typical test-samples signals
with respect to the oscillation function
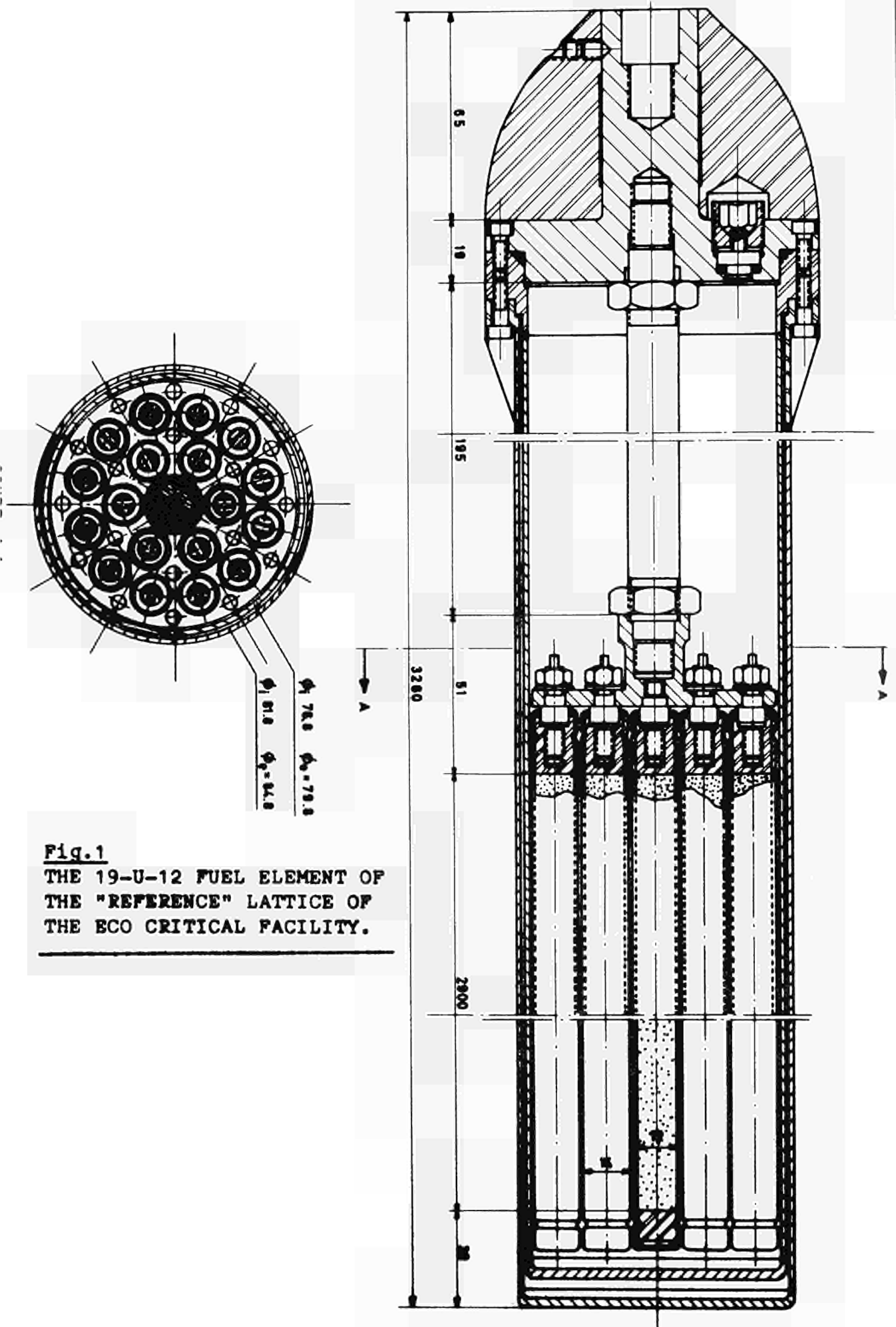
Fig.1
THE 19-U-12 FUEL ELEMENT OF
THE "REFERENCE" LATTICE OF
THE ECO CRITICAL FACILITY.
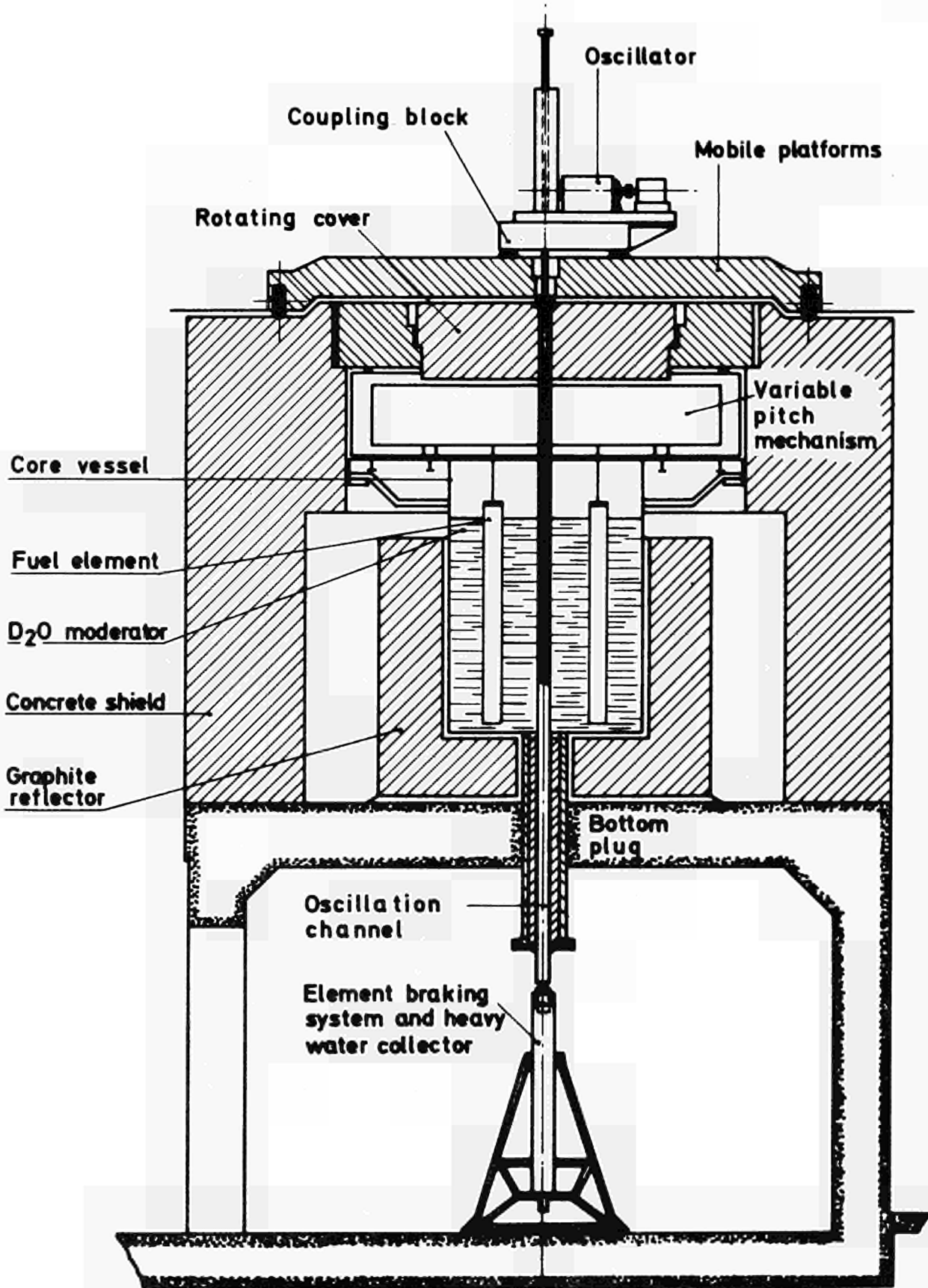
Fig.2 : CROSS SECTION OF THE ECO REACTOR WITH THE FACILITY FOR OSCILLATING THE CENTRAL FUEL ELEMENT.

Fig. 3 : THE TRAPEZOIDAL OSCILLATION FUNCTION

Oscillation period

Upward run

Reference line

Translation amplitude (run)

Downward run

Transit time (rise time)

Transit time (descent time)

Rest time
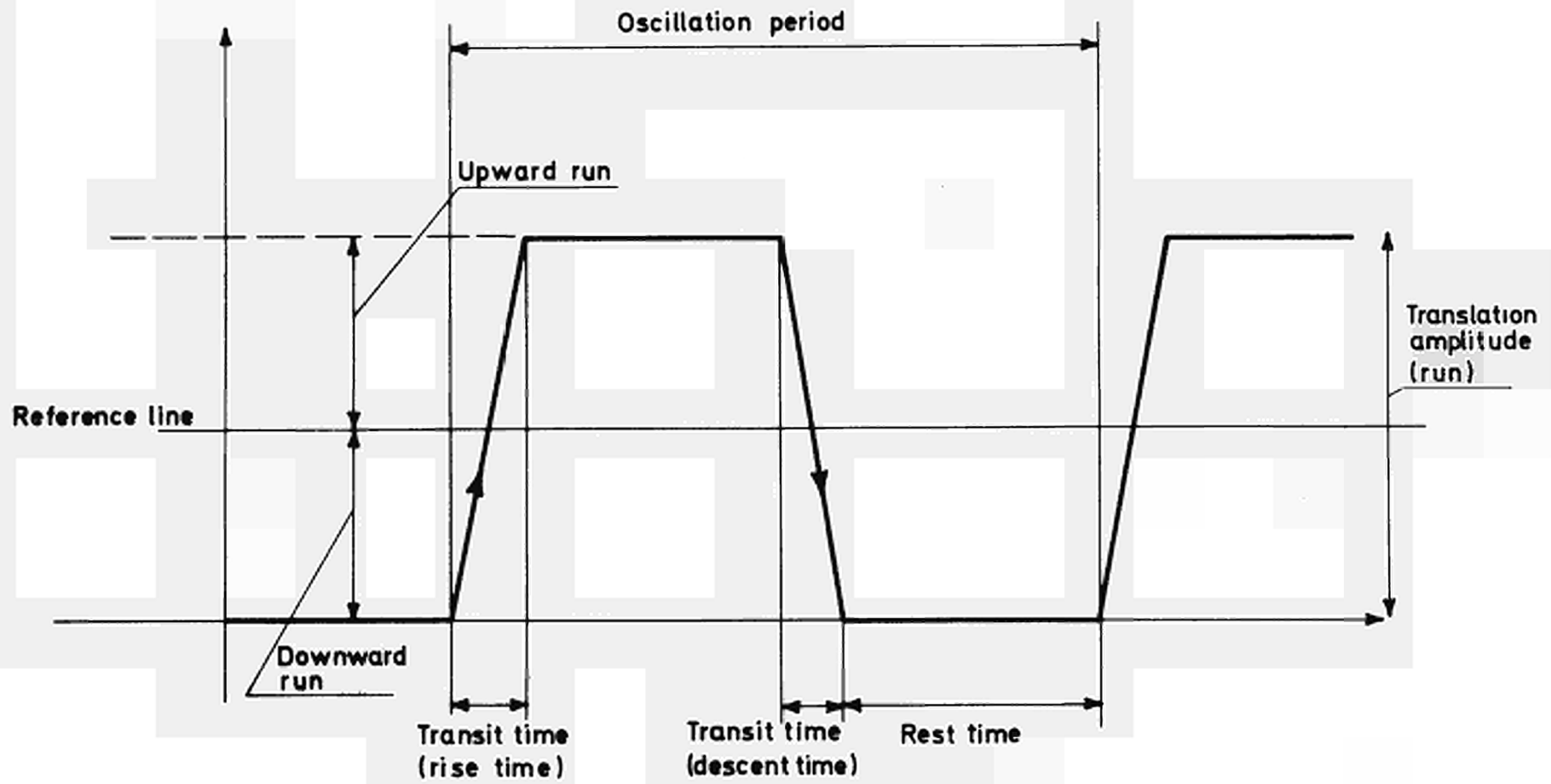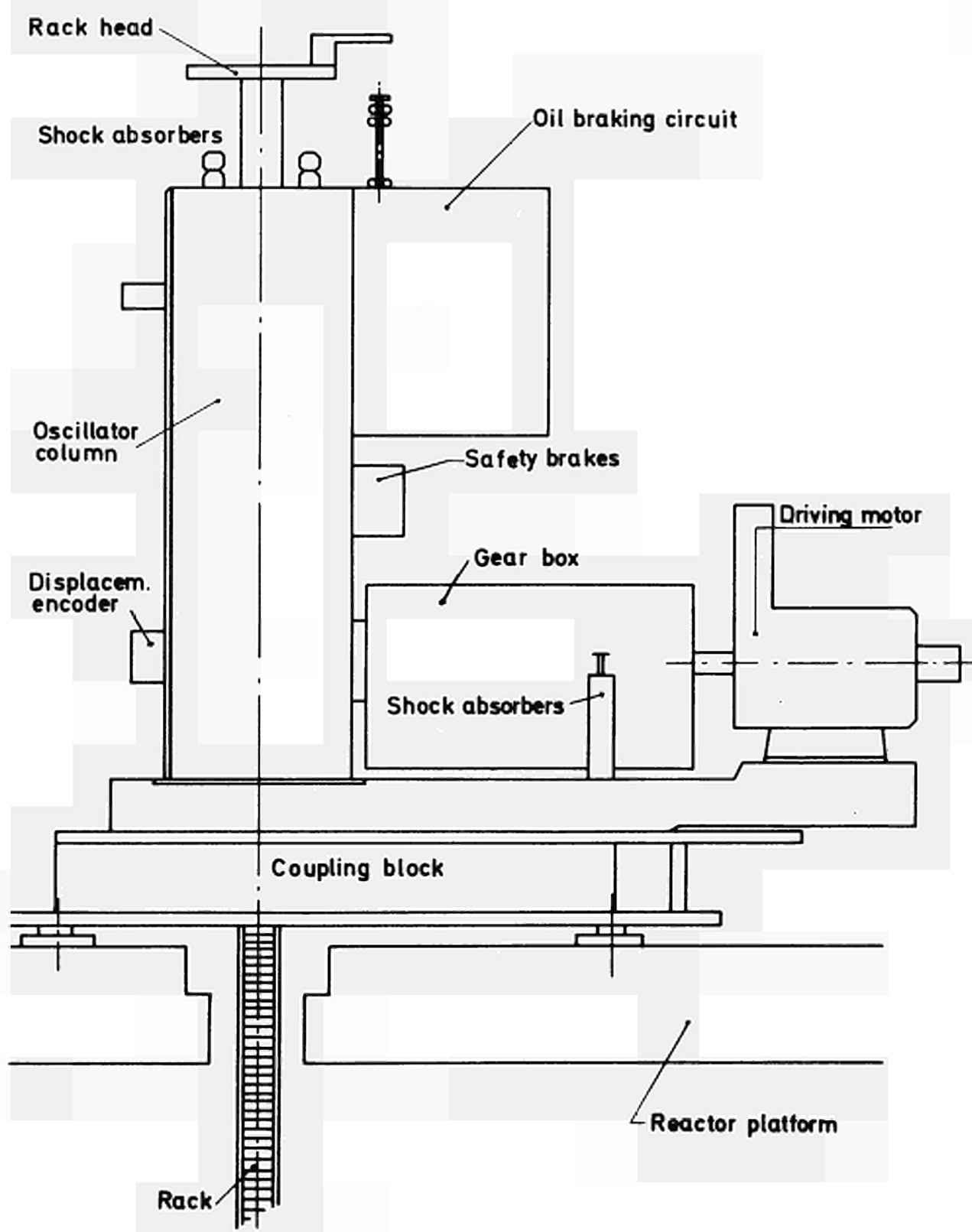
Fig.4. : THE MECHANICAL OSCILLATOR
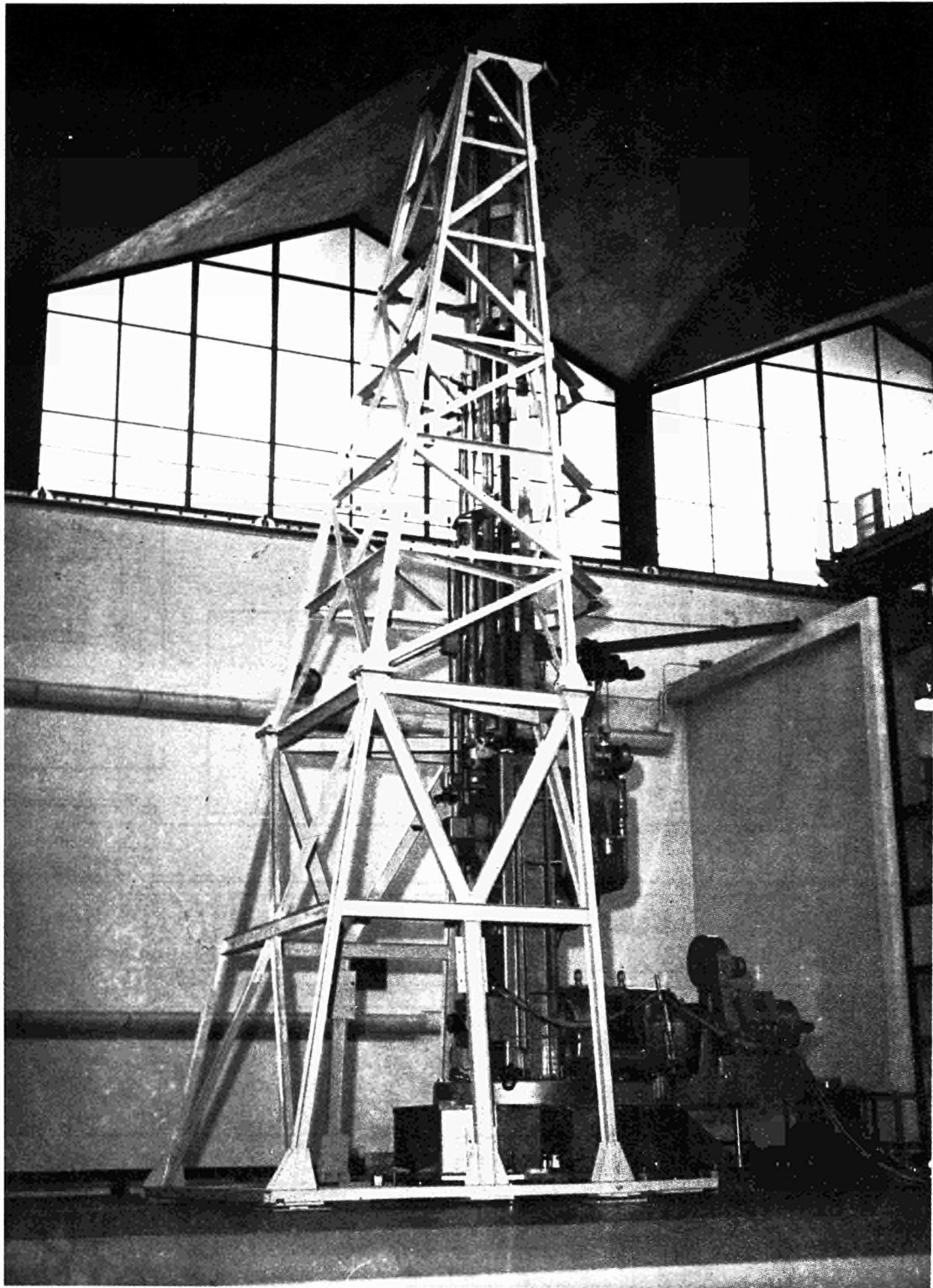
Fig.5 : Oscillator assembly on reactor top plate
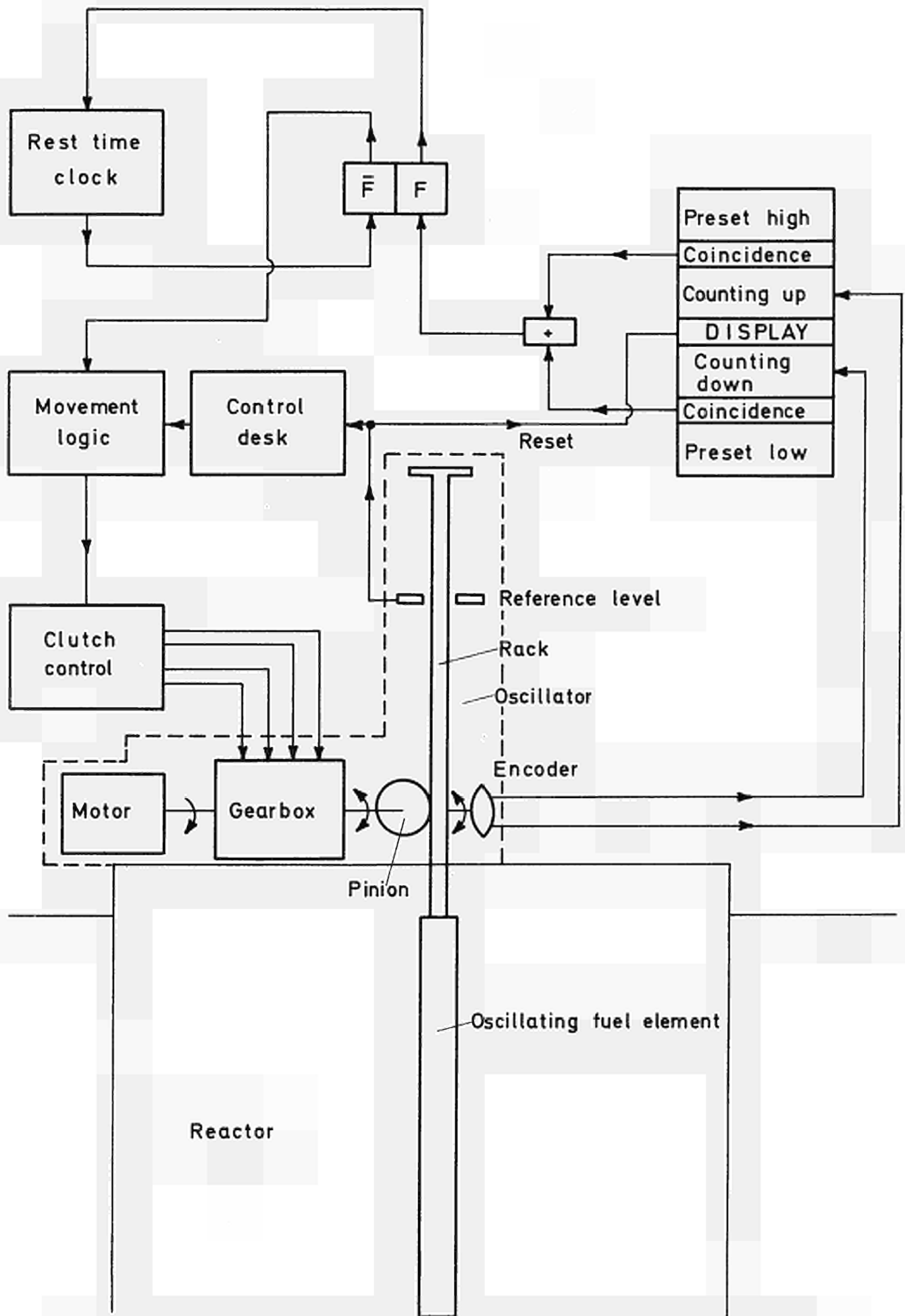
Fig.6 : BLOCK DIAGRAM SHOWING THE OPERATION PRINCIPLE
OF THE OSCILLATOR.
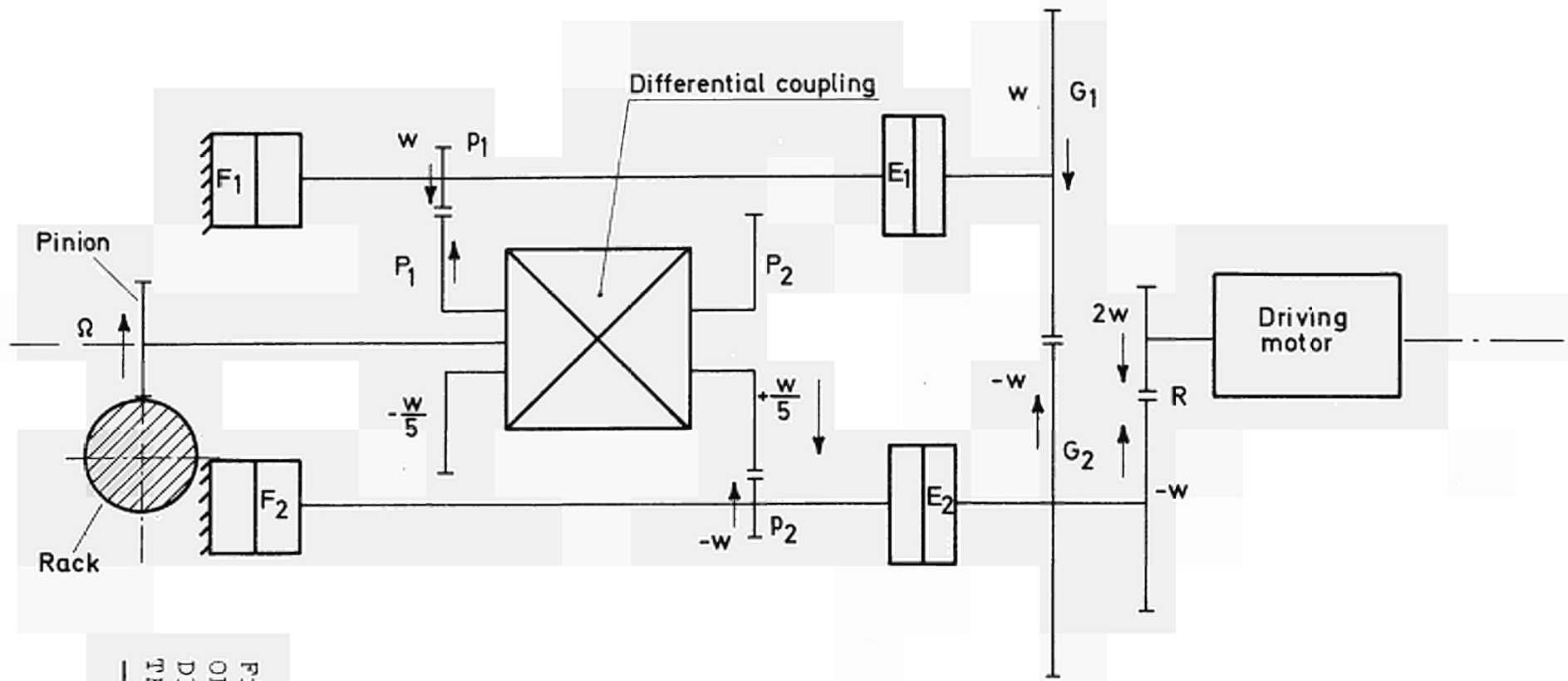
Fig.7
OPERATION PRINCIPLE OF THE
DIFFERENTIAL COUPLING OF
THE OSCILLATOR.

Movement of rack	Magnetic clutches			
	E1	F1	E2	F2
Up wards	1	0	0	1
Stop	1	0	1	0
Down wards	0	1	1	0

0 = open
1 = closed
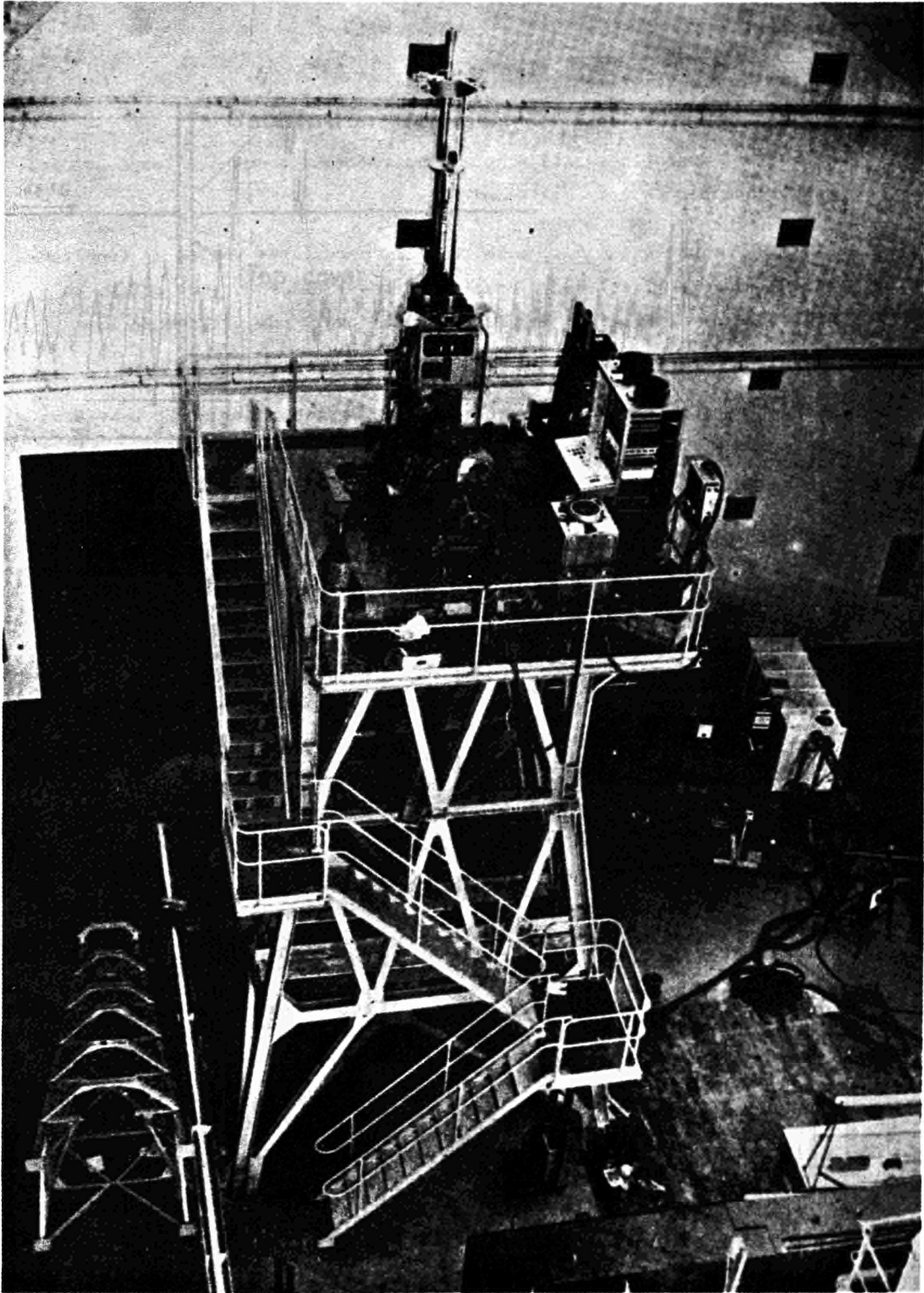
Fig.8 : Oscillation assembly on testing tower

Low rest
position

Start
upward run

Upward run

1g

01 sec

Stop
upward run

High rest position

01sec

1g

High rest position

Start
downward run

Downward run

Stop
downward run

Low rest
position
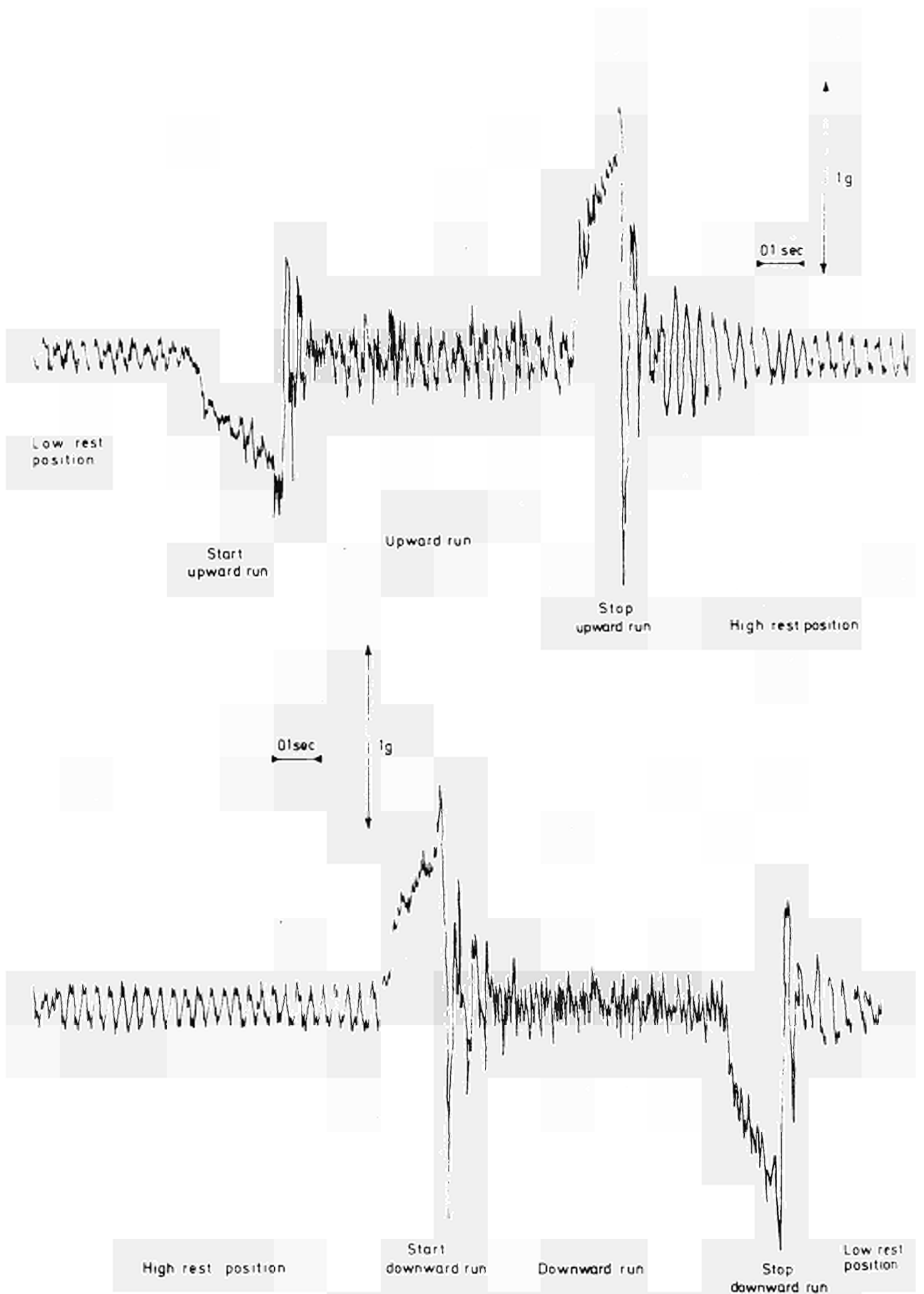
Fig. 9   RECORD OF RACK ACCELERATIONS DURING TRANSIENTS
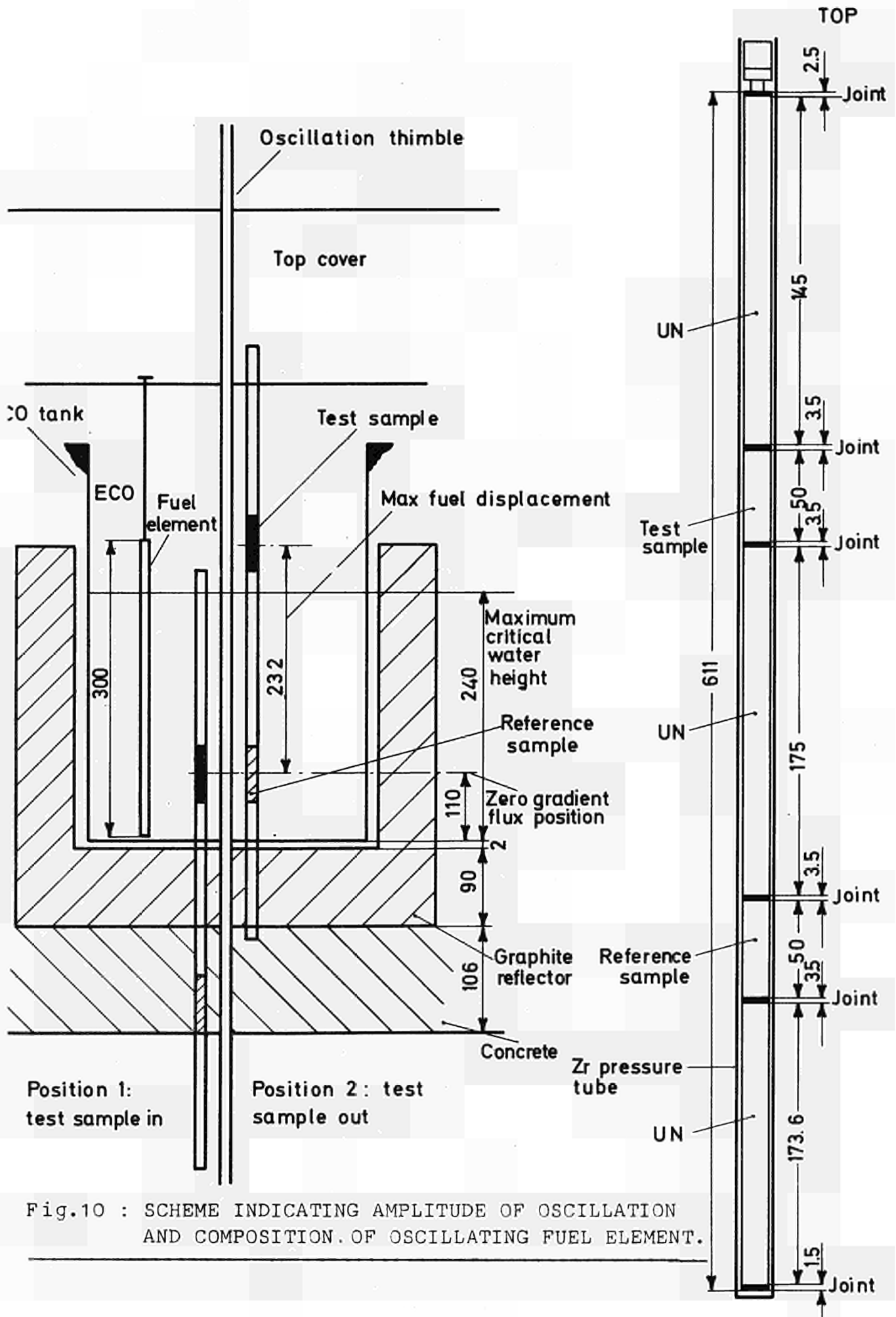
Fig. 10 : SCHEME INDICATING AMPLITUDE OF OSCILLATION
AND COMPOSITION OF OSCILLATING FUEL ELEMENT.

Connection to
head of rack

68

257

297

Upper plug

40

Oscillation tube

Fuel segment

Solid organic matrix
(coolant mock-up)

Fuel element
containment tube

Zirconium joints
between fuel segments

Double action
spring system

Lower plug

185

Centering roller

φ 110
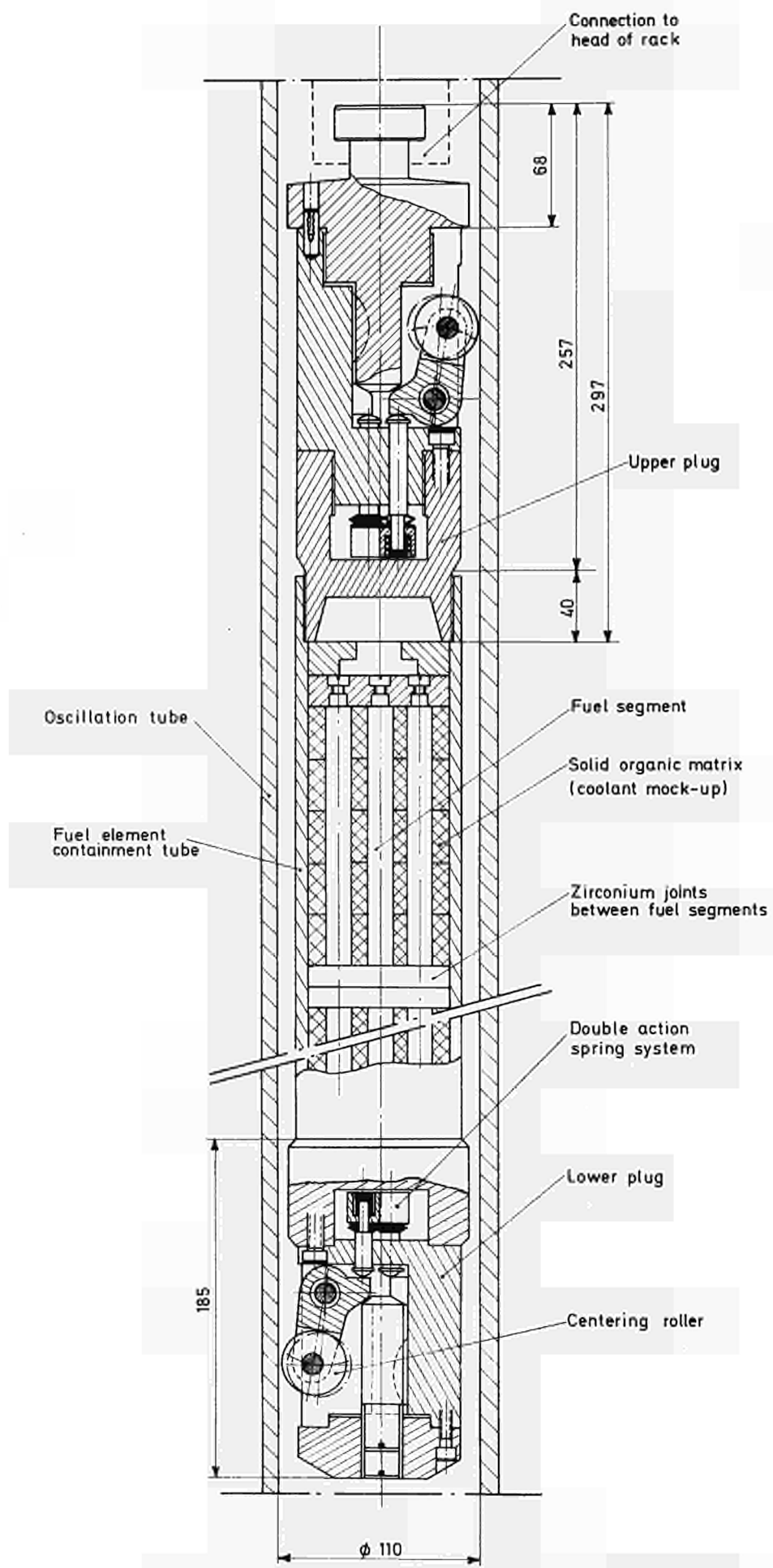
Fig.11. : THE OSCILLATING FUEL ELEMENT. GENERAL VIEW.
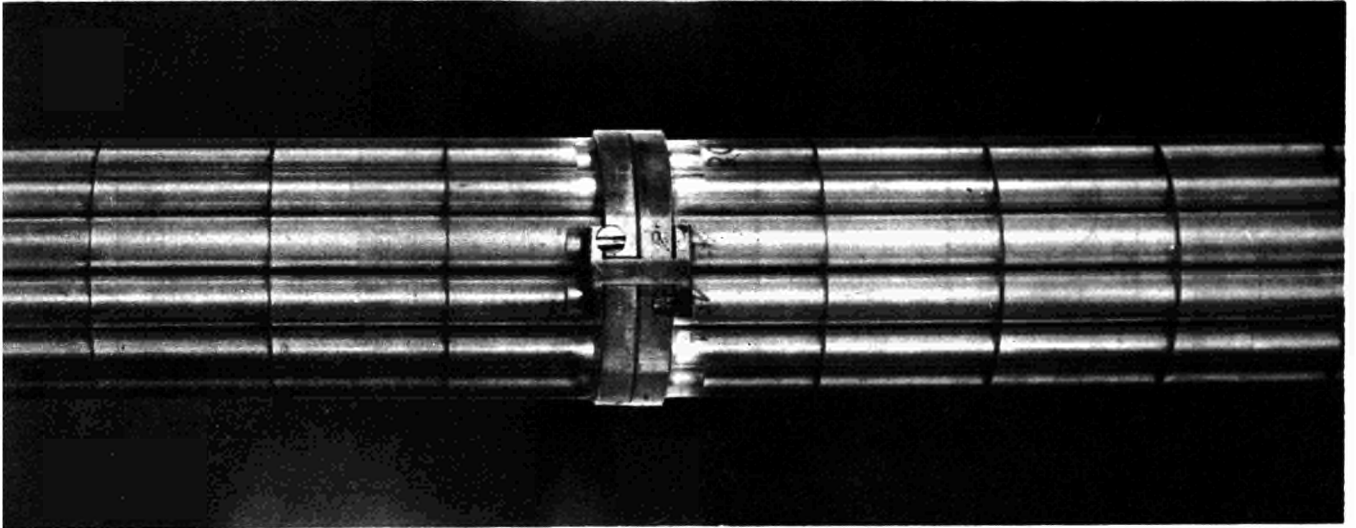
Fig.12 : The oscillation fuel element.
Detail of fuel segments.
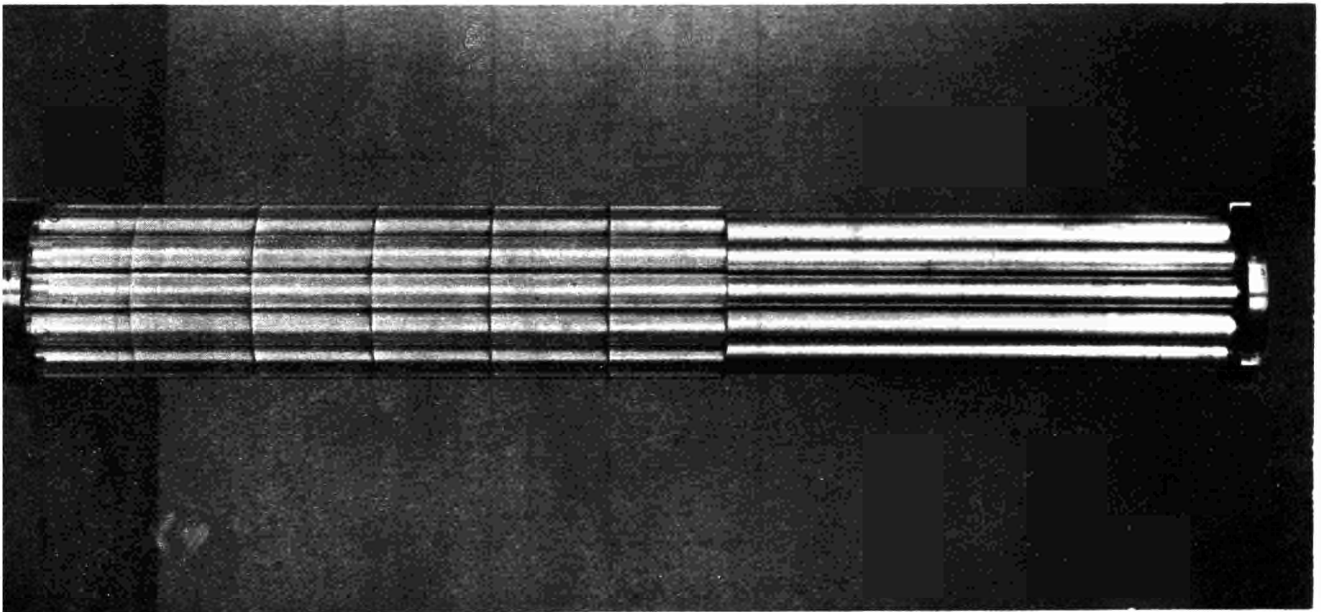
Fig.13 : The fuel test section.
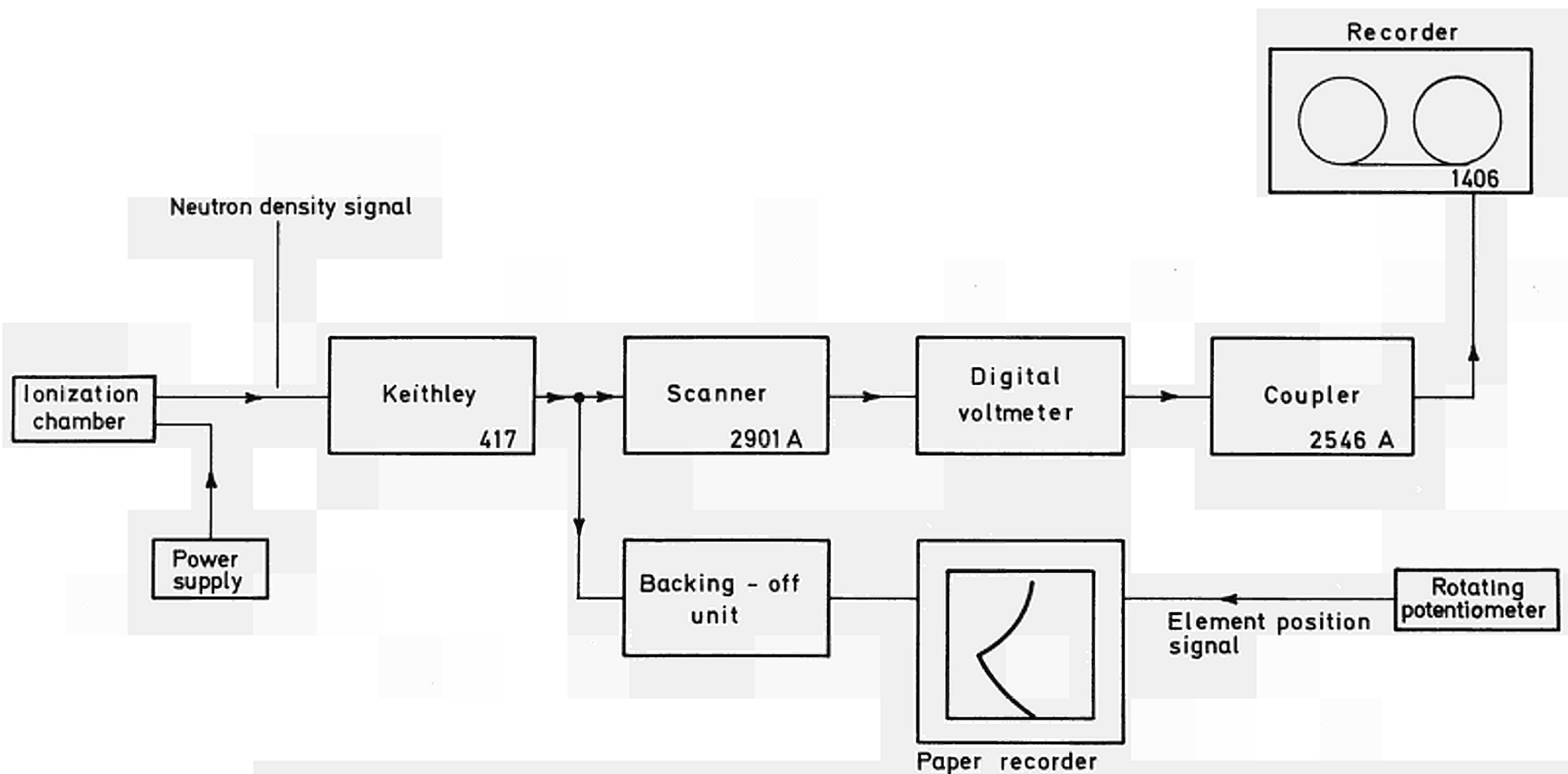
Fig.14 : BLOCK DIAGRAM OF THE INSTRUMENTATION USED FOR RECORDING THE EXPERIMENTAL DATA.

Test fuel
position

Reference
line (zero)

Neutron
density

Single
reading
(for digitalized
neutron
density)

End of
record
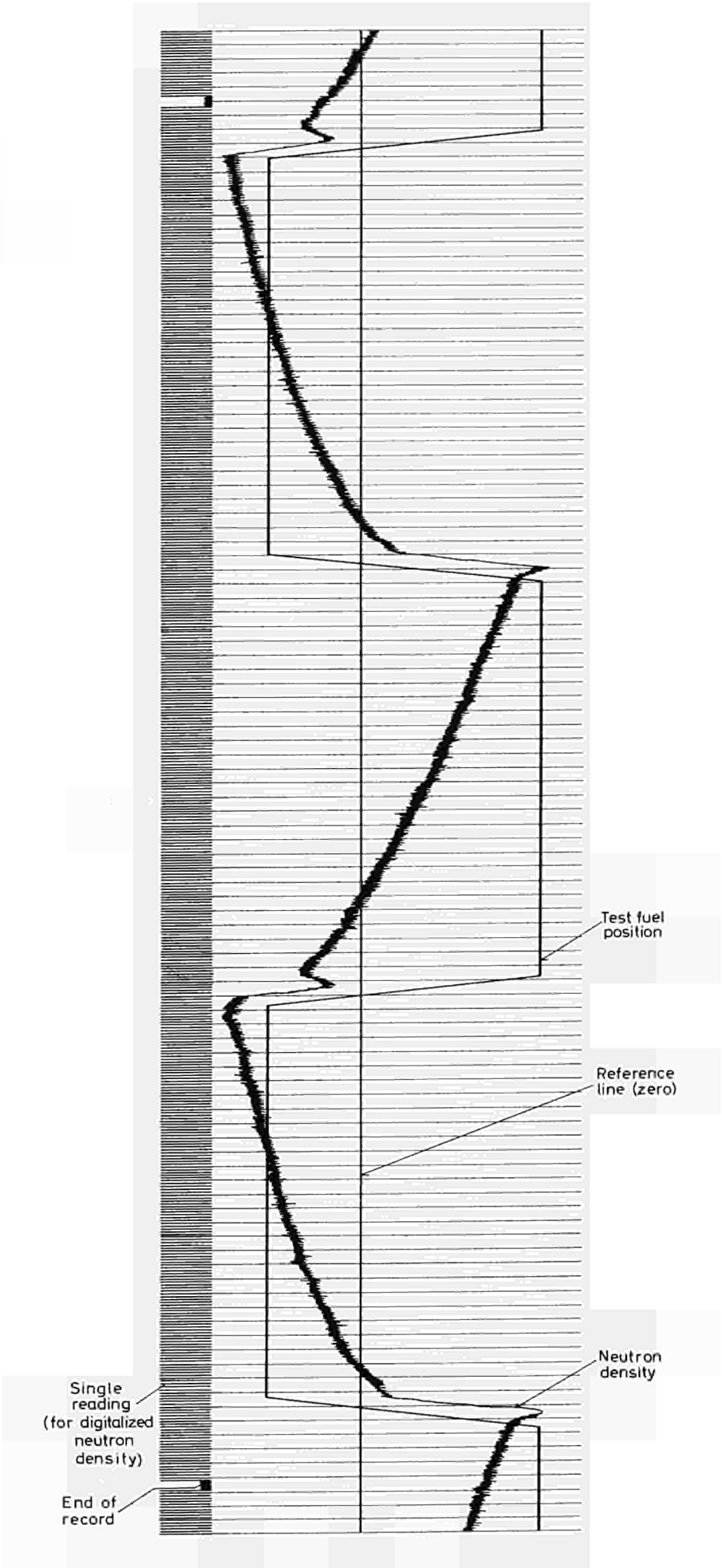
Fig. 15 : EXAMPLE OF FOUR-TRACK RECORD
OF EXPERIMENTAL DATA
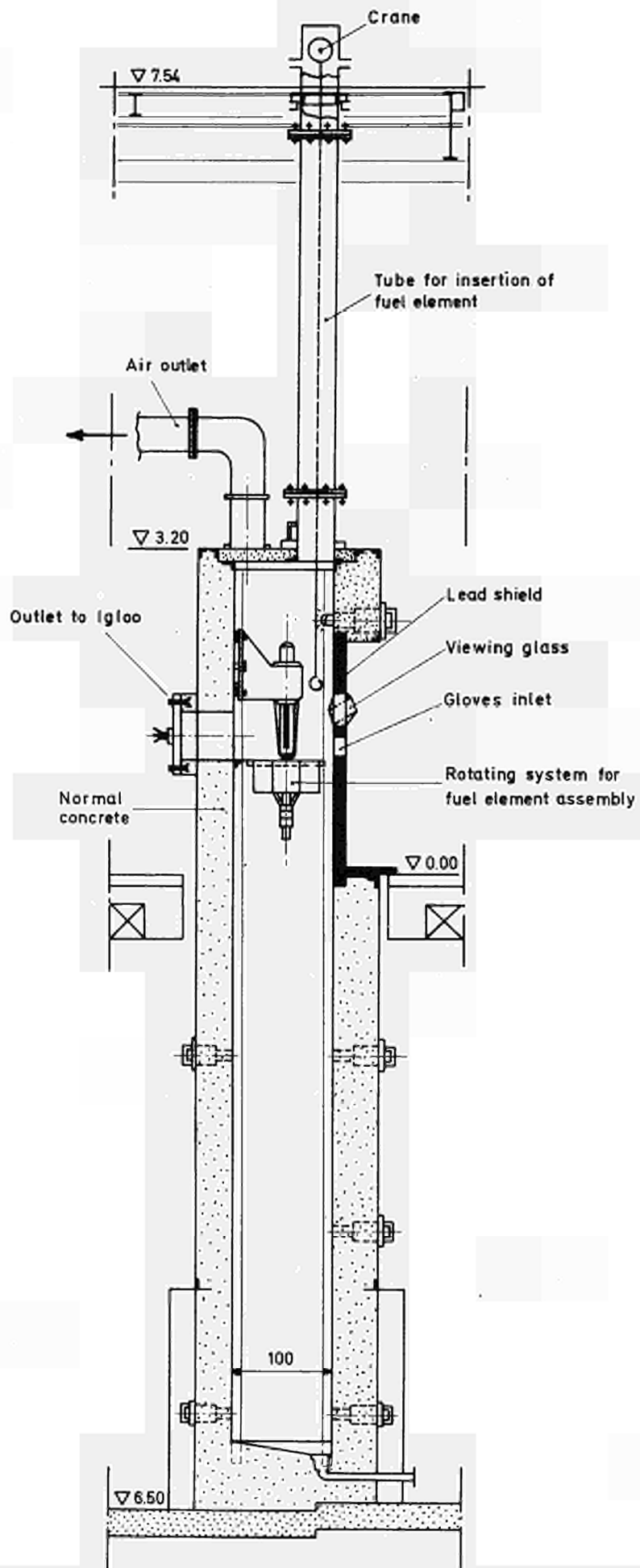
Fig.16 : THE RADIATION SHIELDED CELL FOR THE ASSEMBLY OF THE OSCILLATING FUEL ELEMENT.

4.37

Hood

Glove box

2.50

Filtered air
ventilation
system

Igloo

Radiation shielded
cell

1.80

REACTOR

2.35
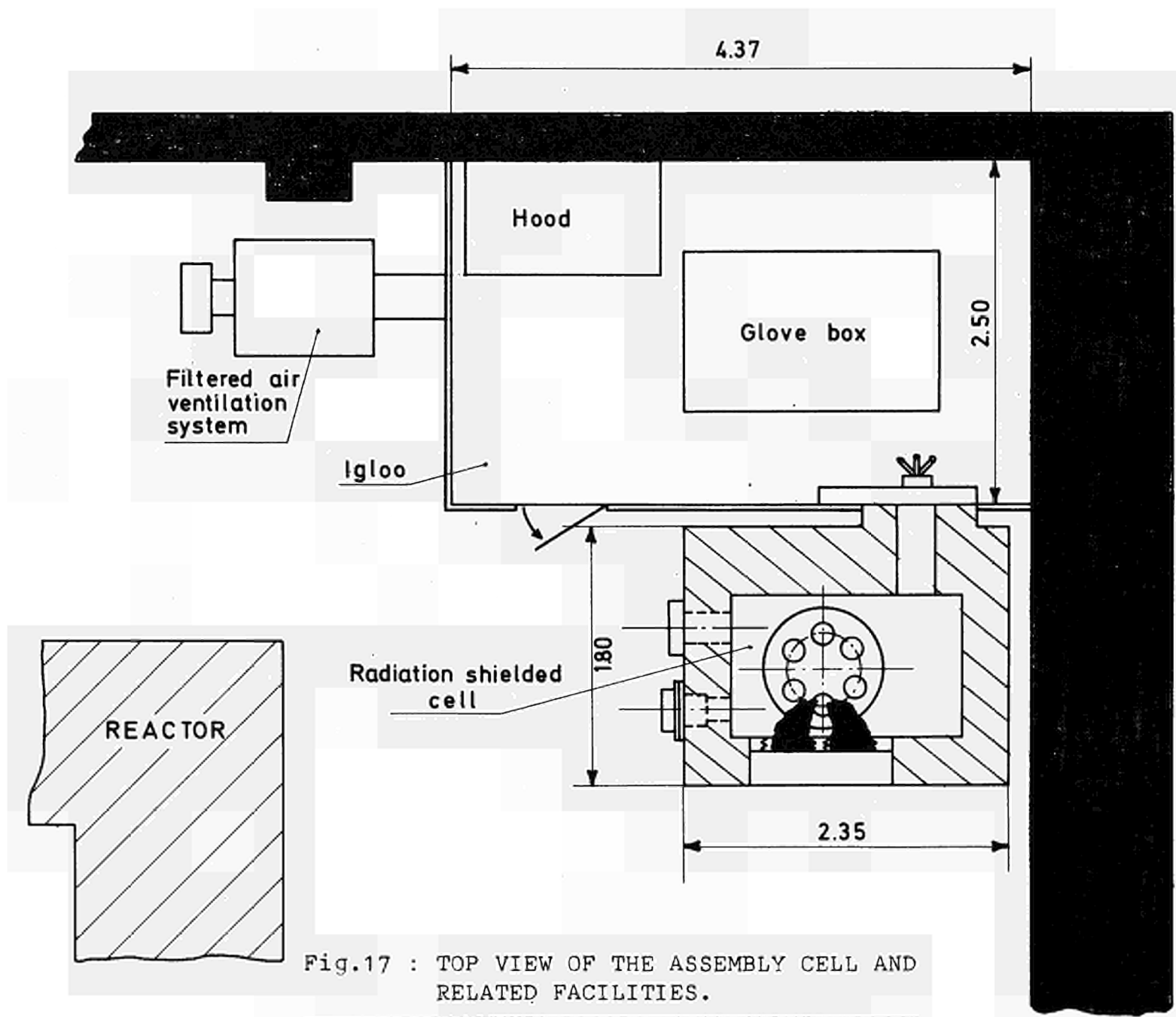
Fig.17 : TOP VIEW OF THE ASSEMBLY CELL AND
RELATED FACILITIES.
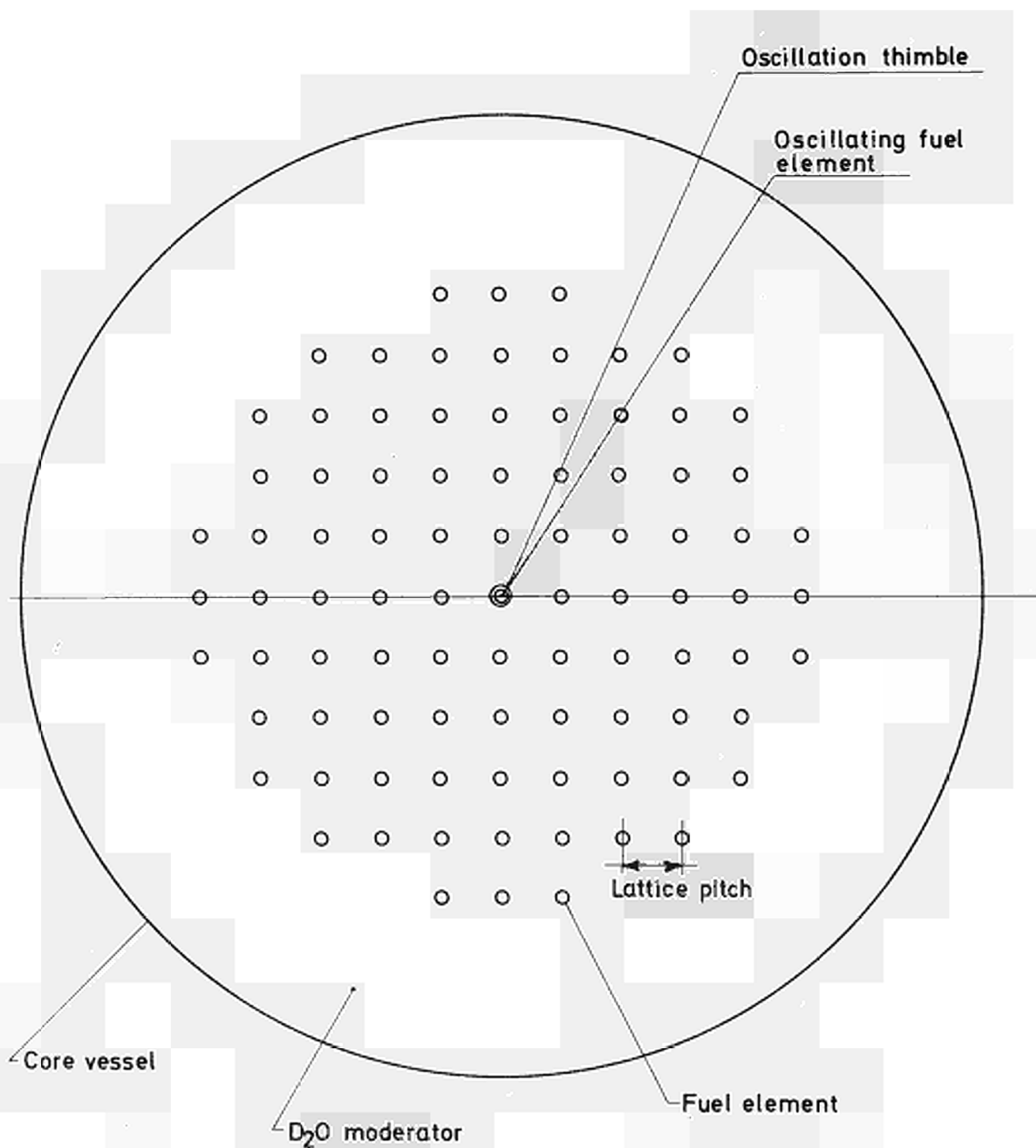
Fig.18a. : ECO LATTICE ARRANGEMENT FOR THE REACTOR OSCILLATION
EXPERIMENT.   LATTICE PITCH 18.8 CM
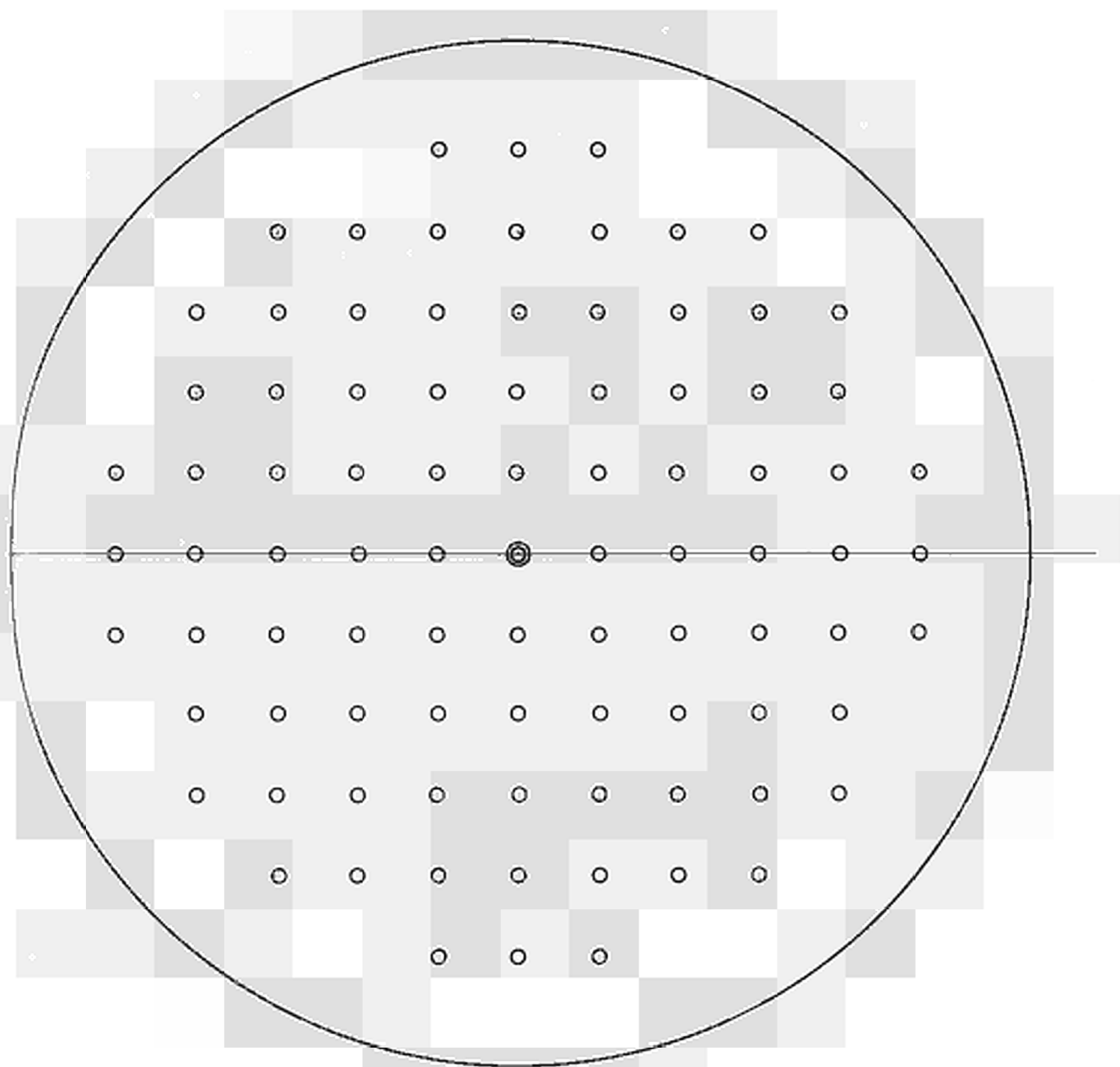
Fig.18b. : ECO LATTICE ARRANGEMENT FOR THE REACTOR OSCILLATION
EXPERIMENT. LATTICE   PITCH 23.5 CM
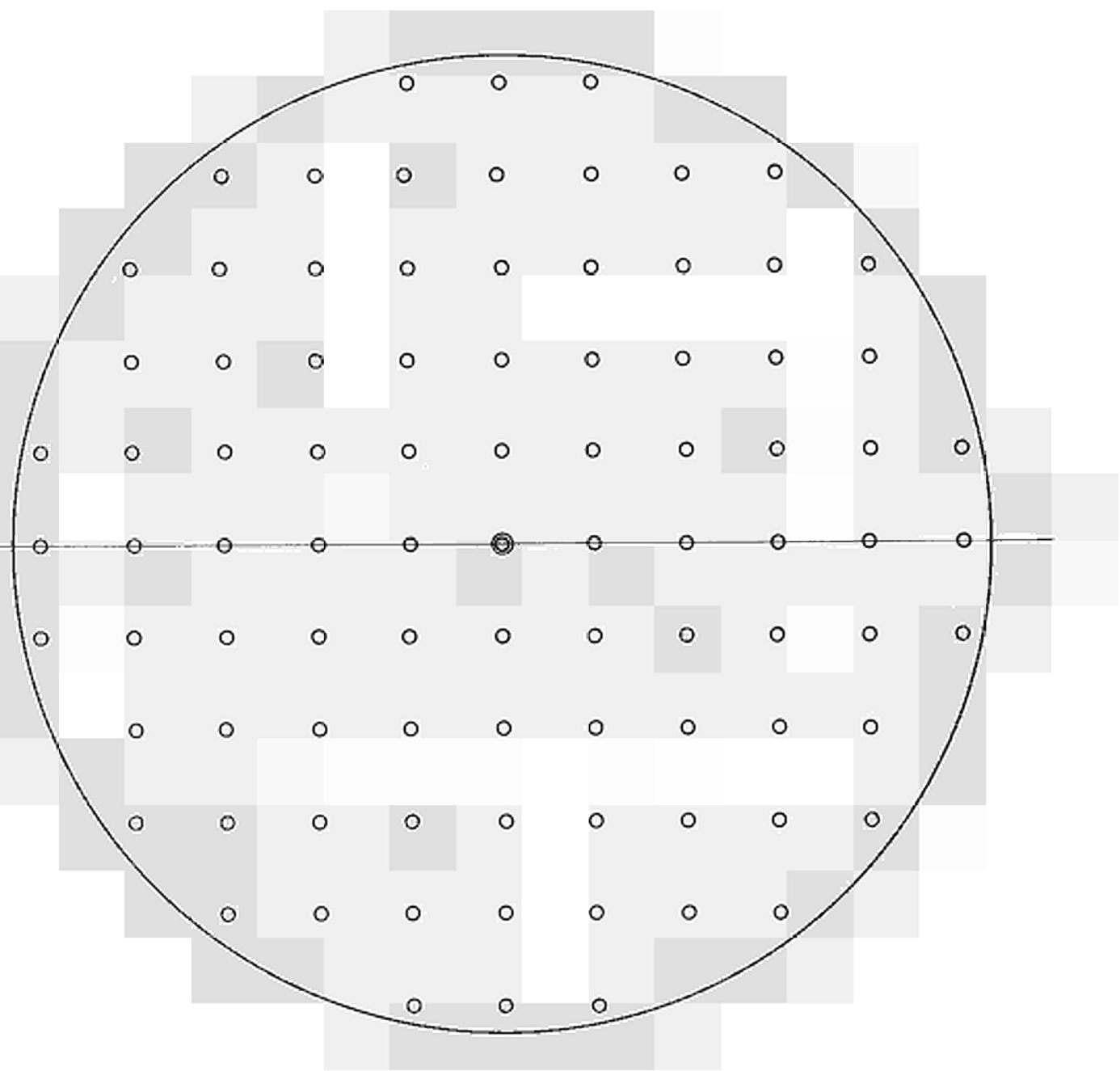
Fig.18c. : ECO LATTICE ARRANGEMENT FOR THE REACTOR
OSCILLATION EXPERIMENT. LATTICE PITCH 28.05 CM.
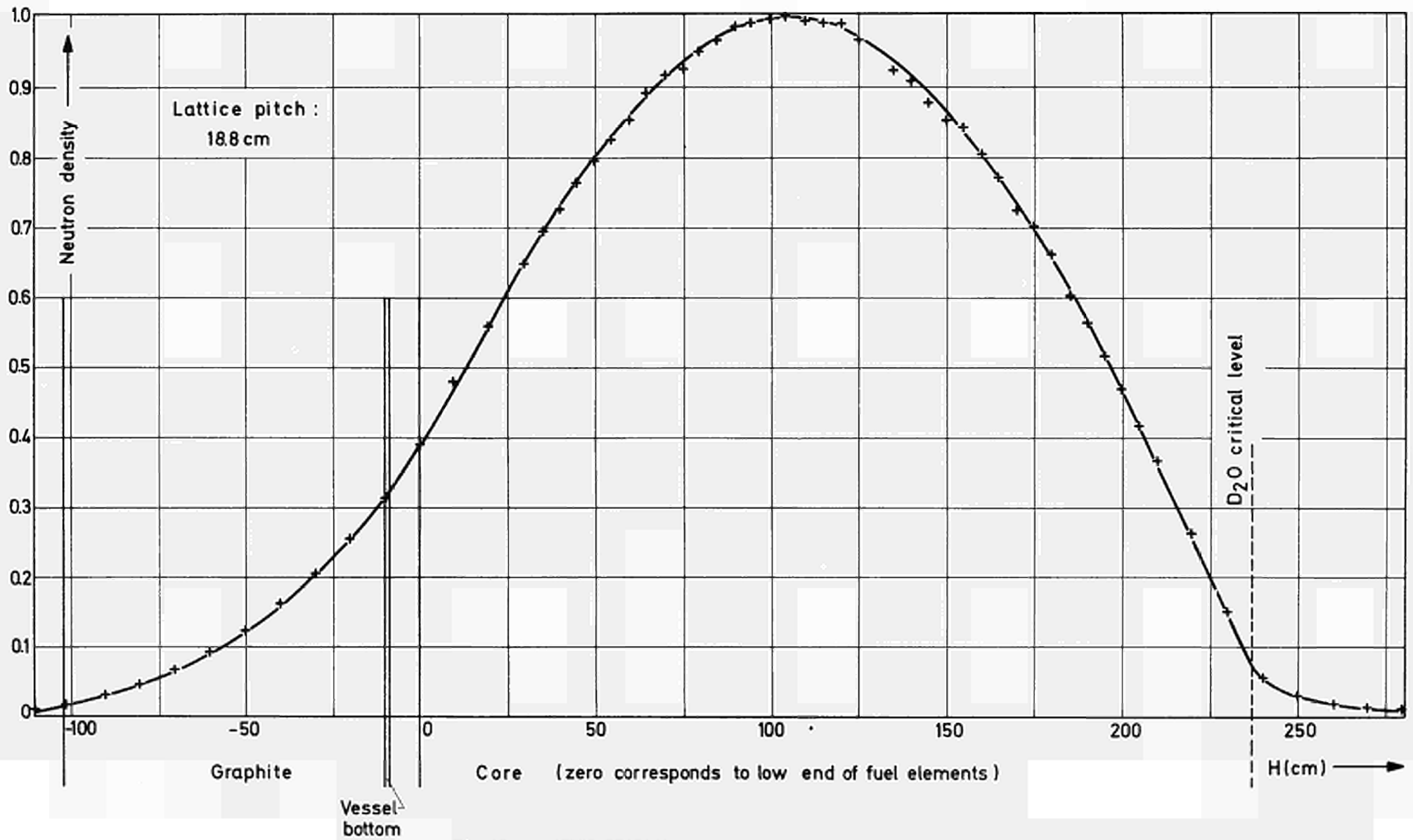
Fig.19a. : AXIAL DISTRIBUTION OF THE NEUTRON DENSITY IN THE OSCILLATION TUBE. LATTICE PITCH 18.8 CM.
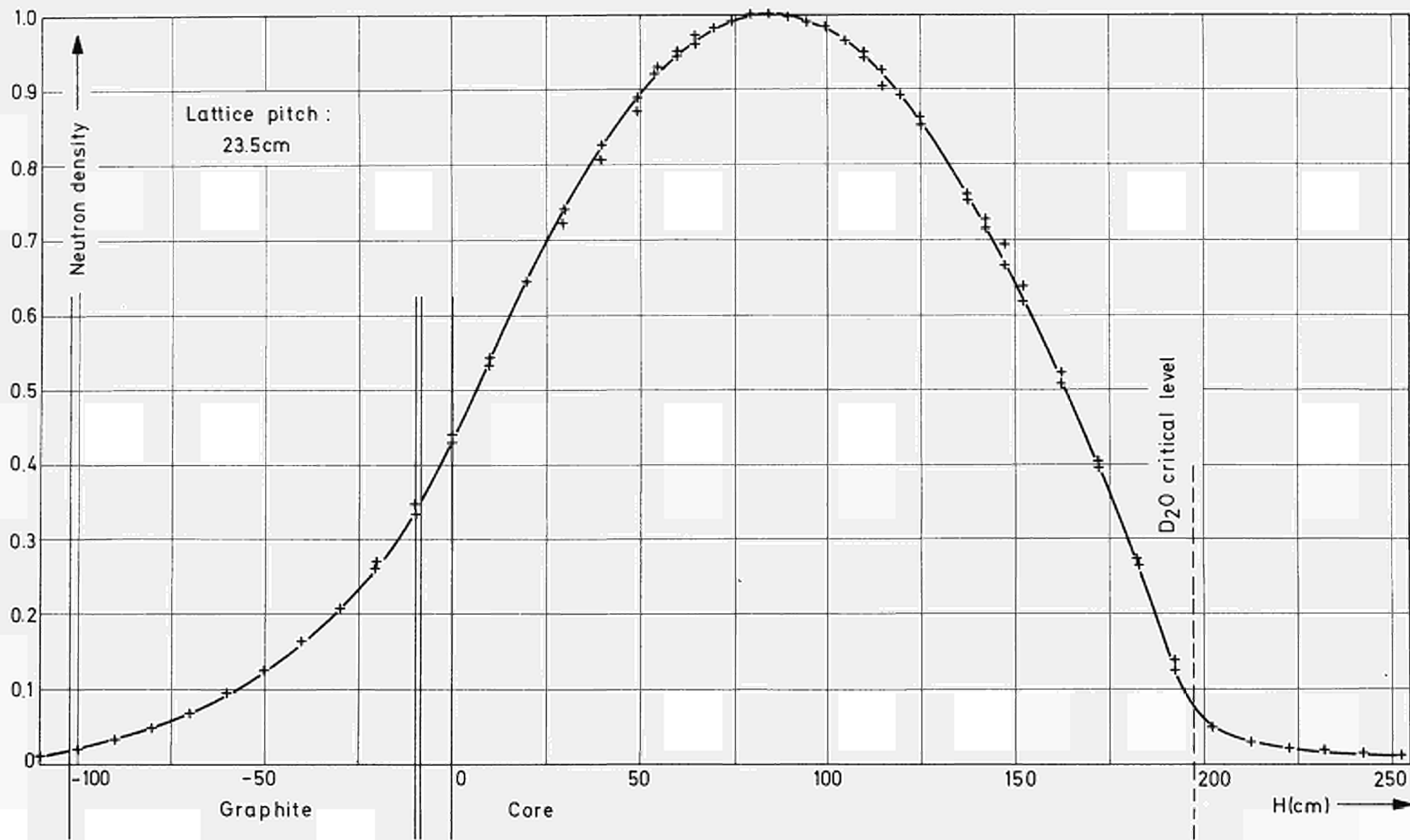
Fig.19b. : AXIAL DISTRIBUTION OF THE NEUTRON DENSITY IN THE OSCILLATION TUBE.
LATTICE PITCH : 23.5 CM.
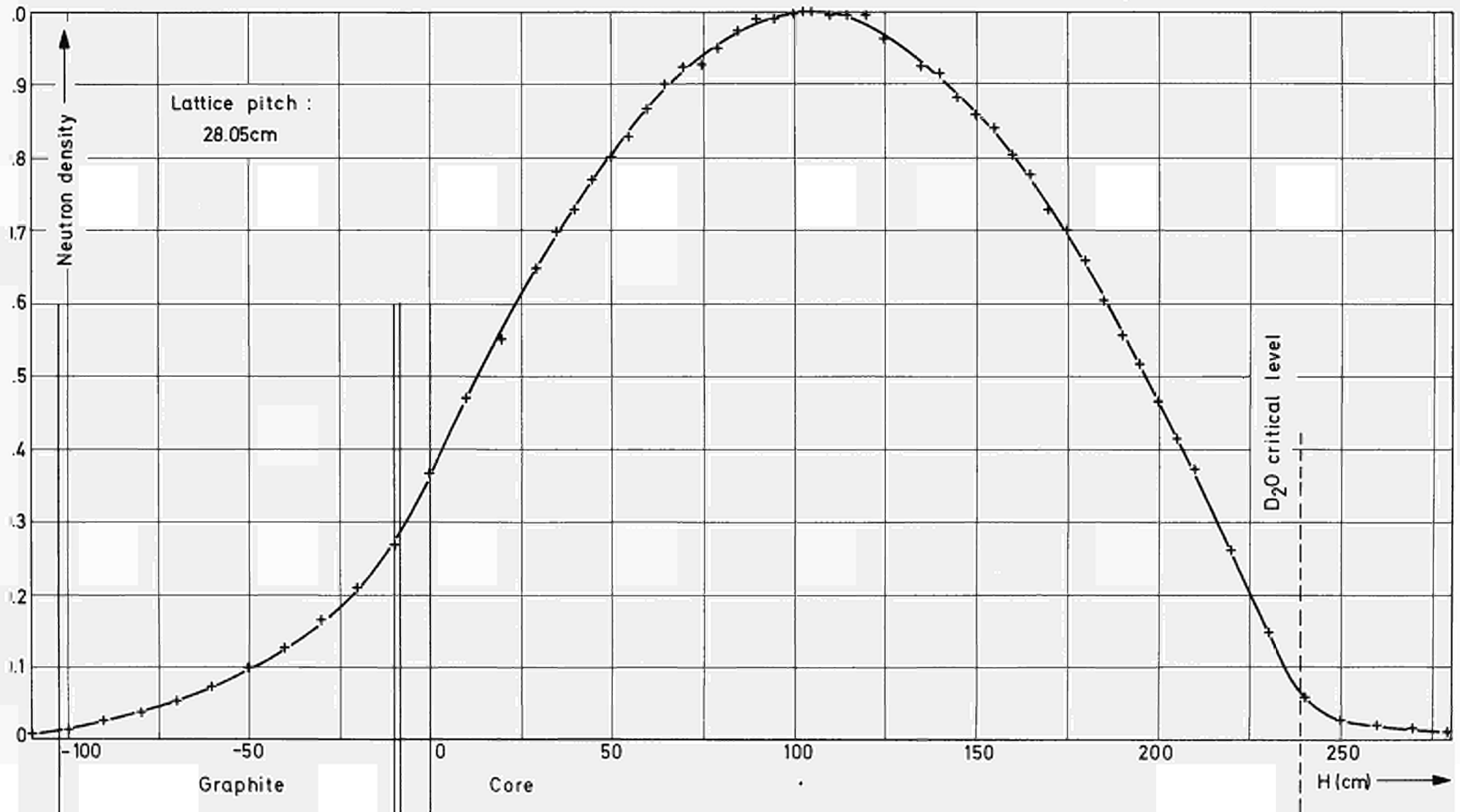
Fig.19e. : AXIAL DISTRIBUTION OF THE NEUTRON DENSITY IN THE OSCILLATION TUBE.
LATTICE PITCH 28.05 CM.
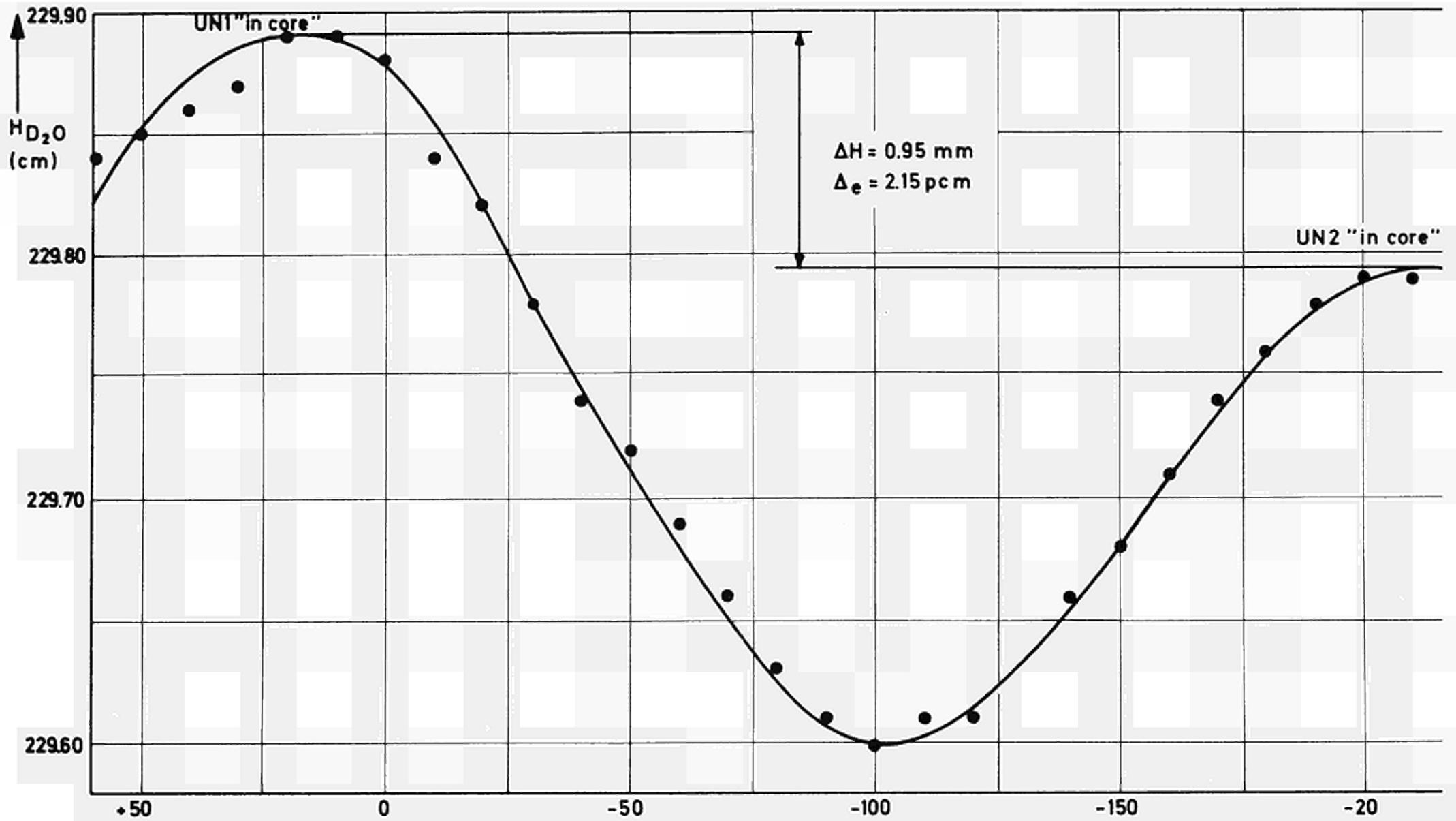
Fig.20a. : REACTIVITY WORTH OF THE OSCILLATING FUEL ELEMENT VERSUS THE AXIAL POSITION OF THE ELEMENT IN THE OSCILLATION TUBE. TEST SECTION UN, LATTICE PITCH 18.8 CM.
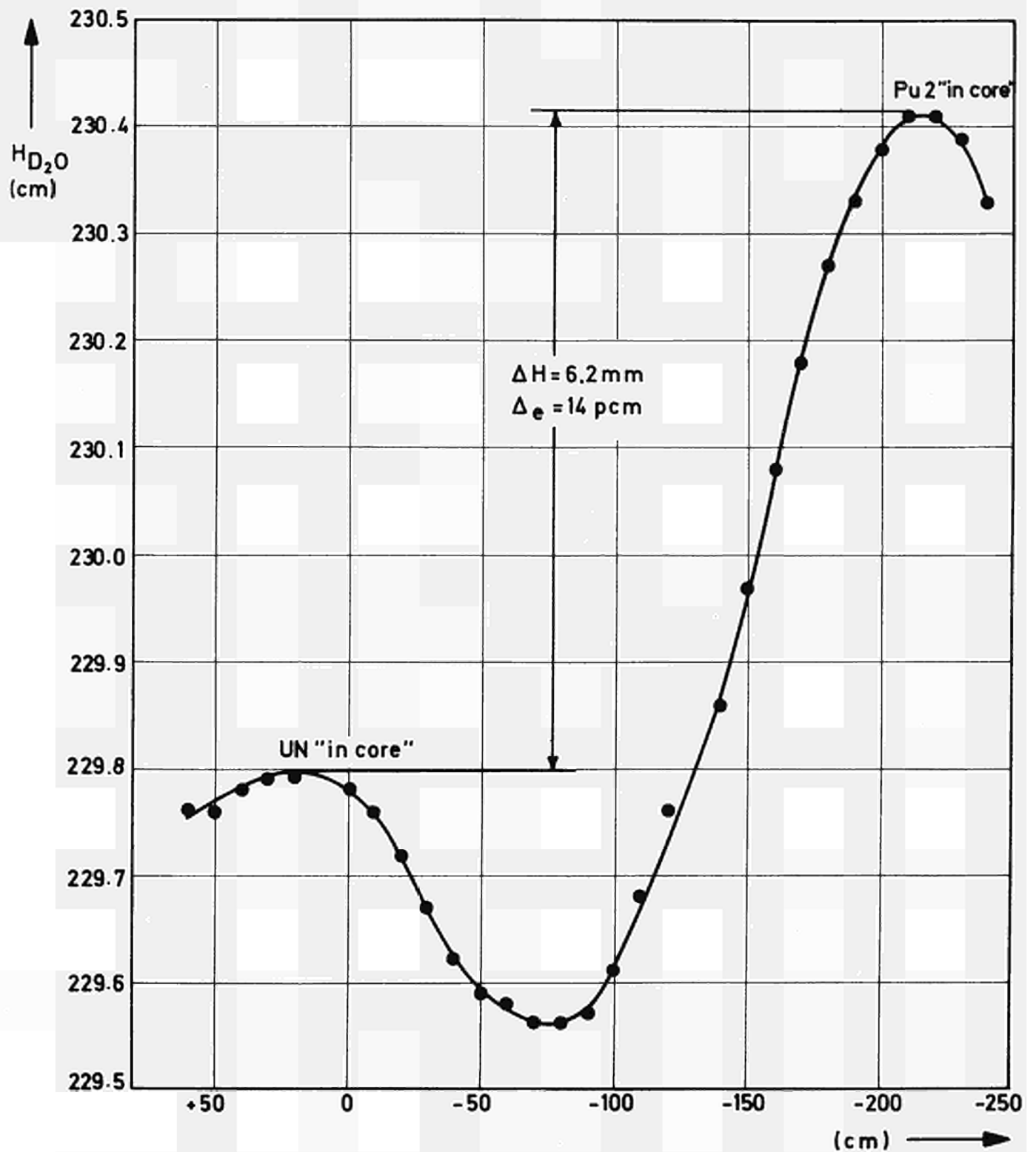
Fig.20b. : REACTIVITY WORTH OF THE OSCILLATING FUEL ELEMENT VERSUS
THE AXIAL POSITION OF THE ELEMENT IN THE OSCILLATION
TUBE.   TEST SECTION Pu II, LATTICE PITCH 18.8 CM.
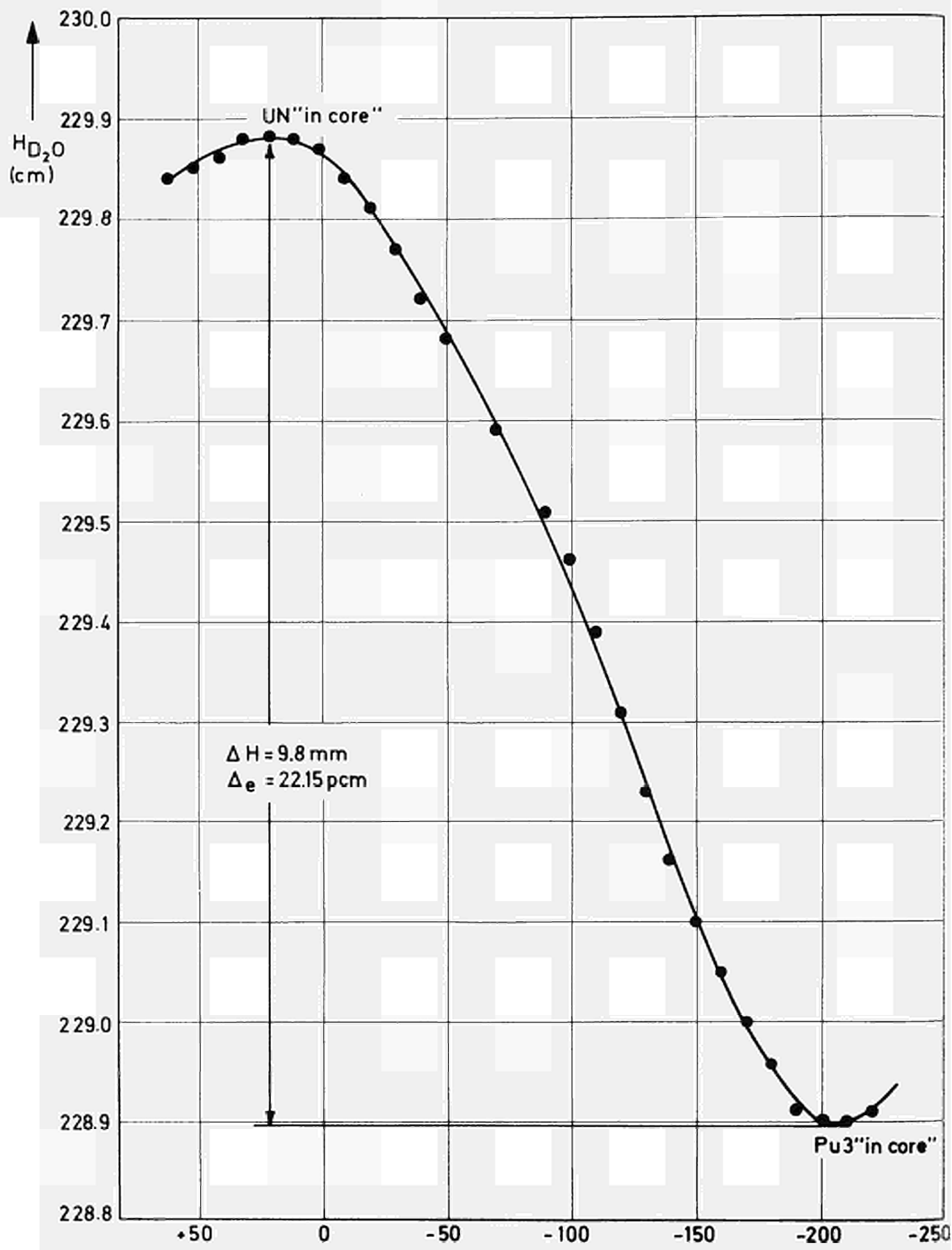
Fig.20c. : REACTIVITY WORTH OF THE OSCILLATING FUEL ELEMENT VERSUS THE AXIAL POSITION OF THE ELEMENT IN THE OSCILLATION TUBE. TEST SECTION PUIII, LATTICE PITCH 18.8CM
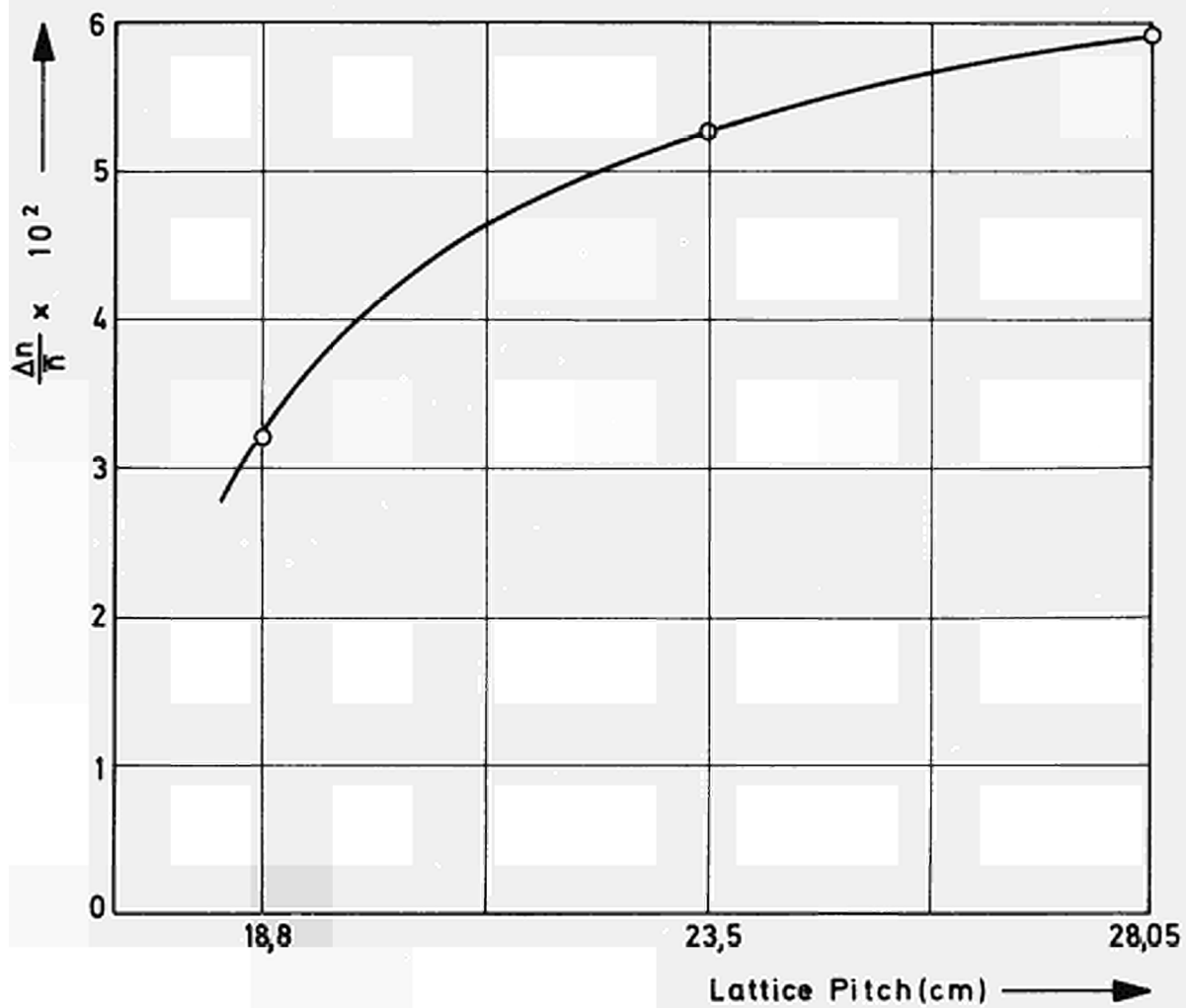
Fig.21 : DEPENDENCE OF THE EXPERIMENTAL RESULT(Δ n/n)
ON THE ECO LATTICE PITCH FOR THE PU II TEST
SECTION.
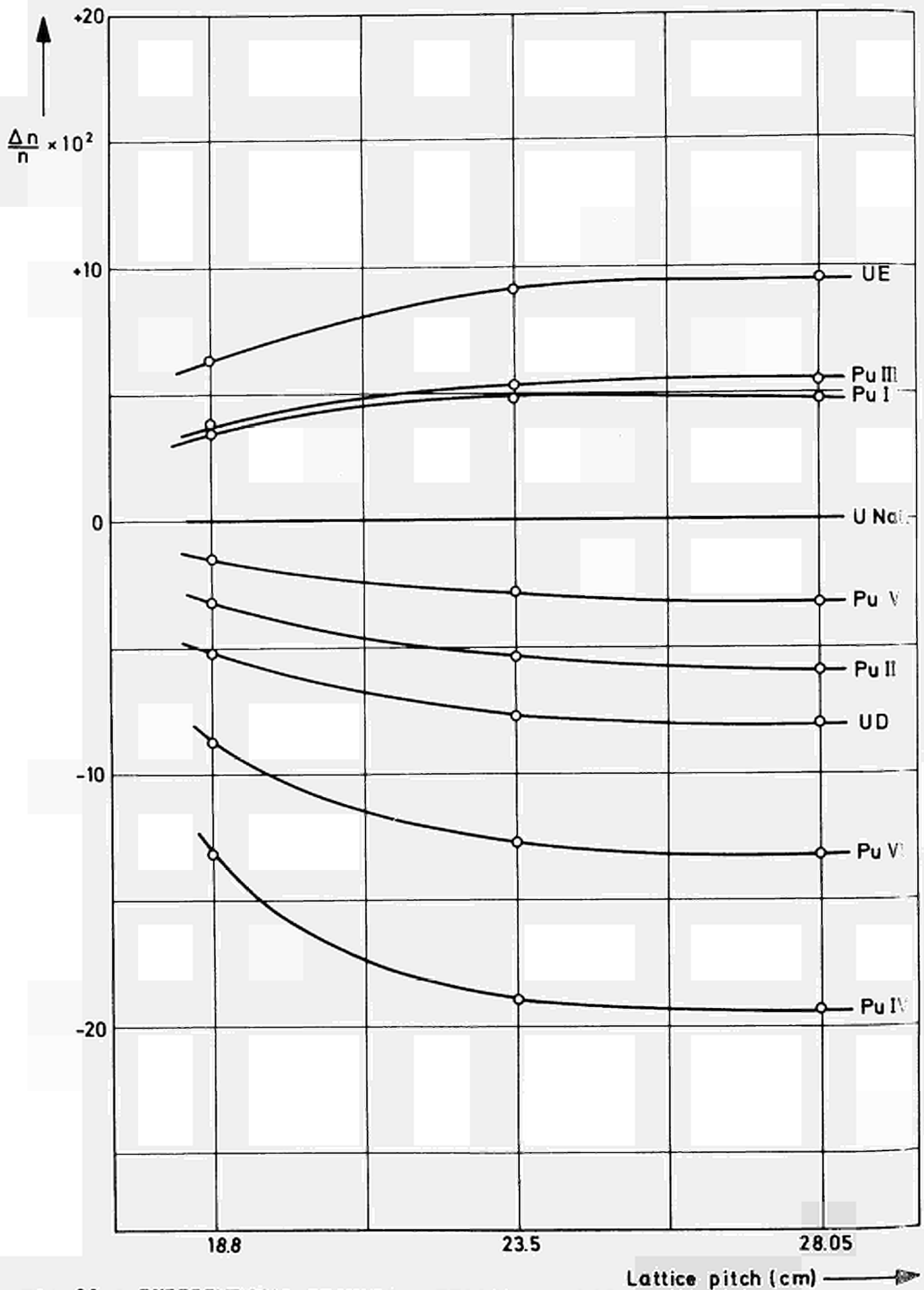
Fig.22 : EXPERIMENTAL RESULTS. REACTIVITY WORTHS OF TEST-FUELS IN PLEXIGLASS MATRIX RELATIVE TO UN IN PLEXIGLASS MATRIX.
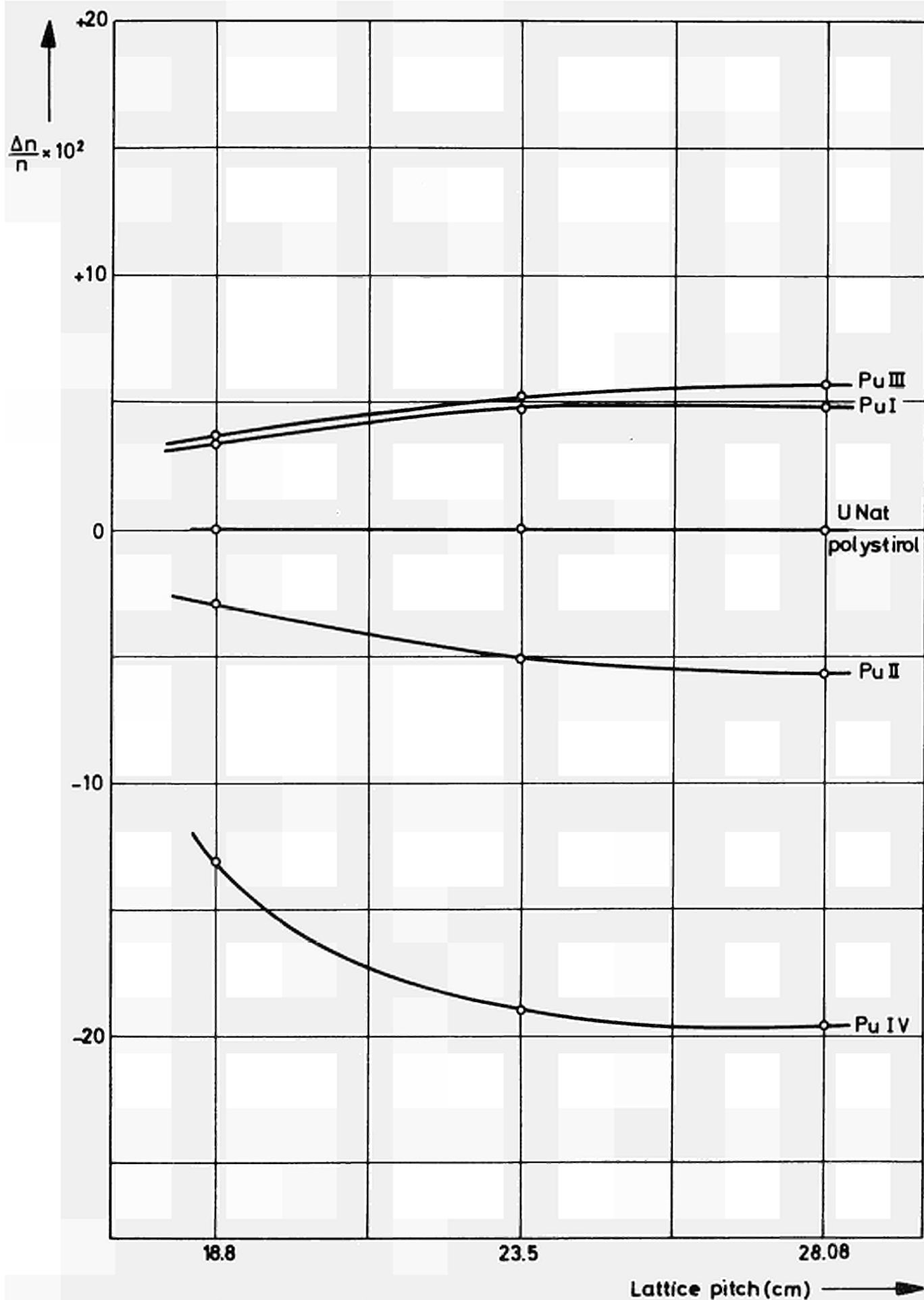
Fig.23 : EXPERIMENTAL RESULTS. REACTIVITY WORTHS OF THE FUELS IN POLYSTIROL MATRIX RELATIVE TO UN IN POLYSTIROL MATRIX.
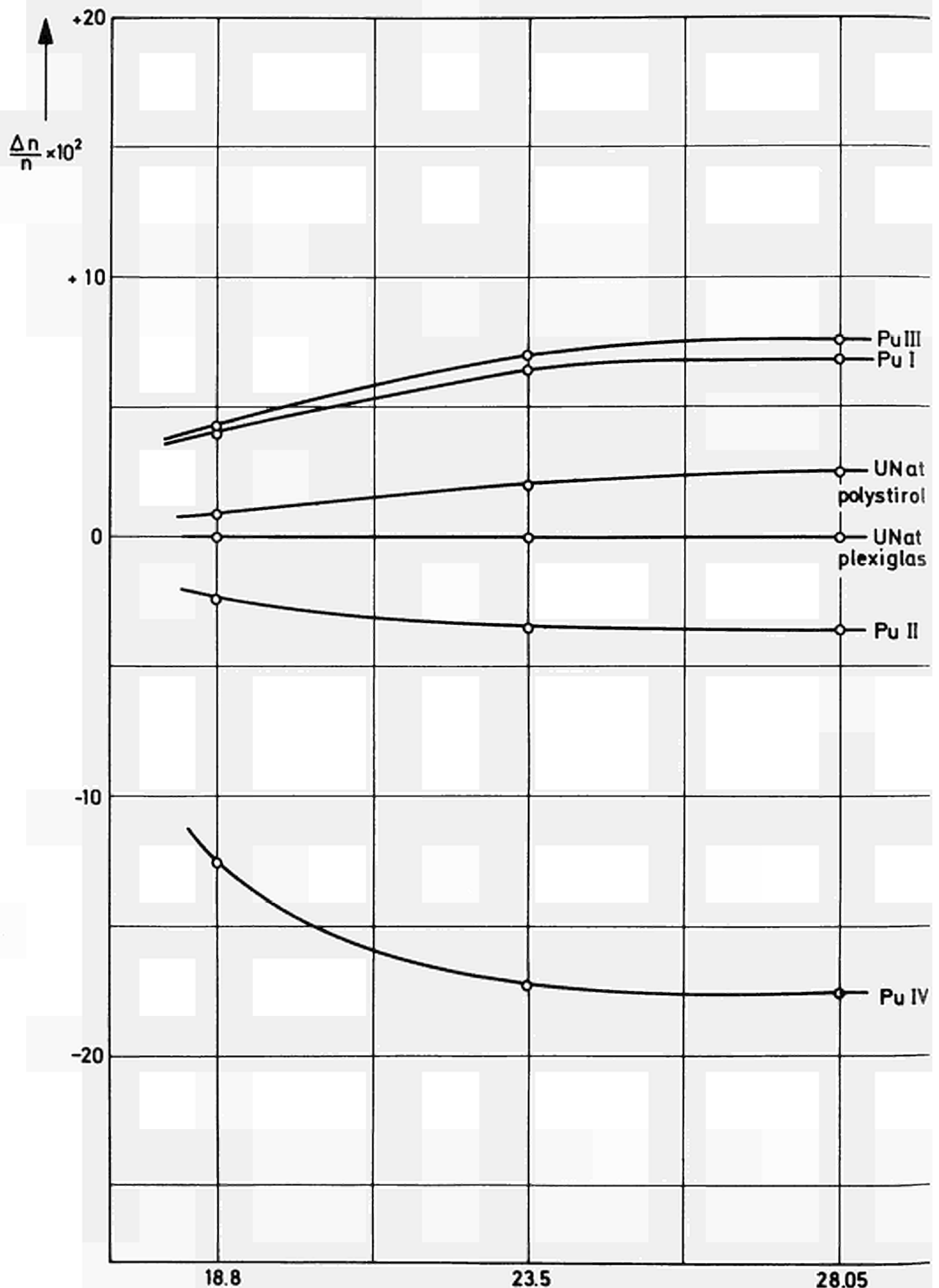
Fig.24 : EXPERIMENTAL RESULTS. REACTIVITY
WORTHS OF TEST FUELS IN POLYSTIROL MATRIX RELATIVE
to UN IN PLEXIGLASS MATRIX.
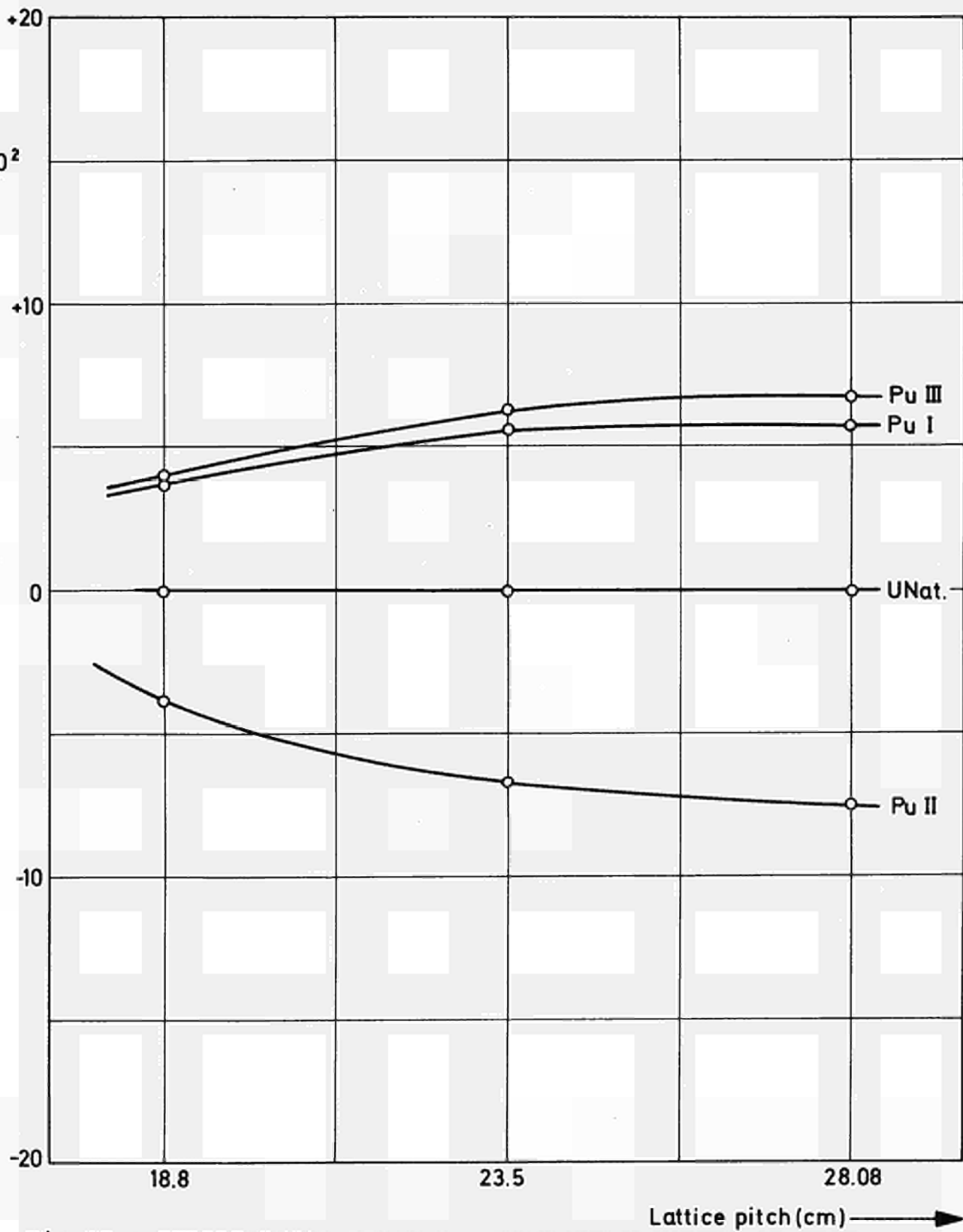
Fig.25 : EXPERIMENTAL RESULTS. REACTIVITY WORTHS OF TEST
FUELS IN AIR RELATIVE TO UN IN AIR.
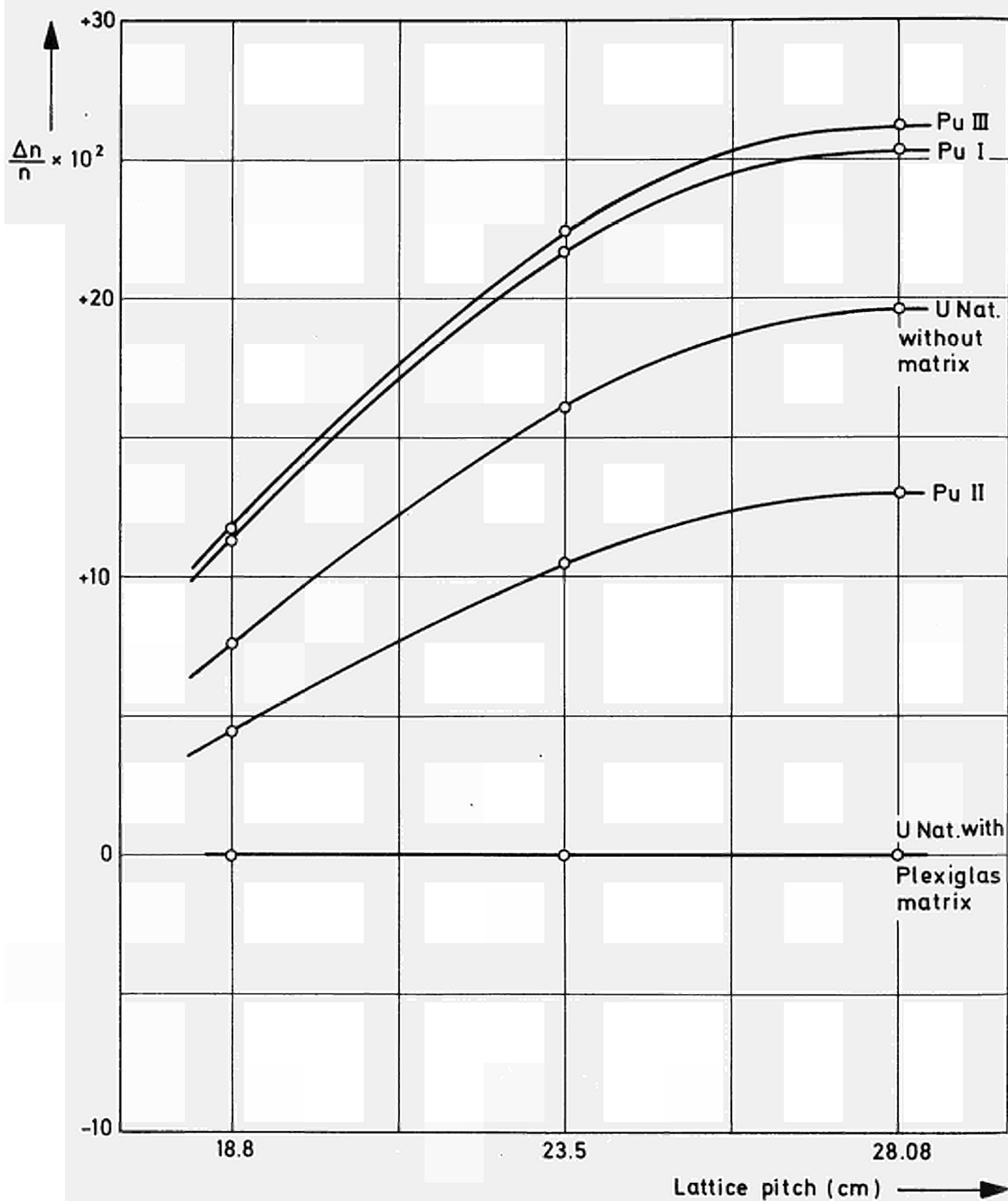
Fig.26 : EXPERIMENTAL RESULTS. REACTIVITY WORTHS OF TEST FUELS
IN AIR RELATIVE TO UN IN PLEXIGLASS MATRIX.

Fig. 27: COMPARISON BETWEEN THE RESULTS OF THE REACTOR OSCILLATION EXPERIMENTS AND OF THE REACTIVITY MEASUREMENT BY THE STATIC METHOD. LATTICE PITCH 18.8 cm
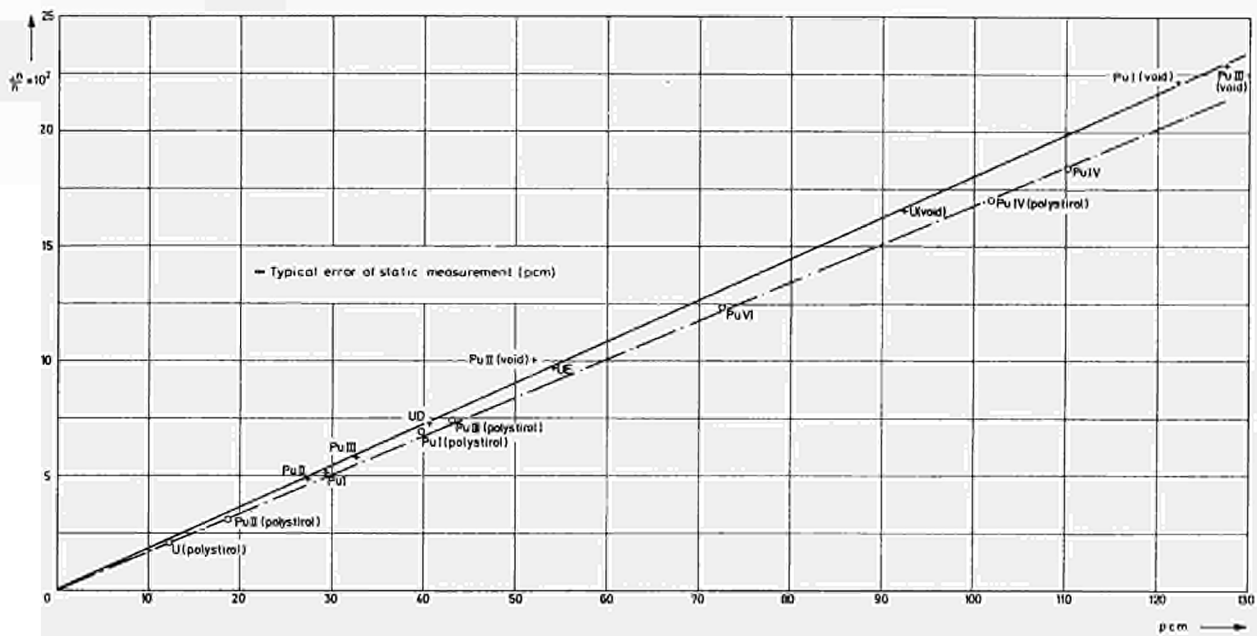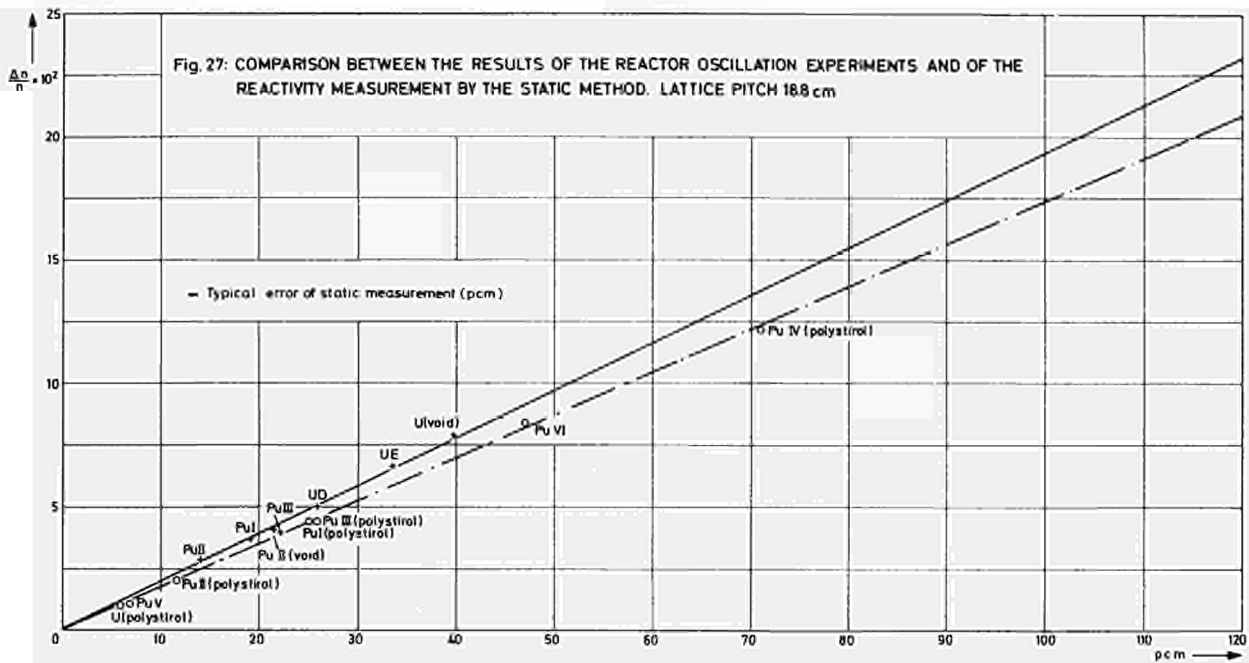
Fig. 28: COMPARISON BETWEEN THE RESULTS OF THE REACTOR OSCILLATION EXPERIMENTS AND OF THE REACTIVITY MEASUREMENT BY THE STATIC METHOD. LATTICE PITCH 23.5 cm
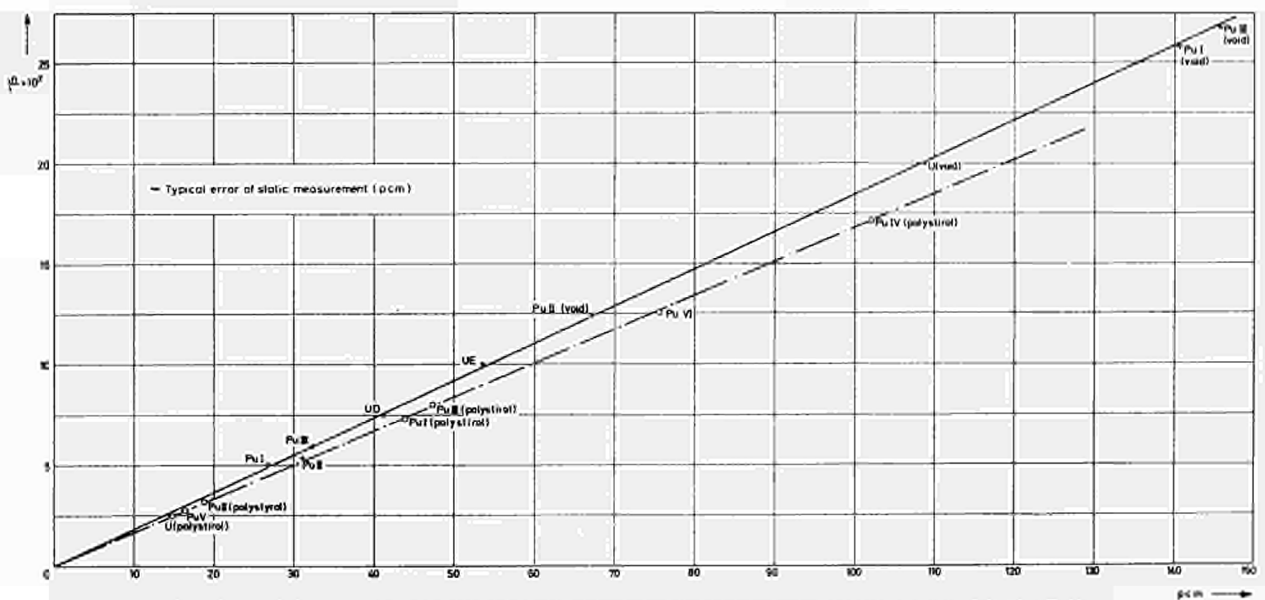
Fig. 29: COMPARISON BETWEEN THE RESULTS OF THE REACTOR OSCILLATION EXPERIMENTS AND OF THE REACTIVITY MEASUREMENT BY THE STATIC METHOD.
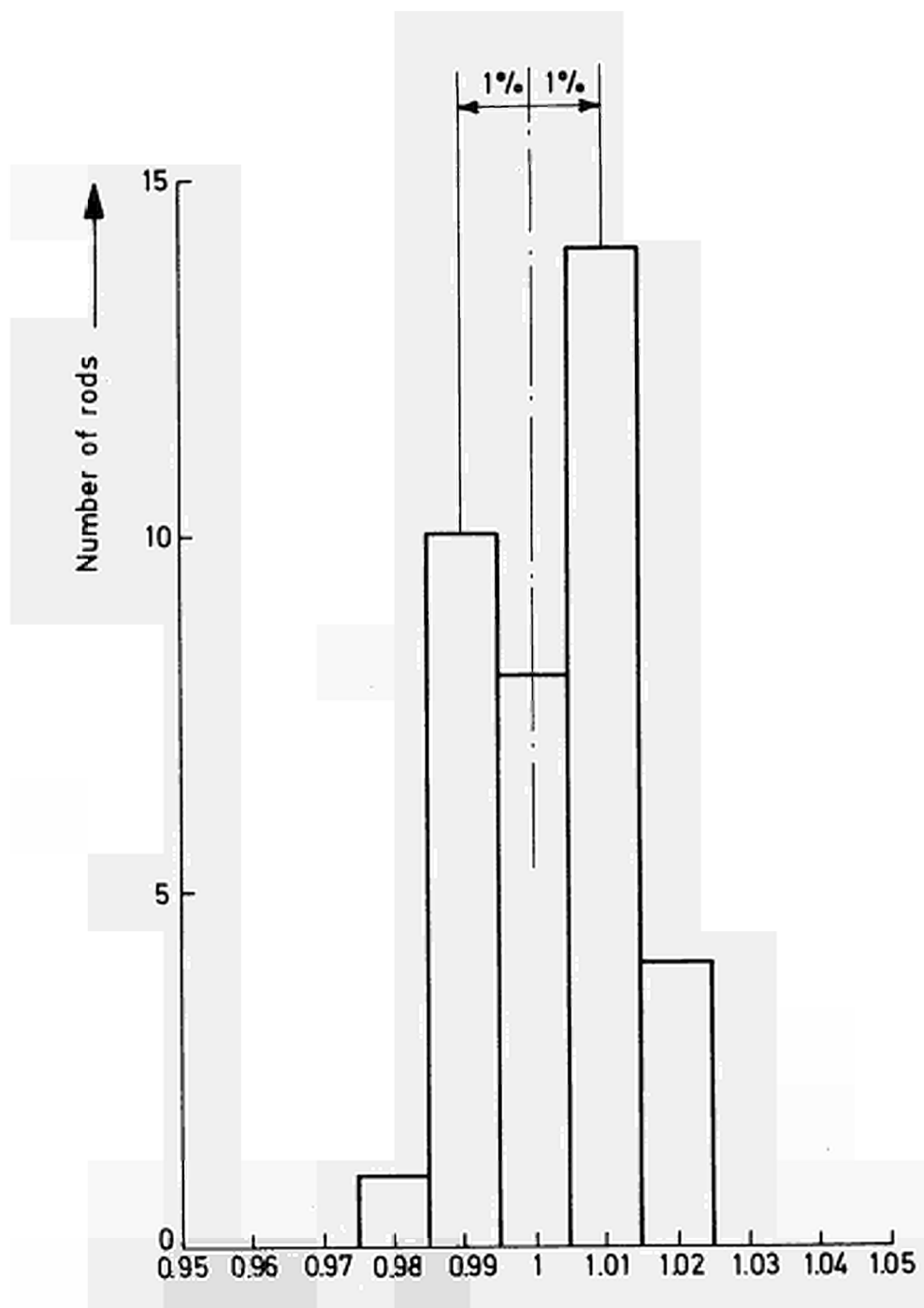
Fig.30 : DISTRIBUTION OF THE Pu/U VALUES FOR THE
RODS OF THE PUI TEST FUEL, NORMALIZED
TO THE MEAN VALUE.
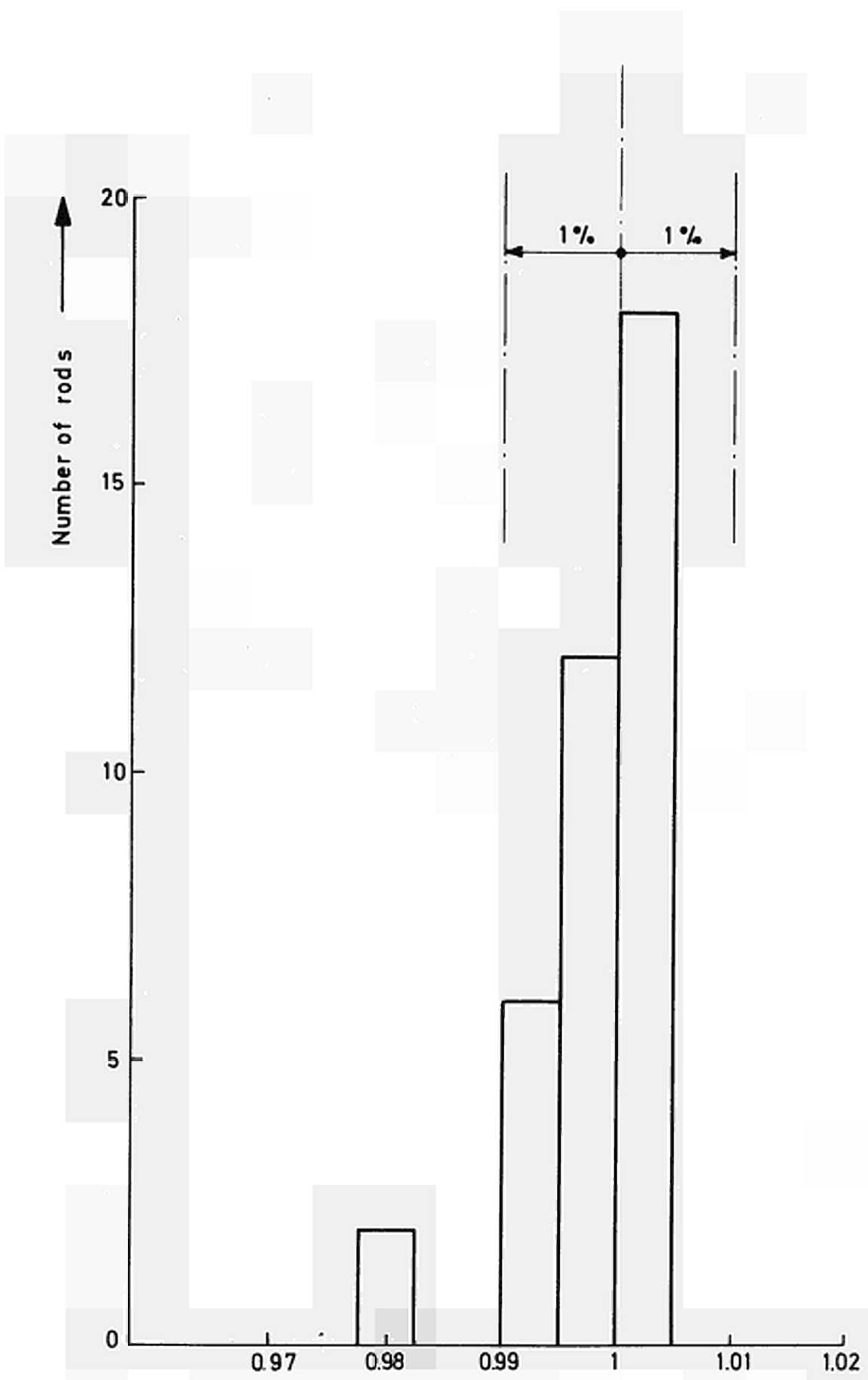
Fig.31 : DISTRIBUTION OF THE PU/U VALUES FOR THE RODS
OF THE PUII TEST FUEL, NORMALIZED TO THE MEAN
VALUE.
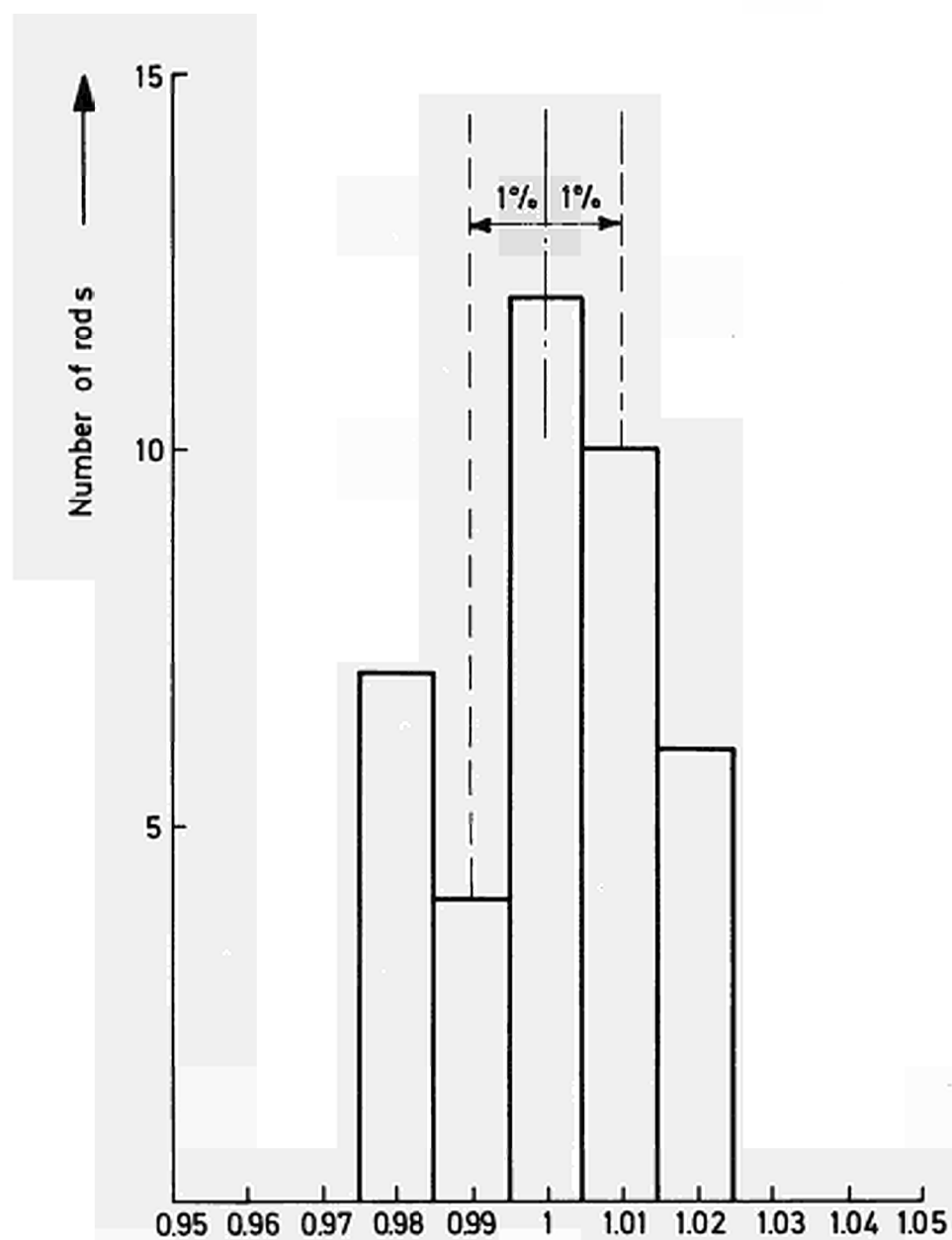
Fig.32 : DISTRIBUTION OF THE PU/U VALUES FOR THE RODS OF
THE PUIII TEST FUEL, NORMALIZED TO THE MEAN VALUE.

Test-section in

Mean neutron density level

Time

Test-section out
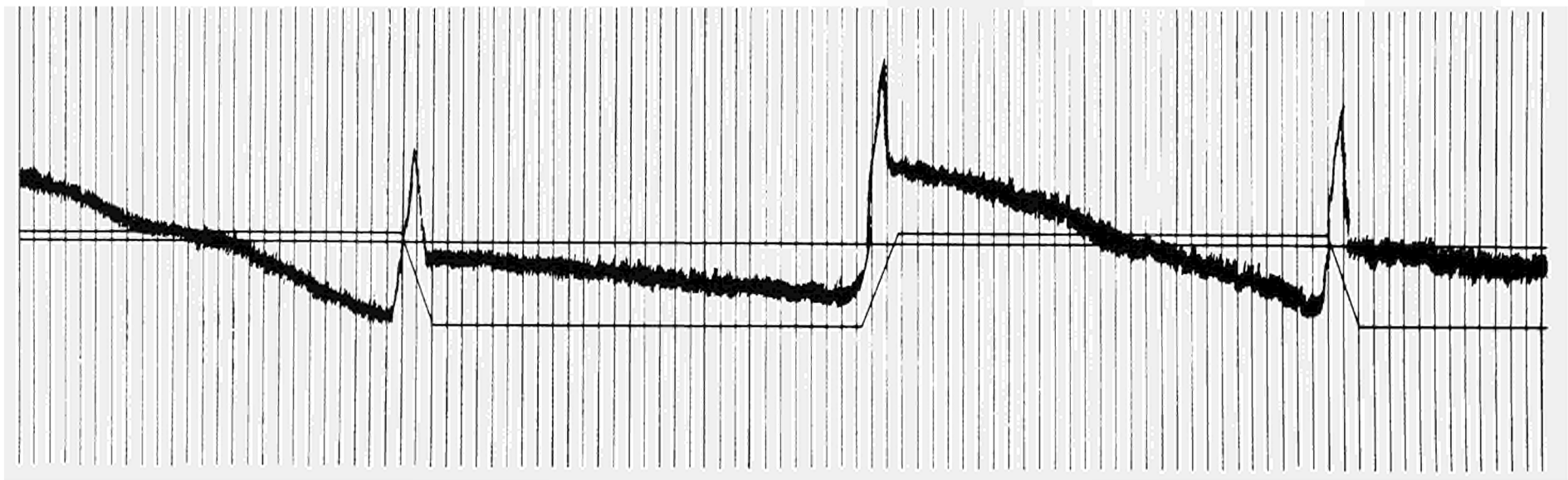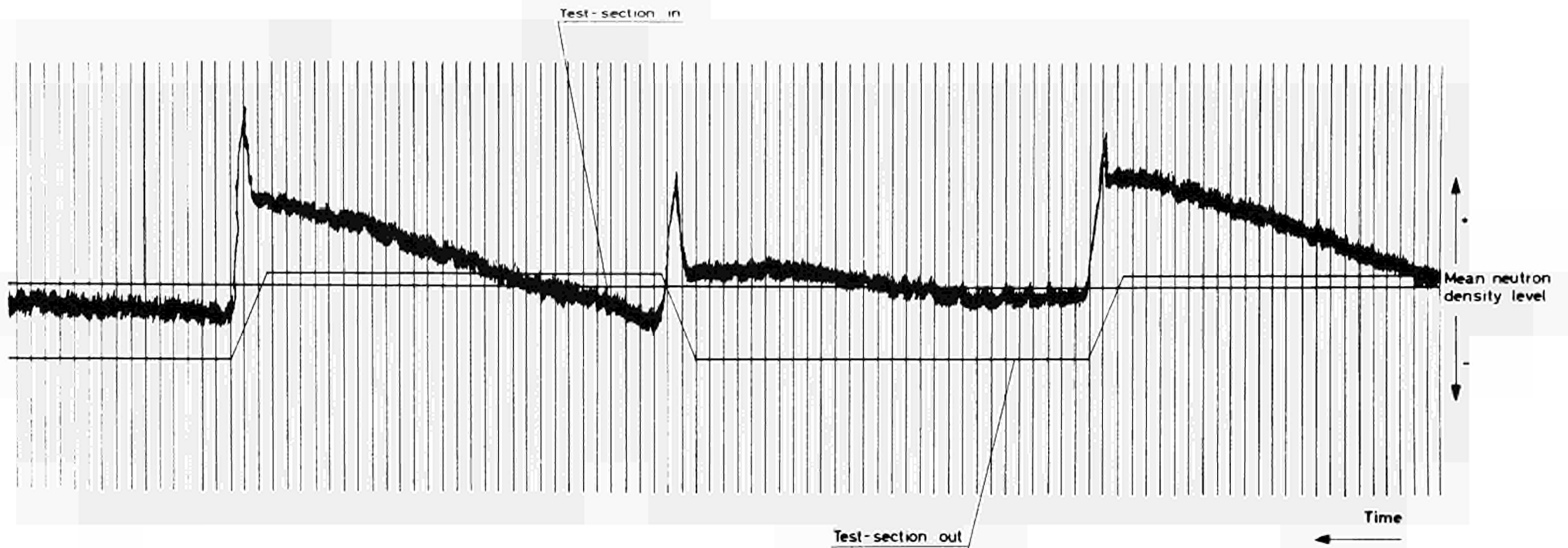
FIG. 33   TYPICAL RECORD OF PRIMARY DATA.
TEST FUEL UN, TRANSIT SPEED 1 M/S
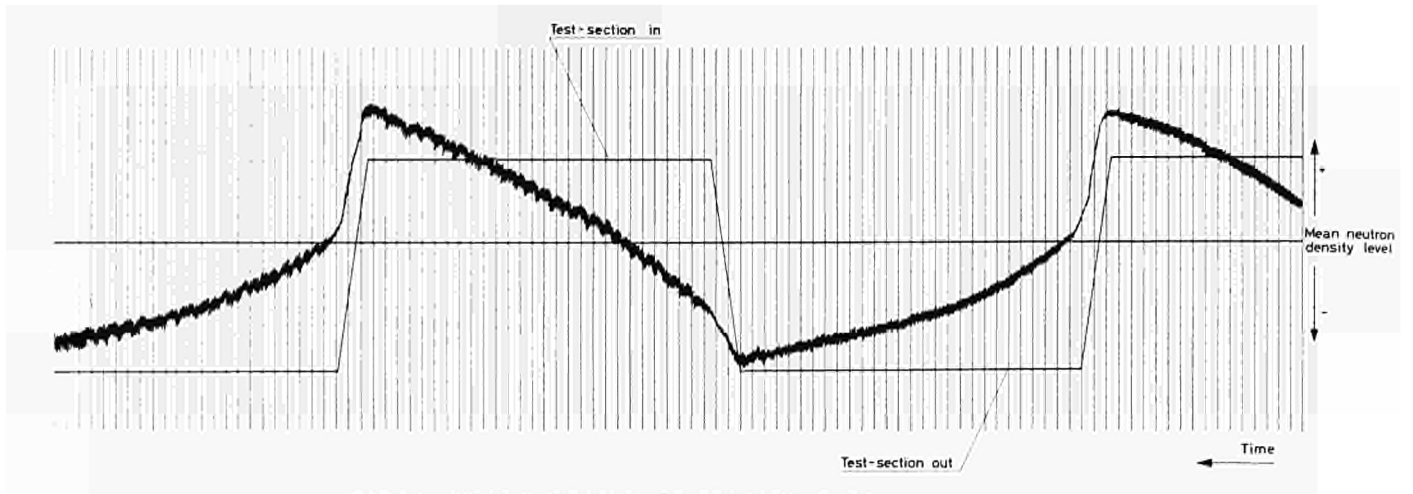
FIG.34 TYPICAL RECORD OF PRIMARY DATA.
TEST FUEL PUI, TRANSIT SPEED 1 M/S.
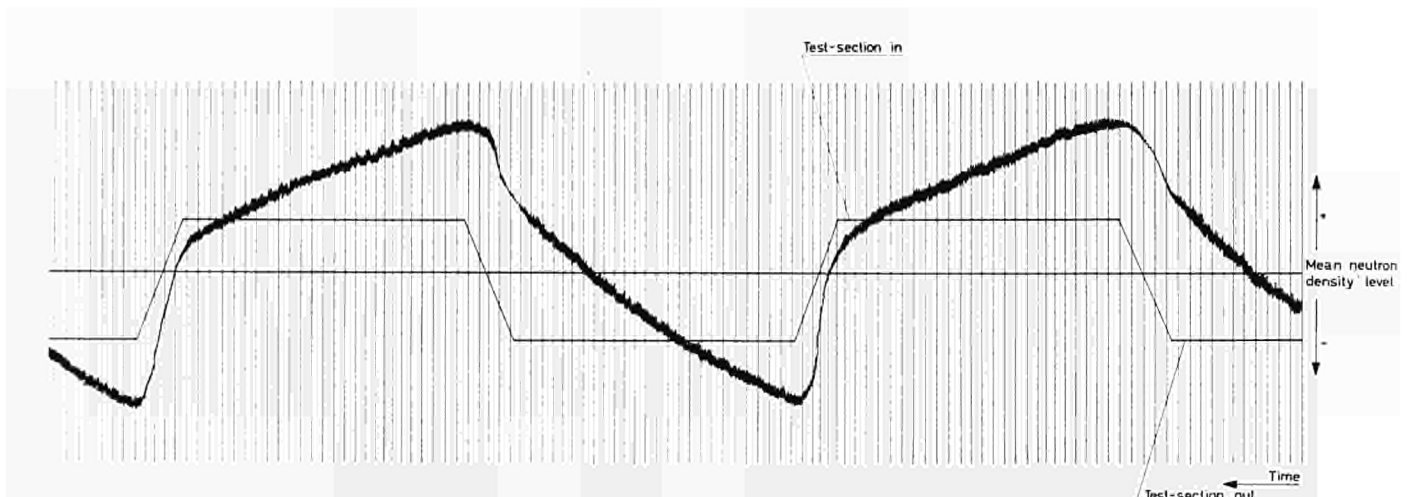
FIG. 35 TYPICAL RECORD OF PRIMARY DATA.
TEST FUEL PUI, TRANSIT SPEED 0,5 M/S
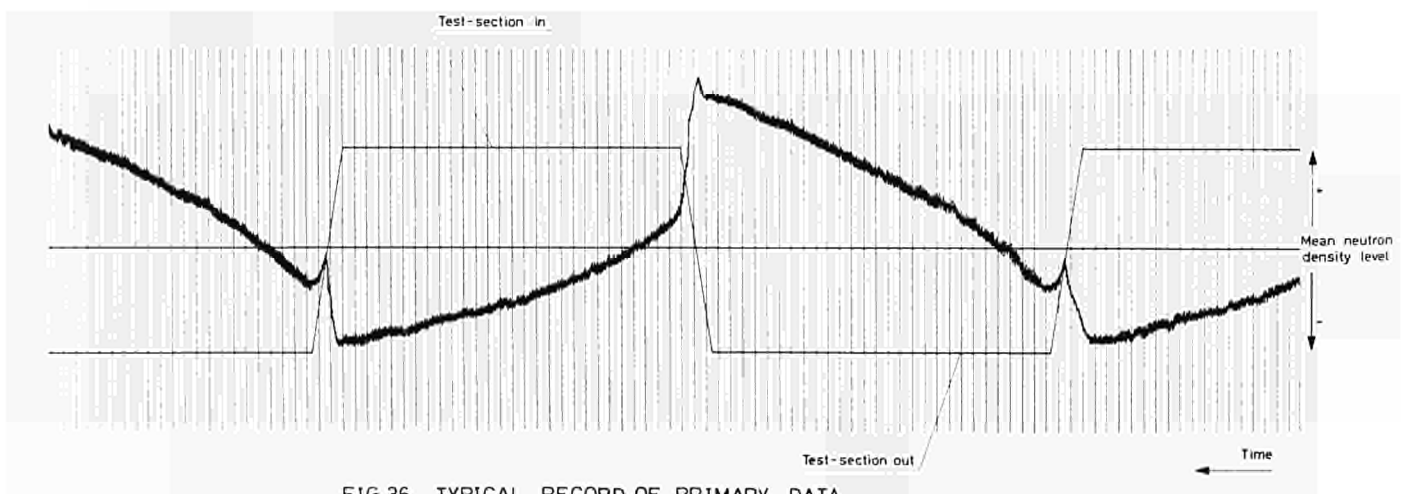
FIG.36 TYPICAL RECORD OF PRIMARY DATA.
TEST FUEL PUII, TRANSIT SPEED 1 M/S

A D D E N D U M

After the conclusion of the work presented in the previous
report an additional series of reactivity worth determina-
tions was performed, primarily in order to provide comple-
mentary data to aid in the theoretical analysis of the
body of the experimental results. The experimental
equipment and method used being those extensively described
in the report, only the essential features of the comple-
mentary experiments are mentioned in the following addendum.

The test-sections considered were composite fuel clusters,
assembled with rods from the available test-fuels, i.e. :
UN, UE, UD, PuI, PuIII, PuIV. Heterogeneous arrays were
obtained by using different test-fuels for the central,
inner-ring and outer-ring rods of the cluster. Mixed
arrays were assembled by alternating rods from two diffe-
rent test-fuels throughout the cluster. In addition,
the PuI test-section was remeasured, having replaced
those rods whose composition seemed to be incorrectly
evaluated (see 12.3). A description of fuel rods arran-
gement in the 10 composite test-sections studied is shown
in Table Ad-1.

The test-sections UE and UD were remeasured, in order to
provide a normalization to the results of the previous
measurements (which was required due to some degradation
meanwhile occurred in the title of the heavy water moderator).

All measurements were carried out at the three standard
lattice pitches of 18.8, 23.5 and 28.05 cm. The test-
sections were assembled in either one of the two plexi-
glass matrices whose composition is listed in Table Ad-2.
From each of the measured reactivity values of the test-
sections was subtracted the reactivity value of the UN-
section assembled in the same matrix.

The compositions of the U and Pu-U test-sections are
listed in Table Ad-3 and Ad-4, respectively. The
experimental results ($\Delta n/n$) are presented in Tables Ad-5,
Ad-6 and Figg.ad-1, ad-2. The uncertainty (not quoted)
is typically that defined in the previous report (see
11.15 to 11.17).

Also reported are the absolute reactivity values (expressed
as pcm, i.e. $\Delta k/k \times 10^{-5}$) inferred from the critical
heavy water levels by asymptotic period measurements
(Table Ad-7 and Figg.ad-3, ad-4, ad-5, for lattice pitch
18.8, 23.5, 28.05 cm, respectively). As noted previously
(see 12.2), the agreement between these results and the
oscillation measurements data is generally satisfactory.

For completeness, the measured distributions of Dy
activation in the representative rods of the UN test-
section at lattice pitches 18.8 and 28.05 cm, are also
presented (Fig.ad-5).

—

Identification	Fuel	Comment
UND-I	UN:center rod UD:other 18 rods	
UND-II	UN:7 inner rods UD:12 outer rods	
UND-III	UN:center rod, 12 outer rods UD:6 inner rods	
UNE-I	UN:center rod UE:other 18 rods	
UNE-II	UN:7 inner rods UE:12 outer rods	
UNE-III	UN :center rod , 12 outer rods UE: 6 inner rods	
UDE(m)	UD, UE mixed by alternating UD, UE throughout 19-rod cluster	
Pu-VI	Pu-I:inner rods Pu-IV:12 outer rods	
Pu-VII	Pu-III:7 inner rods Pu-IV:12 outer rods	
Pu-VII(m)	Pu-III, IV mixed by alternating Pu-III, IV throughout 19-rod cluster	
Pu I	Pu I	Those fuel rods which showed wide discrepancies between chemical analysis and spontaneous fission values replaced
UD	UD	For normalization to previous experiment
UE	UE	For normalization to previous experiment

Table Ad-1 : Description of measured test-sections

material	I	II
plexiglass	927.25 gr	929.58 gr
Zr2 end-plates	508.60 "	508.40 "
Zr2 screws	77.80 "	77.88 "

Table Ad-2 : Composition of matrices used for the
test-sections assembly

Identifi-cation	central rod		inner-ring rods		outer-ring rods	
	U^{235}/U tot (%)	weight (kg)	U^{235}/U tot (%)	weight (kg)	U^{235}/U tot (%)	weight(kg)
UN	0.714	1.0700	0.714	6.4202	0.714	12.8461
UND I	0.714	1.0700	0.643	6.4151	0.643	12.8296
UND II	0.714	1.0705	0.714	6.4202	0.643	12.8296
UND III	0.714	1.0705	0.643	6.4151	0.714	12.8441
UNE I	0.714	1.0700	0.804	6.4401	0.804	12.8808
UNE II	0.714	1.0700	0.714	6.4227	0.804	12.8808
UNE III	0.714	1.0700	0.804	6.4401	0.714	12.8461
UDE (m)	0.804	1.0733	0.804	3.2236	0.804	6.4386
			0.643	3.2082	0.643	6.4175
UD	0.643	1.0695	0.643	6.4151	0.643	12.8296
UE	0.804	1.0736	0.804	6.4401	0.804	12.8803

Table Ad-3 : Compositions of U test-sections

Identifi-cation	central rod weight(gr)		composition(%)			inner-ring rods weight(gr)		composition(%)			outer-ring rods weight(gr)		composition(%)		
	U+Pu	Pu	$\frac{Pu}{U+Pu}$	$\frac{U235}{Utot}$	$\frac{Pu240}{Pu239}$	U+Pu	Pu	$\frac{Pu}{U+Pu}$	$\frac{U235}{Utot}$	$\frac{Pu240}{Pu239}$	U+Pu	Pu	$\frac{Pu}{U+Pu}$	$\frac{U235}{U\ tot}$	$\frac{Pu240}{Pu239}$
Pu I	1063.8	0.4840	0.046	0.714	6.20	6.357.3	2.9457	0.046	0.714	6.20	12.721.4	5.7772	0.046	0.714	6.20
Pu VI	1063.8	0.4840	0.046	0.714	6.20	6.357.3	2.9457	0.046	0.714	6.20	12.803.7	32.3460	0.26	0.227	27.8
Pu VII	1055.8	0.4791	0.046	0.714	25.5	6303.6	2.8856	0.046	0.714	25.5	12.803.7	32.8460	0.26	0.227	27.8
PuVII(m)	1055.8	0.4791	0.046	0.714	25.5	3161.1	1.4407	0.046	0.714	25.5	6303.8	2.8805	0.046	0.714	25.5
						3201.9	8.2650	0.26	0.227	27.8	6400.3	16.3007	0.26	0.227	27.8

Table Ad-4 : Compositions of Pu-U test-sections

lattice pitch (cm)	UE	UNE I	UNE II	UNE III	UDE(m)	UD	UND I	UND II	UND III
18.8	+5.251	+5.007	+3.837	+1.298	+0.697	−4.474	−4.239	−3.176	−1.101
23.5	+7.927	+7.578	+5.812	+1.843	+1.037	−6.621	−6.402	−4.782	−1.606
28.05	+7.727	+7.421	+5.729	+1.744	+1.009	−6.462	−6.225	−4.632	

Table Ad-5 : Experimental results ($\Delta n/n \times 10^2$) for the U test-sections

Lattice pitch (cm)	Pu I	Pu VI	Pu VII	Pu VII(m)
18.8	+2.693	−7.575	−7.533	−4.001
23.5	+3.768	−11.353	−11.287	−5.878
28.05	+3.561	−11.154	−11.087	−5.727

Table Ad-6 : Experimental results ($\Delta n/n \times 10^2$) for the Pu-U test-sections

Identifi- cation	lattice pitch(cm)		
	18.8	23.5	28.05
UE	+28.65	+44.10	+44.00
UD	−21.45	−32.90	−32.25
UND I	−20.10	−31.50	−31.50
UND II	−15.15	−22.75	−23.00
UND III	− 4.80	− 5.95	− 5.50
UNE I	+27.45	+43.35	+41.50
UNE II	+20.70	+33.25	+32.75
UNE III	+ 8.25		+11.50
UDE(m)	+ 5.10	+ 7.70	+ 7.75
Pu I	+15.30	+21.70	+20.00
Pu VI	−38.40	−58.80	
Pu VII	−38.25	−58.10	−57.25
Pu VII(m)	−19.05	−26.60	−29.00

Table Ad-7 : Absolute reactivity values (pcm), as
inferred from asymptotic period
determinations

Fig. ad-1   Experimental results : U test-sections
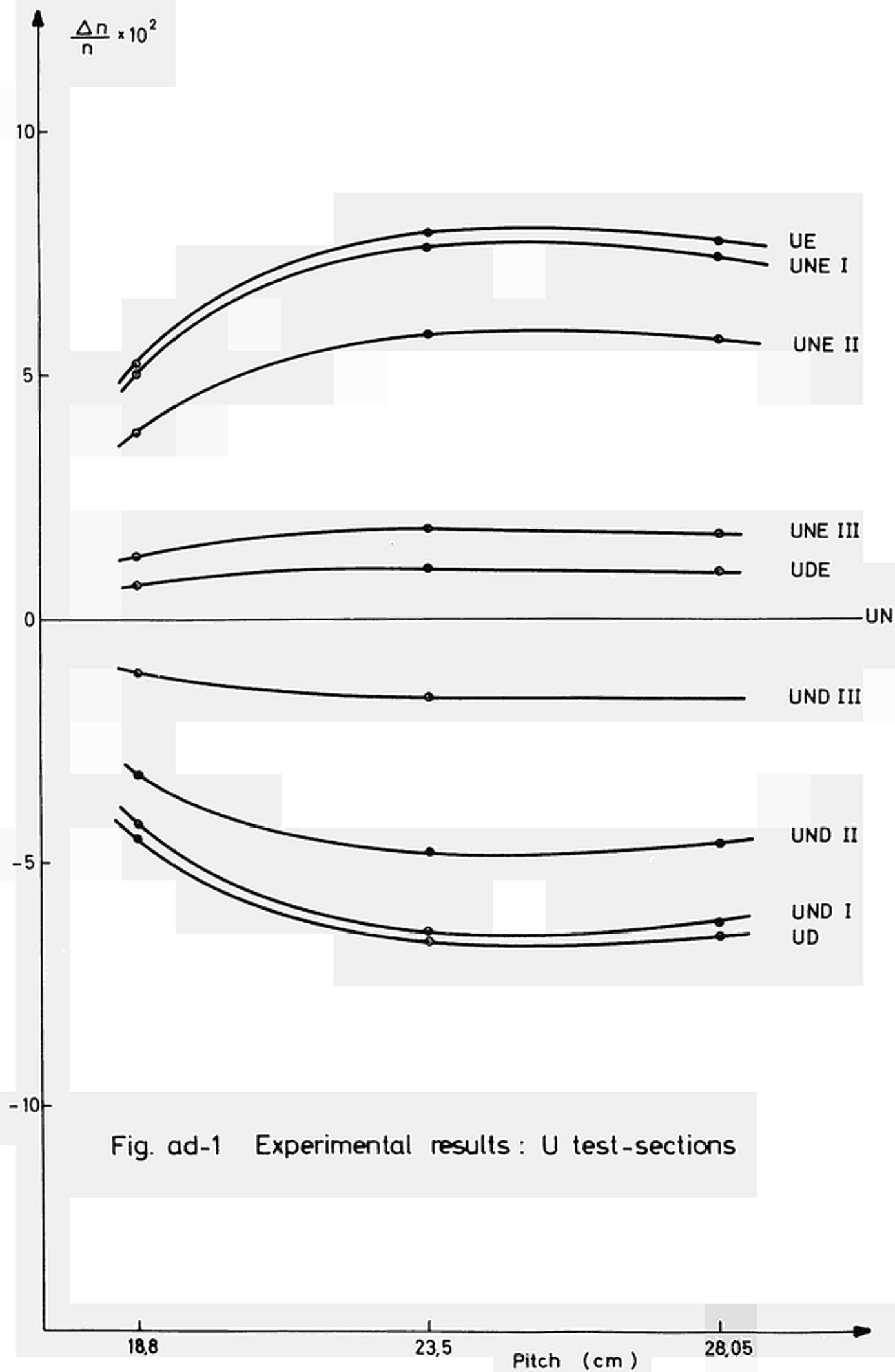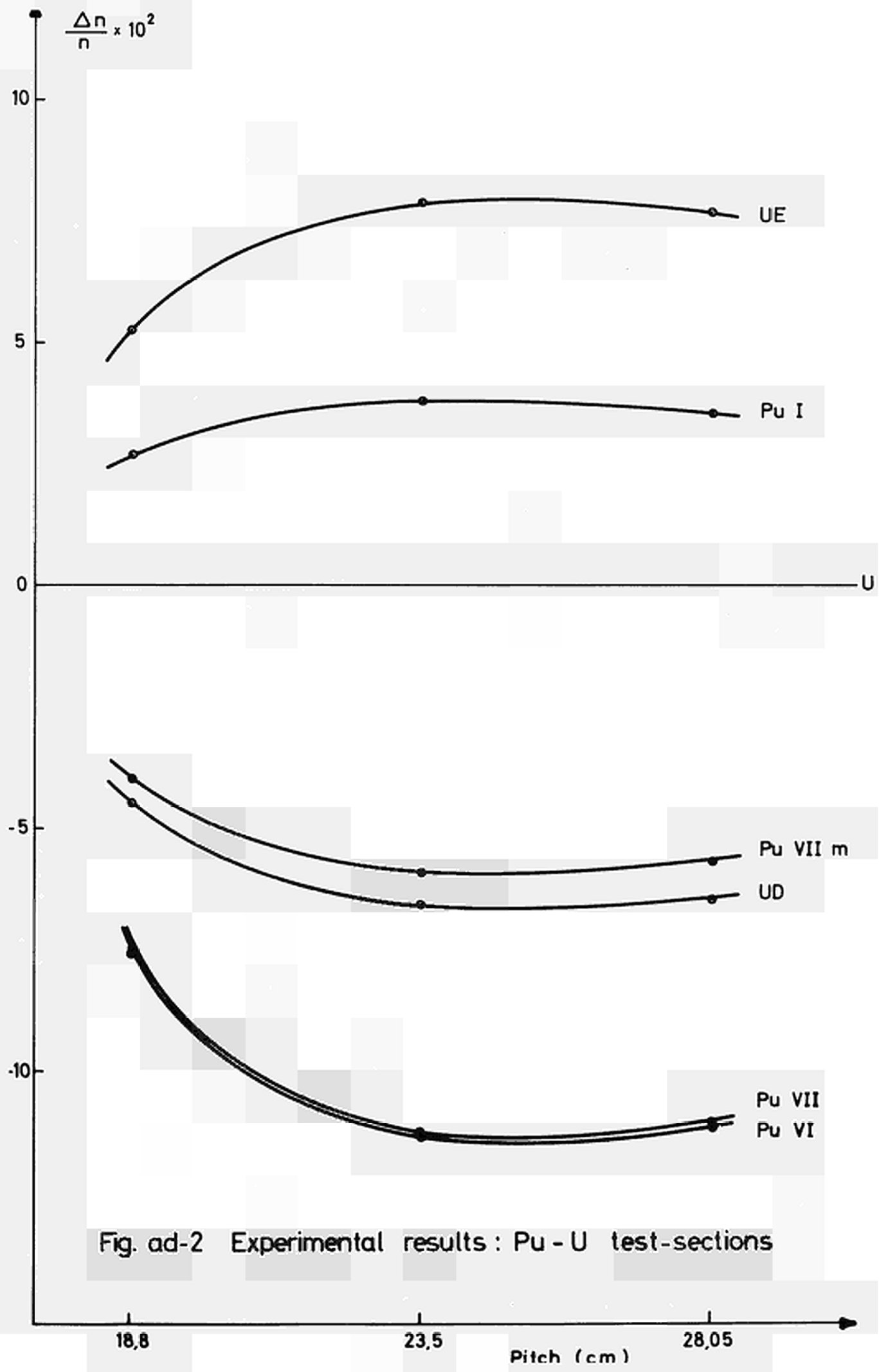
Fig. ad-2 Experimental results : Pu – U test-sections
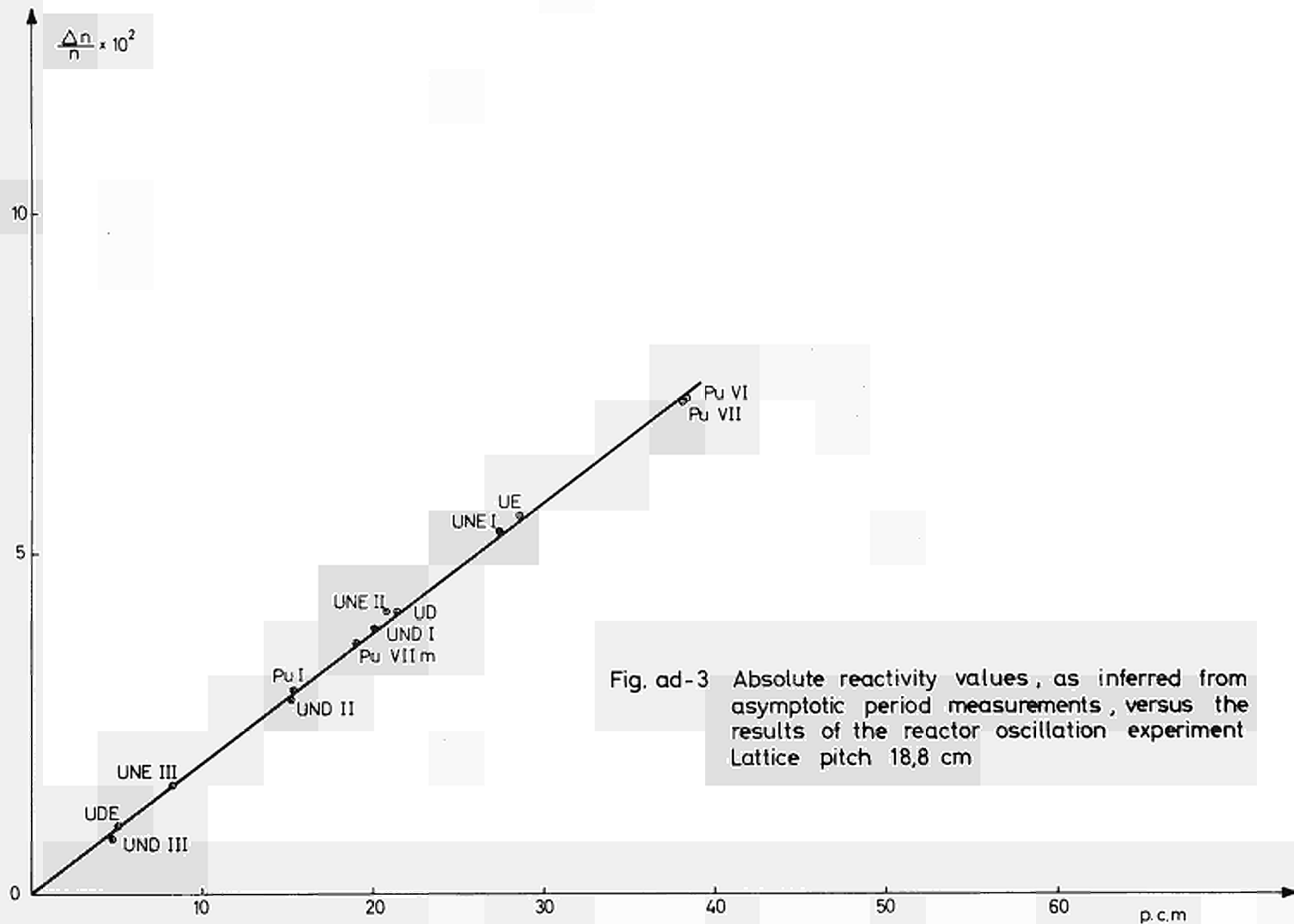
Fig. ad-3 Absolute reactivity values, as inferred from asymptotic period measurements, versus the results of the reactor oscillation experiment Lattice pitch 18,8 cm

Fig. ad-4 Absolute reactivity values, as inferred from asymptotic period measurements, versus the results of the reactor oscillation experiment Lattice pitch 23,5 cm
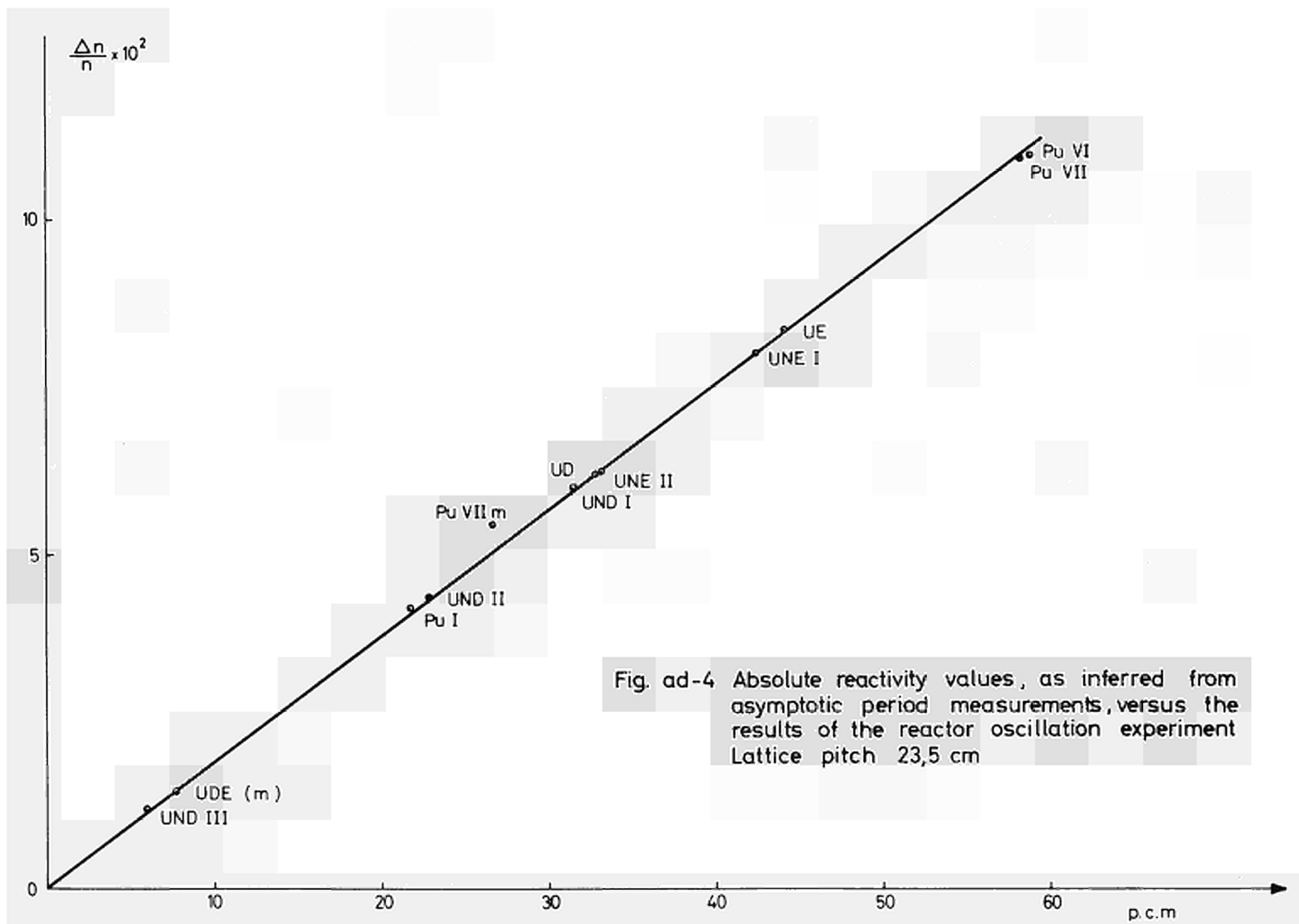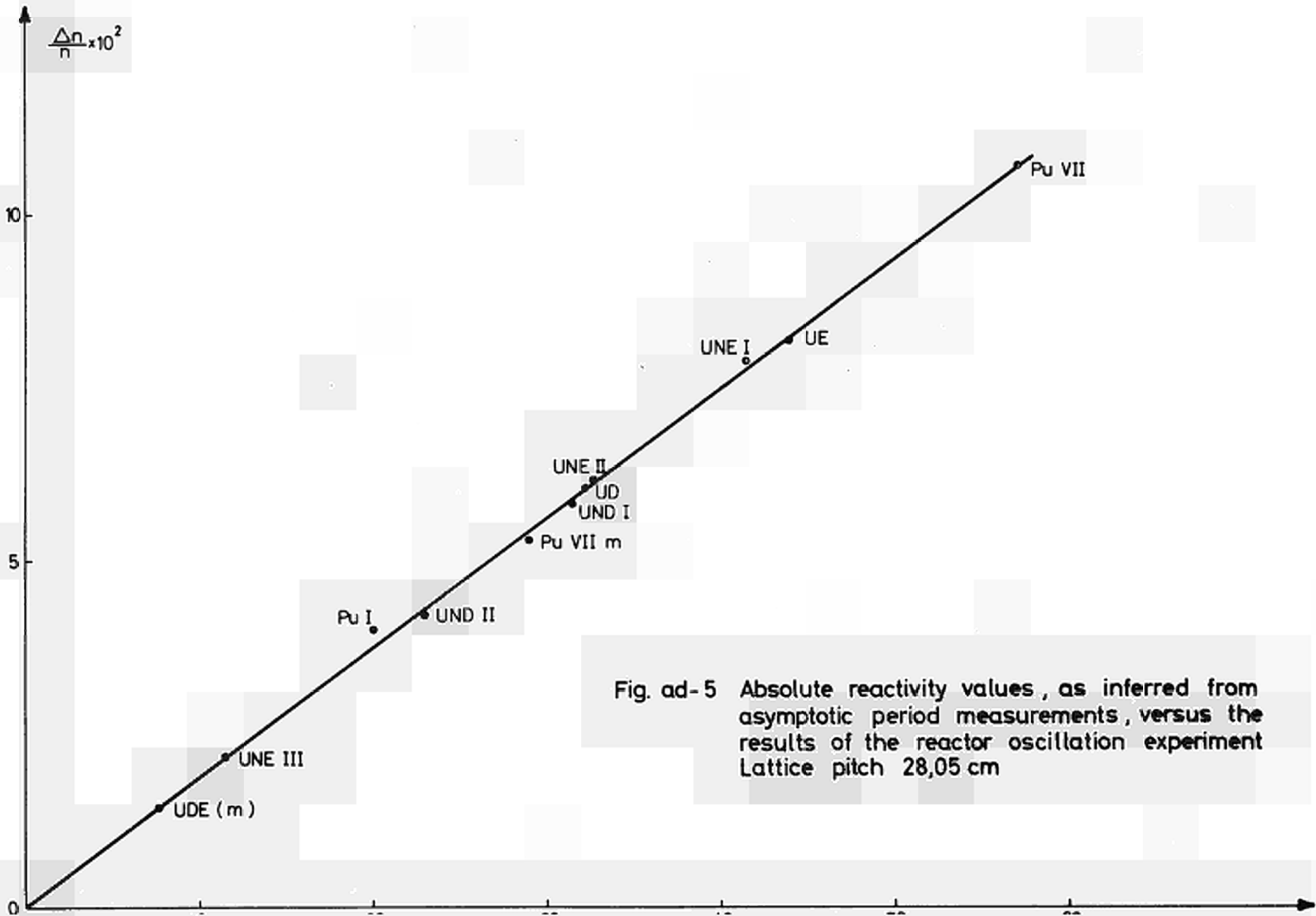
Fig. ad-5 Absolute reactivity values, as inferred from
asymptotic period measurements, versus the
results of the reactor oscillation experiment
Lattice pitch 28,05 cm
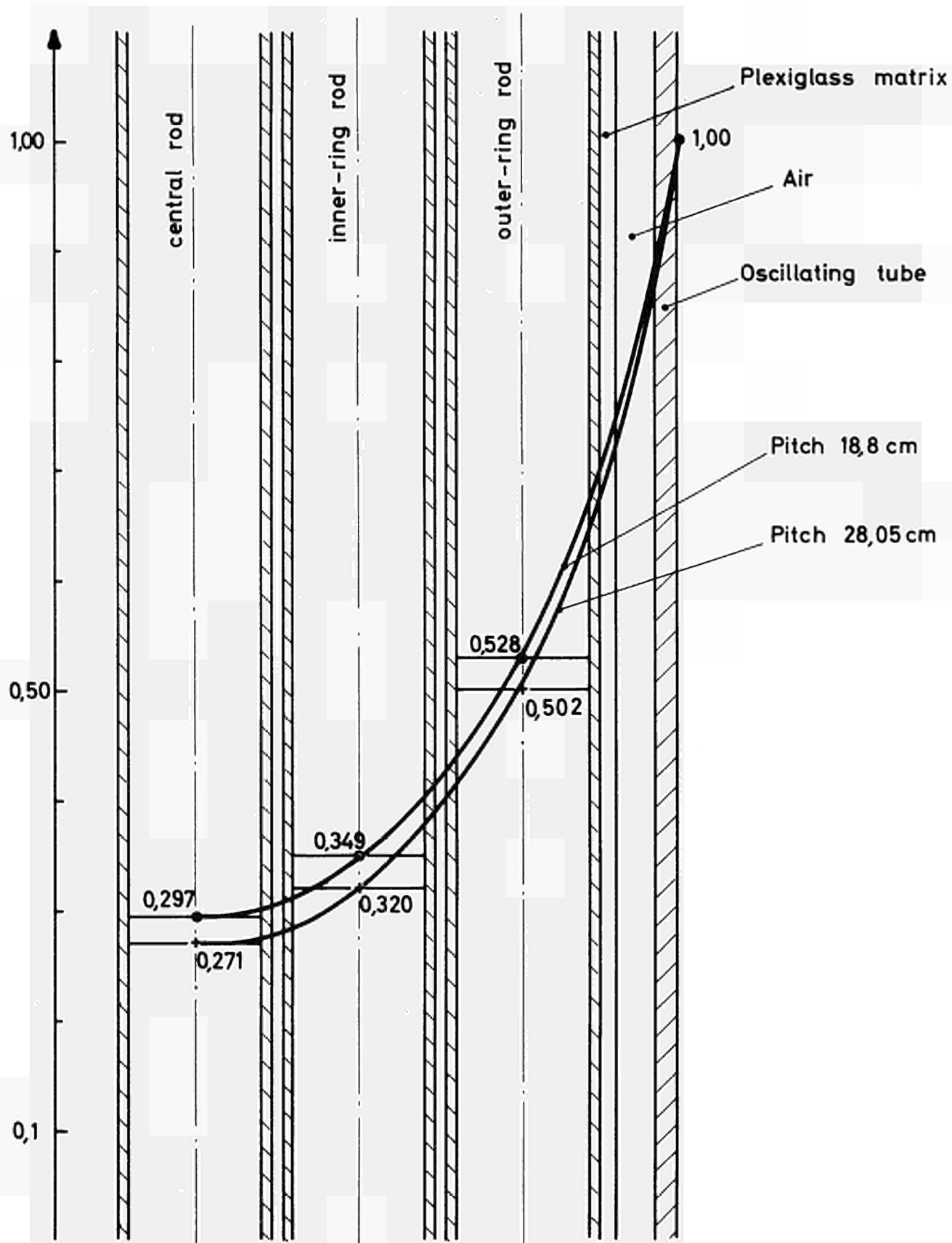
Fig. ad-6   Dysprosium activation distributions in UN
test-section at lattice pitches 18,8 and 28,05 cm
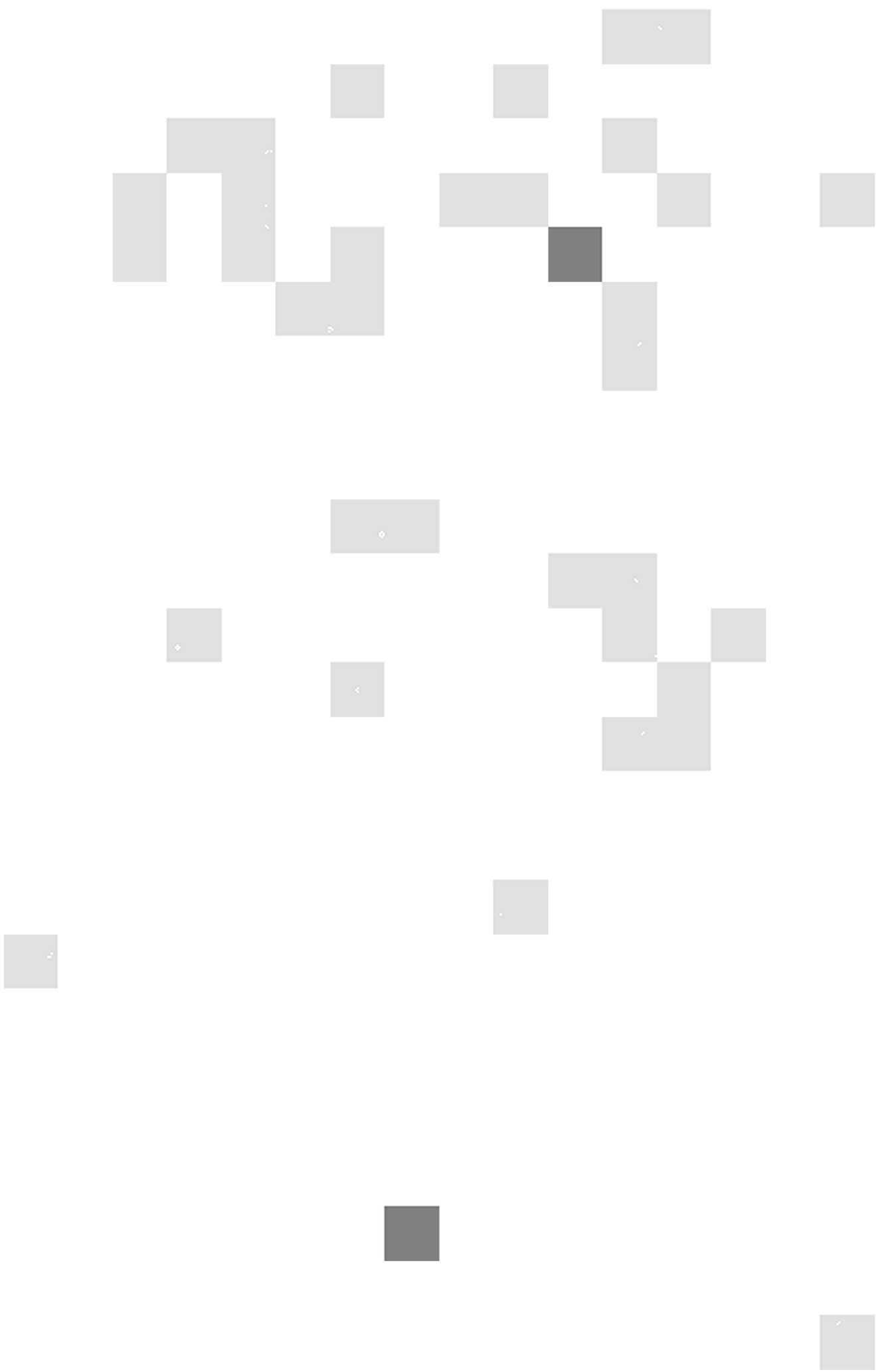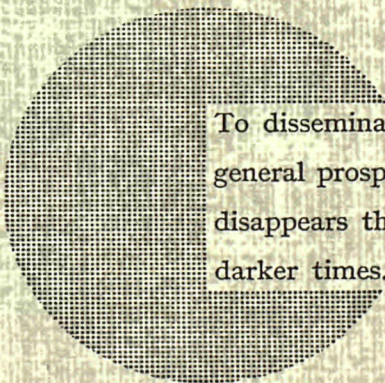
To disseminate knowledge is to disseminate prosperity — I mean general prosperity and not individual riches — and with prosperity disappears the greater part of the evil which is our heritage from darker times.

Alfred Nobel

SALES OFFICES

CDNA04486ENC